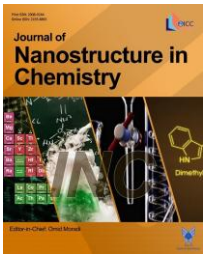

J. Nanostruct Chem. 2026; 16(1): 72-111

Journal of Nanostructure in Chemistry (JNSC)

https://doi.org/10.57647/jnsc.2026.1601.05

Review Article

MXene-Based Wearable Sweat Biosensors for Personalized Health Monitoring: Materials Innovation and Data-Driven Approaches

Ceren Karaman[1,*], Onur Karaman[2,*], Jun Jiang[3], Taotao Zhao [3,*]

[1]*Akdeniz University, Department of Electricity and Energy, Antalya, Turkey*

[2]*Akdeniz University, Department of Medical Services and Techniques, Antalya, Turkey*

[3]*Zhejiang Province Engineering Research Center for Endoscope Instruments and Technology Development, Quzhou People's Hospital, The Quzhou Affiliated Hospital of Wenzhou Medical University, Quzhou, China*

*Corresponding authors: cerenkaraman@akdeniz.edu.tr, onurkaraman@akdeniz.edu.tr, 344607699@wmu.edu.cn

Article History:

Received:
21 October 2025

Revised:
25 November 2025

Accepted:
20 December 2025

Published in Issue:
28 February 2026

Abstract

MXenes, a diverse family of two-dimensional transition metal carbides and nitrides, have emerged as highly promising materials for wearable biosensors due to their exceptional conductivity, tunable surface chemistry, and mechanical flexibility. Among their most compelling applications is sweat-based health monitoring, which enables non-invasive, real-time access to dynamic physiological information. Unlike previous reviews that broadly survey MXene-enabled wearables, this work provides a unified perspective that integrates human-specific sweat variability, sweat-relevant structure–property relationships of MXene compositions, and data-driven methodologies for adaptive, personalized sensing. Translating MXene-based sensors into robust, personalized platforms requires innovations that extend beyond material design into adaptive signal processing, machine learning calibration, and individualized digital modeling. This review critically examines the structure–property relationships of various MXene compositions and outlines material engineering strategies for enhancing sensitivity, selectivity, and operational stability in sweat environments. Furthermore, it highlights how computational frameworks can calibrate, adapt, and simulate sensor behavior under individualized biochemical conditions. In silico sweat simulation and architecture optimization are also discussed as transformative tools for accelerating biosensor development. By bridging advanced materials with data-driven methodologies, this review establishes a blueprint for the next generation of MXene-based wearable systems capable of intelligent, personalized health monitoring.

Keywords: Digital Twin; Electrochemical Sensors; In-silico Optimization; Machine Learning; MXenes; Personalized Bioelectronics; Sweat Analysis; Wearable Biosensors

Cite this article: Karaman, C., Karaman, O., Jiang, J., Taotao, Z., MXene-Based Wearable Sweat Biosensors for Personalized Health Monitoring: Materials Innovation and Data-Driven Approaches. *J Nanostruct Chem* **16,** 72-111(2026).
https://doi.org/10.57647/jnsc.2026.1601.05

1. Introduction

The evolution of wearable bioelectronics has ushered in a new era of non-invasive, real-time health monitoring systems that seamlessly integrate with the human body [1, 2]. These systems offer the unprecedented ability to track physiological signals and biochemical analytes continuously, enabling early disease detection, personalized therapy adjustment, and predictive health analytics [3–5].

Among various bodily fluids used in diagnostic applications, sweat stands out as an attractive candidate

due to its accessibility, non-invasiveness, and rich content of physiological biomarkers, including electrolytes, metabolites, proteins, and hormones [6, 7].

Consequently, sweat-based wearable biosensors have gained significant traction for applications ranging from glucose monitoring and electrolyte balance to stress and dehydration tracking [3, 8–10].

Despite rapid advances in the field, a critical challenge remains largely unaddressed in current literature and device development pipelines. The high degree of inter-individual and intra-individual variability in sweat composition is still crucial to be addressed [11].

Unlike blood, sweat is highly influenced by a wide range of biological and environmental factors such as age, sex, genetics, hydration status, stress levels, physical activity, circadian rhythms, ambient temperature, and underlying medical conditions [12, 13]. These variables alter sweat's ionic strength, pH, metabolite concentrations, protein content, and volume rate, creating a biochemically dynamic and heterogeneous environment that directly impacts sensor response, reliability, calibration, and clinical relevance [14, 15].

However, most wearable biosensors are still designed based on standardized artificial sweat models that fail to capture this biochemical diversity, limiting their accuracy, user specificity, and widespread applicability[16–18]. Addressing this gap necessitates a paradigm shift in sensor material design from static and universal to dynamic and personalized interfaces that can adapt to the complex chemical signatures of individual users. Within this context, MXenes, a class of two-dimensional transition metal carbides, nitrides, and carbonitrides, have emerged as promising materials for advanced biosensing platforms [19–21].

Exhibiting a unique combination of metallic conductivity, hydrophilicity, surface functional tunability, redox activity, and mechanical flexibility, MXenes are particularly well-suited for integration into skin-interfaced devices [22].

Their surface terminations (–OH, –O, –F) enable strong interactions with aqueous and ionic species, while their solution processability allows for scalable fabrication of thin films, membranes, and composite structures [23–25].

Fig. 1 illustrates a personalized bioelectronic platform integrating MXene-based electrochemical sensors for real-time, non-invasive sweat biomarker monitoring. The system addresses the inherent variability in sweat composition across individuals and physiological states, influenced by environmental, dietary, and activity-related factors.

By combining the chemical specificity of MXenes with machine learning (ML) algorithms and digital twin frameworks, the platform enables adaptive signal processing and individualized health tracking tailored to each user's biochemical profile. The integration of MXenes into wearable sweat sensors has largely followed a conventional approach maximizing conductivity and surface area for improved electrochemical signal generation [20, 26].

While such strategies have led to significant progress in analyte detection (e.g., glucose, lactate, sodium, cortisol), they often overlook the crucial influence of sweat variability and user-specific biochemical environments on material performance, degradation behavior, and signal fidelity [12, 14, 27].

For instance, changes in pH or ion concentration may modulate surface charge distribution on MXenes, affect redox reactions, alter enzymatic activities, or trigger aggregation or delamination [28].

Moreover, the influence of interfacial hydration, electrolyte diffusion, and long-term biofouling on MXene-based sensors in real sweat conditions is not well-characterized in the literature.

This review seeks to address this critical knowledge gap by presenting a first-of-its-kind analysis of the interplay between human-specific sweat chemistry and MXene-based sensor materials.

A materials-centric framework for understanding and optimizing MXene structures and hybrid systems in the context of biochemical personalization is proposed. This includes comprehensive discussions on sweat composition variability, structure–property relationships of MXenes in physiological environments, material engineering strategies for personalized selectivity and robustness, and performance benchmarking under variable sweat conditions.

Furthermore, we explore emerging directions in adaptive sensor systems that incorporate AI-guided calibration, digital twin modeling, and biosensor matching to individual user profiles, transforming wearable sensors into truly personalized bioelectronic platforms.

By bridging the domains of advanced functional materials, sweat biochemistry, and personalized healthcare engineering, this review offers a novel, cross-disciplinary perspective that is absent from existing literature.

It aims to serve not only as a scientific synthesis but also as a strategic guide for the rational design of next-generation wearable sensors tailored to the individual at the molecular, material, and system levels.

Although several reviews have discussed MXene-based bioelectronics or wearable sweat sensors, these works have primarily focused on general device architectures, broad material classifications, or application overviews without explicitly integrating the biochemical variability of human sweat into materials design.

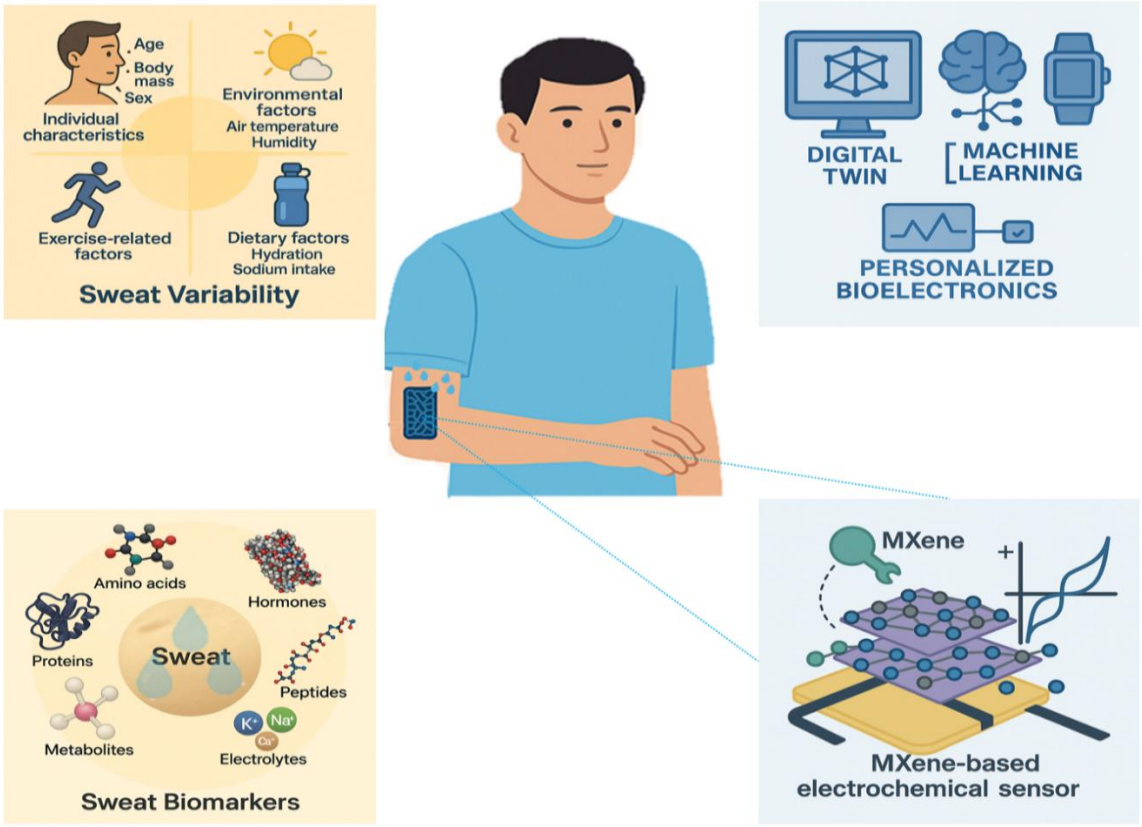

Figure 1. Illustration of the concept of personalized bioelectronics through sweat sensing

The present review is distinct in three critical ways. First, it introduces a sweat-centric framework that treats inter- and intra-individual variability in sweat composition as a fundamental engineering parameter, linking these biochemical variations directly to MXene surface terminations, ion-exchange behavior, and electrochemical stability. Second, it systematically analyzes structure–property relationships of MXenes under sweat-relevant mechanical, chemical, and environmental conditions. Third, it uniquely incorporates data-driven methodologies, including real-time ML calibration, in silico sweat modeling, and digital-twin architectures, to outline how MXene-based sensors can evolve into adaptive, personalized bioelectronic systems. By combining sweat biochemistry, MXene materials science, and computational personalization, this review frames a new cross-disciplinary perspective that is not limitedly addressed in the current literature and provides a targeted roadmap for next-generation personalized sweat biosensing.

2. Sweat Composition and Human-Specific Variability

2.1. Core Components of Human Sweat

Human sweat is a complex aqueous biofluid composed of a wide array of physiologically relevant constituents [7, 12]. Although primarily composed of water (~98–99%), the remaining 1–2% comprises a dynamic mixture of electrolytes, metabolites, proteins, hormones, and trace biomolecules, many of which serve as critical indicators of health status, metabolic activity, and environmental adaptation [14, 29, 30]. The complexity of sweat composition stems from the active and passive transport mechanisms governing its production, as well as from systemic influences such as endocrine regulation, renal function, and skin surface interactions [12, 14].

Electrolytes are among the most abundant and functionally significant components in sweat [13]. Sodium (Na^+) and chloride (Cl^-) ions are secreted in the highest concentrations depending on sweat rate, acclimatization status, and ductal reabsorption efficiency [30, 31]. Potassium (K^+), calcium (Ca^{2+}), and magnesium (Mg^{2+}) are also present in lower concentrations but contribute to osmotic regulation and electrochemical balance [31, 32]. These ions influence the ionic conductivity and interfacial capacitance of sensor materials and can modulate the performance of electrochemical biosensors based on redox and impedance mechanisms.

Sweat also contains key metabolites such as glucose, lactate, urea, and ammonia, which serve as real-time indicators of metabolic and physiological activity [7, 32]. Glucose concentrations in sweat generally range from 10 µM to 1 mM, reflecting plasma levels with a time lag that

varies based on skin permeability and sweat gland physiology [14, 33]. Lactate, a byproduct of anaerobic metabolism, is often detected at concentrations between 5–25 mM during intense physical activity and is an important marker of muscle fatigue and tissue oxygenation [34, 35]. Urea and ammonia arise from protein catabolism and nitrogen excretion pathways, and their levels are influenced by renal function and hydration state [32, 36, 37]. Human sweat urea concentration in healthy individuals typically ranges from about 5 to 40 millimolar (mM), with an average around 20 to 25 mM. This level is substantially higher than the urea concentration in blood serum, which is generally around 6.2 mM (typically 2.5 to 7.5 mM depending on the source). The urea concentration in sweat can increase significantly in people with kidney dysfunction or end-stage renal disease, sometimes reaching levels above 100 mM [38–40]. Meanwhile, ammonia concentration in human sweat varies widely but typically ranges from about 10 to 110 μM. The highest concentrations are often observed in the initial stages of sweating when sweat secretion is low, and the levels decrease as sweating becomes more profuse [32, 41–43].

Hormones such as cortisol, aldosterone, and epidermal growth factor are secreted into sweat at nanomolar to micromolar levels and reflect endocrine activity, psychological stress, and circadian rhythm [44]. Cortisol is gaining attention as a non-invasive stress biomarker due to its measurable correlation with serum levels and its implications in fatigue, depression, and metabolic syndromes [45]. Cortisol levels in human sweat generally range between about 8 to 142 ng/mL, which is slightly broader than the stated 5–30 ng/mL. These levels reflect circadian rhythms and stress responses, with variations by time of day, sweat rate, collection site, exercise, and hydration status. Some studies report average sweat cortisol concentrations around 20-70 ng/mL, with peaks up to 141.7 ng/mL post-exercise [44, 46–48]. This makes sweat cortisol a viable biomarker reflecting systemic cortisol fluctuations related to stress. These biochemical ranges underscore the complexity of sweat as an analytical matrix and highlight the need for wearable sensors to maintain high selectivity and stability across wide dynamic concentration spans. These low-abundance analytes require highly sensitive and selective sensor platforms with engineered surface chemistries to ensure accurate detection amidst interfering species.

In addition to small molecules, sweat contains a variety of proteins, peptides, and enzymes such as lysozyme, dermcidin, interleukins (e.g., IL-6), and lactate dehydrogenase. These constituents are associated with immune function, inflammation, and skin microbiome interaction [14]. Their presence may also contribute to biofouling on sensor surfaces and affect the long-term reliability and stability of biosensing membranes. The interplay between these macromolecules and sensor materials, especially two-dimensional (2D) materials like MXenes, requires detailed interfacial design to mitigate nonspecific adsorption and maintain sensor selectivity [49–51]. Moreover, the pH of sweat varies widely, typically between 4.5 and 7.5, depending on anatomical location, microbiota, and sweating rate [52, 53]. This variation in hydrogen ion concentration can affect the electrochemical behavior of redox-active materials, enzyme kinetics in bio-functionalized sensors, and the stability of surface terminations on MXenes, especially in hybrid structures. Similarly, sweat viscosity influence the diffusion and mass transport of analytes to the sensor surface, thereby affecting response time and analytical accuracy. Human sweat is a biochemically rich and dynamically fluctuating fluid, with its core components influencing multiple aspects of biosensor function from ion exchange and redox activity to signal stability and mechanical interface behavior.

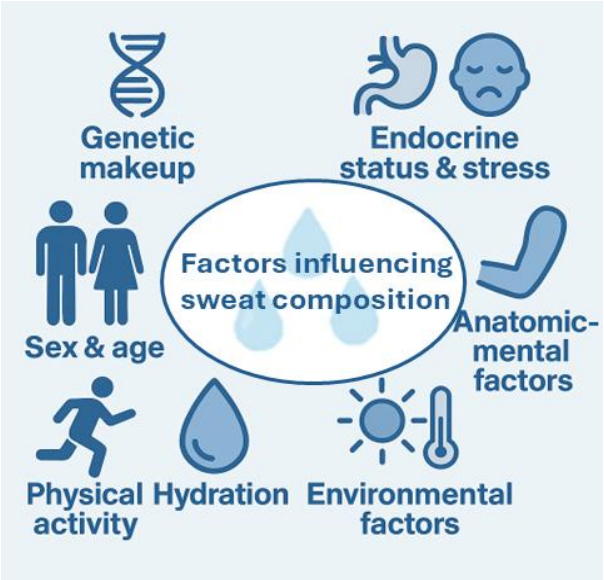

Figure 2. Generalized illustration of factors influencing sweat composition

Any material system intended for reliable sweat-based biosensing, such as MXenes, must be carefully engineered to operate across a broad range of concentrations, ionic environments, and biochemical contexts. Understanding these core components is thus essential as a foundation for the subsequent development of personalized, adaptive biosensing platforms.

2.2. Factors Influencing Sweat Composition

The biochemical composition of sweat is not static rather, it is shaped by a complex interplay of intrinsic and extrinsic factors that contribute to significant inter- and intra-individual variability (Fig. 2) [54, 55]. This variability poses a critical challenge to the standardization and calibration of wearable biosensors and necessitates sensor materials that are both adaptable and robust under fluctuating physiological and environmental conditions. Understanding the sources and mechanisms of this variability is crucial for the rational design of biosensors, particularly those based on surface-sensitive materials such as MXenes, whose electrochemical behavior is intimately linked to the local ionic and biochemical milieu.

One of the most prominent intrinsic factors influencing sweat composition is genetic makeup, which governs the baseline function of sweat glands, ion transport channels, and systemic metabolism. For instance, individuals with cystic fibrosis exhibit elevated concentrations of sodium and chloride in their sweat due to mutations in the CFTR (CF Transmembrane Conductance Regulator) gene, which impairs ion reabsorption in the sweat ducts [56, 57]. Similarly, polymorphisms in genes regulating glucose metabolism or hormone secretion can affect sweat glucose and cortisol levels, respectively. These genetic variations not only modulate analyte concentration ranges but also affect the baseline electrochemical profile encountered by the sensor. Sex and age also exert considerable influence. It has been observed that males typically produce sweat with higher sodium content compared to females, owing to differences in hormonal regulation and sweat gland density [13, 58]. Age-related changes affect both sweat rate and composition, with elderly individuals showing reduced sweating capacity, altered electrolyte balance, and diminished buffering capacity, which can shift pH profiles[59, 60]. These physiological variations have direct implications for biosensor design, particularly in relation to surface functionalization and enzyme stability in pH-sensitive detection systems. Hydration status is another major determinant of sweat composition. Hypohydration reduces overall sweat volume and increases the relative concentration of electrolytes and urea, thereby enhancing solution viscosity and ionic strength [13, 61–63]. This affects the diffusion kinetics and analyte transport to the sensor surface, influencing time-response characteristics and potentially leading to fouling or oversaturation of sensor interfaces. Conversely, hyperhydration dilutes analyte concentrations and may reduce sensitivity, necessitating dynamic calibration mechanisms in the sensing platform [61, 62]. Physical activity and thermal exposure not only increase sweat rate but also alter its chemical profile. During prolonged or high-intensity exercise, lactate concentrations rise significantly due to increased anaerobic metabolism, while sodium and chloride losses can reach levels that trigger heat-related illness if not properly replenished [64–66]. These high-flux sweating conditions result in a continuously changing biochemical environment, requiring sensors to remain functional under high ionic fluxes, mechanical deformation, and variable hydration layers, conditions under which the performance of some 2D materials can degrade unless properly stabilized. Endocrine status and stress levels modulate the secretion of hormones and low-molecular-weight analytes such as cortisol and adrenaline, which are now being targeted in sweat-based diagnostics for mental health, fatigue, and metabolic syndromes [67, 68]. Circadian rhythms add a temporal dimension to this variability, with certain analytes such as cortisol exhibiting peak levels in the early morning and declining throughout the day [69, 70].

Thus, sensors aiming to track these biomarkers must be not only chemically selective but also temporally responsive, with data processing frameworks that can integrate time-series trends. Anatomical location of sweat collection (whether forehead, back, forearm, or armpit) affects both sweat gland type and the local chemical environment [12, 14]. Eccrine glands, which are most commonly targeted in wearable biosensing, differ in density and activity across body regions, leading to site-dependent variations in analyte concentration and pH. Furthermore, interactions with skin microbiota and local epidermal enzymes can degrade or transform analytes post-secretion, affecting the reliability of on-skin biosensors [71, 72]. Moreover, external factors such as ambient temperature, humidity, and air flow conditions alter sweat rate and evaporation kinetics, modifying analyte accumulation on sensor surfaces [73, 74].

These environmental conditions are particularly relevant for long-term or outdoor deployments of wearable devices and must be considered during the materials selection and encapsulation design phases. These variations impact analyte availability, signal strength, sensor fouling, and long-term device performance. For MXene-based biosensors, whose sensing mechanism often relies on interfacial redox activity, ion transport, and surface charge interactions, this variability underscores the need for customizable material interfaces and context-aware calibration frameworks [75, 76]. Recognizing and addressing these influences is a foundational step in

moving from population-level biosensor designs to individual-specific diagnostic platforms.

2.3. Implications for Biosensor Calibration and Design

The dynamic and individualized composition of sweat has profound implications for the design, calibration, and functional reliability of wearable biosensors [20, 77–79]. Traditional biosensing platforms, including those employing MXene-based materials, are often validated using artificial sweat formulations with fixed pH, ionic strength, and analyte concentrations [20, 75, 76]. While these models are useful for baseline performance evaluation, they fail to capture the physiological diversity seen in real-world applications. As a result, wearable devices often exhibit signal drift, inconsistent sensitivity, or false-positive/negative readings when deployed on human skin across different users or under varying physiological states.

From a calibration standpoint, sensors that rely on electrochemical or potentiometric mechanisms are particularly susceptible to compositional fluctuations. For example, changes in sweat pH can significantly alter the protonation state of sensing interfaces, especially for materials with pH-sensitive functional groups. In the context of MXenes, whose surface terminations interact with ionic species, local pH can influence surface charge density, double-layer formation, and redox kinetics [80, 81]. These variations manifest as shifts in open-circuit potential, changes in charge transfer resistance (R_{ct}), or altered chronoamperometric response. All of them impact sensor's output unless properly accounted for in the calibration algorithm.

Ionic strength is another critical parameter. Variability in sodium, potassium, and chloride concentrations affects not only the conductivity of the sweat media but also the Debye screening length at the sensor interface, modulating the effective electrochemical sensing zone [82] . For materials like MXenes, where electron-ion coupling and interfacial capacitance play key roles in signal transduction, variations in ion concentration can attenuate or amplify signals unpredictably [75, 76, 83]. This poses a significant challenge for sensors that aim to provide quantitative outputs rather than binary thresholds, especially in the detection of low-abundance analytes such as cortisol or interleukins.

In addition, sweat flow rate and hydration state can affect both analyte concentration and transport dynamics [61, 62]. At high sweat rates, dilution of target molecules can reduce detection sensitivity, whereas low sweat rates may lead to local accumulation and sensor fouling [84, 85]. Moreover, proteinaceous components and enzymes present in sweat can non-specifically adsorb to the surface of 2D materials, including MXenes, potentially compromising active sites and degrading sensor selectivity over time. These challenges necessitate the use of anti-fouling coatings, hydrogels, or zwitterionic barriers that maintain sensor responsiveness in biofouling-prone environments [86–89].

The variability in analyte concentration ranges across individuals further complicates the issue. For instance, while sweat glucose levels may vary from 10 µM to 1 mM depending on the individual and metabolic condition, many sensors are optimized for narrow detection windows based on average population data. This mismatch can lead to overestimation or underdetection in users with atypical profiles, especially in cases such as prediabetes, dehydration, or stress-induced hyperglycemia [90, 91]. As such, biosensor materials must be engineered with broad dynamic range and high signal-to-noise ratios, while calibration algorithms must incorporate user-specific baselines or adaptive learning models [92–94].

These calibration complexities are further compounded in multi-analyte sensing platforms, where cross-sensitivity between ions (e.g., Na^+/K^+), metabolites (e.g., glucose/lactate), or redox species (e.g., uric acid (UA) /ascorbic acid (AA)) can interfere with signal discrimination [94–96]. The design of selective interfaces, such as MXene-based composites functionalized with molecular recognition elements (enzymes, aptamers, antibodies), becomes essential. However, these biorecognition strategies must also be robust against matrix effects imposed by inter-individual sweat composition, including changes in buffer capacity, ionic competition, and enzyme denaturation at non-physiological pH levels [75, 76, 97].

To address these challenges, emerging strategies include the integration of real-time feedback control, self-calibrating architectures, and data-driven adaptive signal processing into wearable biosensor systems. For MXene-based sensors, the ability to dynamically modulate sensing performance via electrical gating, chemical functionalization, or ML-guided recalibration presents a promising direction. In this framework, calibration is no longer a static, one-time event but a continuous, personalized process informed by both material behavior and real-time biochemical input.

In addition to the challenges posed by compositional variability, the analytical requirements for sweat biosensing must also be aligned with the physiological concentration ranges and temporal dynamics of each biomarker. Electrolytes such as sodium or potassium, which fluctuate on the order of tens of millimoles and exhibit rapid changes during thermoregulation or exercise, demand sensors with wide linear ranges, fast ion-exchange kinetics, and negligible drift under high-sweat-flux conditions. Metabolites including glucose and lactate require high sensitivity and µM–mM resolution, with

architectures capable of suppressing interference from coexisting species such as ascorbate, urea, and uric acid. Hormonal biomarkers such as cortisol, present at nM–pM levels, impose even stricter requirements on limit of detection, signal-to-noise ratio, and recognition selectivity, typically necessitating surface functionalization strategies or engineered MXene terminations that preferentially capture low-abundance targets. For macromolecular biomarkers such as cytokines or enzymes, antifouling interfaces and long-term surface stability become the dominant constraints. These biomarker-specific analytical profiles thus directly inform the choice of MXene composition, termination chemistry, hybrid structure, and polymer environment, enabling the rational matching of material properties to the sensing task. Such coupling between physiological context and material design is essential for future personalized sweat diagnostics and underpins the structure–performance discussions developed in the subsequent sections of this review.

3. MXenes as Sensing Materials: Structure–Property Relationships

3.1. MXene Fundamentals

MXenes, a rapidly expanding family of 2D transition metal carbides, nitrides, and carbonitrides, have emerged as highly versatile materials for a wide range of applications, including electrochemical energy storage, electromagnetic interference shielding, water purification, and more recently, biosensing [98, 99]. First reported in 2011 by Naguib et al., MXenes are typically synthesized by selectively etching the A layers from MAX phases—ternary carbides or nitrides with the general formula $M_{n+1}AX_n$ (n = 1–3), where M is an early transition metal, A is predominantly an element from groups 13–14 (with some reported examples from groups 15–16), and X is carbon and/or nitrogen [100, 101]. The resulting 2D structures have the general formula $M_{n+1}X_nT_x$, where T_x denotes surface terminations (–OH, –F, –O) introduced during the etching process [102, 103].

The intrinsic properties of MXenes such as their high electrical conductivity, large surface area, and hydrophilicity make them highly suitable for multifunctional platforms, including electrochemical biosensors, energy storage devices, and flexible or stretchable electronics [104–106]. In biosensing applications, these properties facilitate rapid electron transfer, strong analyte–surface interactions, and efficient integration with hydrogels, polymers, and microfluidic systems [100, 107].

The synthesis route has a profound impact on MXene physicochemical properties and, consequently, their biosensing performance [99, 107]. Conventional wet-chemical etching using hydrofluoric acid (HF) or in situ generated HF (e.g., LiF/HCl) removes the A-layer and introduces surface terminations that enhance hydrophilicity and compatibility with aqueous environments such as sweat. Alternative routes including molten-salt etching, electrochemical etching, and delamination strategies have been developed to improve yield, structural integrity, and environmental safety[99, 101]. A critical feature that makes MXenes especially attractive for wearable biosensors is their metal-like conductivity combined with solution processability, enabling fabrication into thin films, flexible membranes, and printable inks [17, 26, 108]. Their 2D layered structure also provides a high surface area and the possibility of intercalating ions or functional molecules between the layers, which is beneficial for electrochemical signal amplification [109]. Additionally, their tunable surface chemistry allows precise control over their interaction with target analytes, electrolytes, and biological molecules [17, 110]. The type and density of surface terminations (–OH, –F, –O) are particularly important in determining the zeta potential, electronic structure, and interfacial reactivity of MXenes [110, 111]. For example, $Ti_3C_2T_x$ with a dominant –OH termination behaves differently in terms of redox activity and hydration layer formation compared to one rich in –F terminations [110–112]. These structural features strongly influence MXene interactions with ions and biomolecules. Their specific implications for sweat biosensing are discussed in Section 3.2.

Although $Ti_3C_2T_x$ remains the predominant MXene employed in sweat biosensing owing to its high conductivity, hydrophilicity, well-established synthesis protocols, and abundant literature. On the other hand, recent studies have begun to explore alternative MXene compositions such as Nb_2C, Mo_2CT_x, and V_2CT_x. These emerging materials offer distinct surface terminations, redox behaviors, and stability profiles that may prove advantageous for specific sensing tasks. While the experimental evidence for these non-Ti MXenes is still limited compared to $Ti_3C_2T_x$, they have been explored in this review to provide a comprehensive and forward-looking perspective on the broader MXene family and their potential roles in next-generation sweat biosensors.

3.2. Relevant Properties of MXenes for Sweat Biosensing

Building on the structural and chemical fundamentals outlined in Section 3.1, this section discusses the specific MXene properties that directly influence performance in sweat biosensing applications.

In the context of sweat biosensing, these structural and surface features translate into application-specific functional advantages.

Understanding how these intrinsic and tunable properties influence sensor performance is essential for guiding the rational design of MXene-based platforms that can maintain stability and selectivity under physiological conditions. One of the most critical properties of MXenes is their high intrinsic electrical conductivity, which enables efficient electron transfer and low interfacial resistance when used as transducing elements in electrochemical sensors [83, 113]. The high conductivity of MXenes ensures efficient charge transfer during amperometric or voltammetric measurements, which is crucial when detecting weak redox-active biomarkers such as dopamine, uric acid, or cortisol in low concentrations. For instance, $Ti_3C_2T_x$ films exhibit high electrical conductivity values comparable to or even surpassing conventional carbon-based nanomaterials like graphene or carbon nanotubes under certain conditions [114]. This property supports sensitive amperometric and potentiometric measurements, even in miniaturized or low-power formats. Conductivity in MXenes is strongly influenced by flake size, interlayer spacing, and the density of surface terminations [115], all of which can be tuned via the synthesis route and post-processing conditions such as annealing or solvent treatment [109, 116]. The layered morphology and adjustable interlayer spacing facilitate efficient diffusion of Na^+, K^+, Cl^-, lactate, and other sweat-relevant ions, supporting low-noise electrochemical readout under variable hydration conditions.

Equally important for sweat biosensing is hydrophilicity, which enables effective ion and molecule exchange at the material–biofluid interface. Hydrophilicity promotes rapid sweat wetting and stable skin–sensor adhesion, enabling continuous ion transport and minimizing contact impedance. Unlike many other 2D materials that require surface modification to become hydrophilic, MXenes possess native surface functional groups that render them inherently wettable [117]. This feature enhances the accessibility of target analytes such as glucose, lactate, and electrolytes to electroactive or recognition sites on the material surface. Moreover, hydrophilicity contributes to rapid analyte diffusion and uniform sweat spreading across the sensor area, improving the temporal resolution and reliability of the signal.

The surface chemistry of MXenes, dictated by their terminations and defect sites, plays a central role in determining their interaction with both ionic and molecular species [25, 110, 117]. These terminations affect the material's redox potential, point of zero charge, and overall chemical reactivity. For instance, surface –OH groups participate in hydrogen bonding with polar analytes, while –F groups may reduce electrochemical activity and hinder enzymatic integration [24, 110]. For example, the abundance and tunability of –OH, –O, and –F terminations modulate MXene surface charge and interfacial redox behavior, directly influencing sensitivity to pH, electrolytes, and charged metabolites naturally present in sweat. Importantly, the surface termination profile of MXenes governs multiple sweat-relevant sensing behaviors through well-defined structure–property couplings. For example, hydroxyl-rich $Ti_3C_2T_x$ exhibits higher hydrophilicity, stronger hydrogen bonding interactions, and faster electron–ion coupling compared to fluorine-terminated analogues, which translates into improved sensitivity for metabolites such as glucose [118, 119].

In contrast, –F terminations increase interlayer repulsion and suppress faradaic activity, often reducing redox response and selectivity [120, 121]. The M-site chemistry also plays a decisive role. For instance, early transition metals with higher d-electron density (e.g., Nb_2C, Mo_2C) show accelerated charge transfer and stronger affinity for cationic species, making them promising for electrolyte and hormone sensing [122, 123]. Engineering the termination profile can modulate properties such as binding affinity, pH sensitivity, and enzyme compatibility, which are critical for biosensors targeting diverse sweat biomarkers.

Additionally, MXenes can be functionalized with enzymes, antibodies, aptamers, or redox mediators to impart specific recognition capabilities, while still maintaining a high electron-transfer rate due to their conductive backbone [124, 125].

MXenes exhibit ion permeability and pseudocapacitive behavior, both of which are advantageous in biosensing applications that rely on capacitive or impedance-based readouts [75, 83, 110]. The lamellar structure of MXenes supports interlayer diffusion of hydrated ions [126], allowing dynamic changes in dielectric properties in response to fluctuating ionic strength in sweat. This is particularly useful for sensing electrolytes such as Na^+ and K^+, whose concentration directly influences ionic conductivity, dielectric constant, and electrochemical impedance spectra. These properties also enable the development of multiplexed sensors where different ions or metabolites can be simultaneously monitored through changes in frequency-dependent electrical response [127].

Another dimension of relevance is mechanical adaptability. For skin-mounted or wearable devices, sensor materials must accommodate repeated mechanical deformation, such as stretching, bending, and compression [3, 17]. MXenes, particularly when processed into composite films with polymers or hydrogels, demonstrate excellent mechanical resilience and flexibility without significant loss of conductivity or sensing performance [76, 97, 107].

This enables continuous operation under physical strain typical of real-life wearables, ensuring that signal output remains reliable over prolonged use.

3.3. Mechanical and Electrochemical Stability in Sweat-like Conditions

The long-term operation of wearable biosensors in real-life environments demands sensing materials that are both mechanically robust and electrochemically stable under dynamic, moisture-rich, and chemically complex conditions. MXenes, particularly $Ti_3C_2T_x$, but increasingly also Nb_2CT_x, V_2CT_x, and Mo_2CT_x, are attractive candidates due to their high conductivity, solution processability, and surface chemistry, yet their use in wearable formats necessitates deliberate strategies to address their inherent structural fragility and susceptibility to oxidation [26, 100, 101]. Mechanical behavior is intimately tied to MXene flake size, layer stacking order, and interfacial bonding within composites. Larger lateral flakes improve percolation pathways and conductivity stability under strain, whereas small or defective flakes are more prone to crack propagation and delamination during repeated deformation [128, 129]. Likewise, expanded interlayer spacing, which can be achieved via intercalants, polymer chains, or heteroatom doping, improves stretchability and reduces conductivity loss at high perspiration levels [130, 131]. These structure–property correlations are critical for designing MXene architectures that preserve signal fidelity during dynamic on-body operation. Mechanically, single- and few-layer MXene films exhibit flexibility suitable for integration onto soft substrates but are prone to microcracking and delamination under continuous strain, particularly when used as standalone layers [125, 132]. To overcome this limitation, recent research has focused on hybrid and composite architectures in which MXenes are embedded into stretchable matrices [133, 134]. For instance, Pu *et al.* (2019) developed a multilayered fiber-based sensor by sequentially coating silver nanowire and MXene layers onto a hydrophilic polyurethane substrate via a simple dip-coating process. The composite architecture mitigated crack propagation under deformation, enabling a gauge factor exceeding 100 within a 0–100% strain range, and demonstrated seamless integration into wearable textiles for real-time motion detection [135]. Similarly, Seyedin *et al.* (2020) utilized wet-spinning to fabricate highly conductive MXene/polyurethane fibers with strain endurance up to ~152% and a gauge factor approaching 13,000, demonstrating scalability and suitability for wearable strain-sensing systems [136].

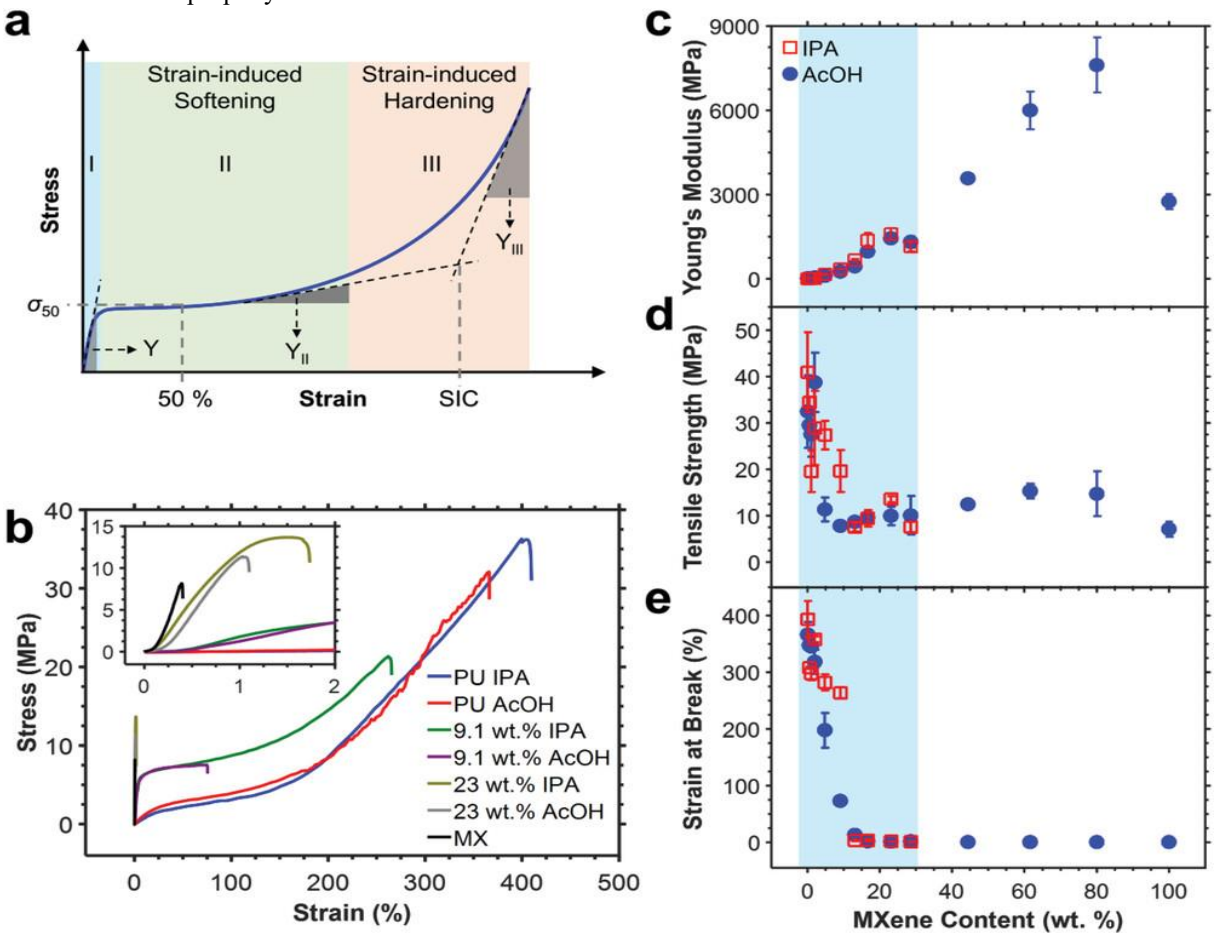

Figure 3. Mechanical behavior of MXene/polyurethane composites as a function of MXene content and solvent processing. (a) Schematic stress–strain curve illustrating softening and strain-induced crystallization regions. (b) Representative stress–strain curves for composites prepared with isopropanol (IPA) and acetic acid (AcOH) at different MXene loadings. (c–e) Variation of Young's modulus, tensile strength, and strain at break with MXene content, highlighting the trade-off between mechanical robustness and filler concentration. Reproduced with permission from [136] © 2020 WILEY-VCH Verlag GmbH & Co. KGaA, Weinheim

Fig. 3 further highlights how MXene loading and solvent processing influence the mechanical performance of MXene/polyurethane composites. As shown in Fig. 3b, increasing MXene content initially enhances the mechanical strength and stretchability, particularly under acetic acid processing conditions. However, beyond a critical MXene concentration, the composite becomes brittle, as reflected in the dramatic decrease in strain at break (Fig. 3e) and tensile strength (Fig. 3d) [136]. This confirms the importance of controlled MXene integration within flexible matrices to preserve both conductivity and mechanical resilience under strain.

In a similar way, a recent study introduced a multidimensional nanocomposite yarn combining silver nanoparticles, silver nanowires, and MXene nanosheets, fabricated through a dip-coating approach [137]. The hierarchical 0D–1D–2D configuration enabled the yarn to achieve good strain sensitivity over a broad strain range of up to 350%. Beyond sensing applications, the composite yarns also functioned as electrically responsive heating elements when woven into fabrics, broadening their utility in smart textile systems [137].

Beyond polymer composites, intercalation or hybridization with conductive nanomaterials such as carbon nanotubes, graphene, or silver nanowires has proven effective in enhancing the mechanical integrity of MXene-based electrodes. These hybrid structures maintain high conductivity while distributing mechanical stress across the network, reducing crack propagation. In one example, MXene was combined with carbon nanotubes to form an interwoven percolation network that synergistically leverages the conductivity of 2D MXene sheets and the flexibility of 1D CNTs [138].

This hybrid design enabled ultrathin, highly stretchable strain sensors capable of detecting minute deformations (as low as 0.1% strain) while maintaining sensitivity over a broad range. The integration of dimensional heterogeneity not only enhanced mechanical durability under repeated strain but also ensured stable electrical performance across thousands of cycles. These results reveal its applicability in wearable systems for continuous physiological monitoring [138].

A layered composite structure integrating $Ti_3C_2T_x$ MXene with graphene and PDMS has been shown to provide both high sensitivity and mechanical adaptability under strain [139]. Upon stretching, the structure separates into a brittle MXene-rich upper layer and a resilient graphene/PDMS foundation, enabling a dynamic balance between conductive pathway disruption and preservation. This architecture delivers stable and tunable sensitivity across a wide deformation range, with excellent linearity and durability, making it ideal for precise motion tracking in applications such as respiratory monitoring [139]. Electrochemical stability is equally critical, particularly in wearable applications involving prolonged exposure to sweat, which contains chloride ions, proteins, and fluctuating pH that accelerate oxidative degradation of MXene flakes. Electrochemical stability is also strongly structure dependent. MXenes with higher oxygen termination density form more stable Ti–O networks that resist chloride-induced oxidation, whereas fluorinated surfaces degrade more rapidly in sweaty, acidic, or high-ionic-strength environments.

Similarly, multilayer MXenes oxidize from their edges inward, while delaminated single layer nanosheets exhibit faster but more uniform degradation. These trends highlight the need for termination control, protective polymer coatings, and composite encapsulation to preserve MXene activity under real-sweat exposure. Surface oxidation disrupts interlayer conductivity and impairs redox performance, especially for sensors relying on faradaic charge transfer or interfacial capacitance. To counteract this, surface passivation techniques have been employed. For instance, to enhance electrochemical resilience in sweat-exposed environments, a recent study by Chen *et al.* (2022) utilized fluoroalkyl silane-functionalized MXene integrated with a polyaniline (PANI) membrane to fabricate a flexible sweat pH sensor. The fluorinated surface treatment significantly improved MXene's environmental stability by mitigating oxidative degradation, while the PANI layer provided enhanced electrochemical response and reversibility. The resulting miniaturized sensor exhibited long-term operational stability and accurate real-time pH monitoring during physical activity, illustrating the effectiveness of surface passivation strategies in preserving MXene performance in biofluids [140].

Another approach to improving electrochemical stability in wearable sensing applications involved directly employing $Ti_3C_2T_x$ MXene as the active layer in a potentiometric pH sensor [80]. By comparing MXene etched via LiF/HCl and HF routes, Liang *et al.* (2023) demonstrated that deeper HF etching produced a more responsive and reversible pH-sensitive material. The resulting flexible sensor, combined with a solid-contact Ag/AgCl electrode, delivered reliable real-time sweat pH readings, maintaining consistent performance in physiological conditions. This highlights the role of controlled etching and structural refinement in optimizing MXene's stability and sensing efficiency in chloride-rich environments like human sweat [80].

In addition to surface modifications, encapsulation within hydrogel or polymeric membranes has been used to protect MXene films while maintaining their ionic permeability [141].

The choice of encapsulant not only affects chemical protection but also contributes to mechanical damping, further enhancing operational durability. Encapsulated

systems have demonstrated multi-day stability under physiological conditions, a key metric for real-time, on-body biosensing [142]. For instance, MXene-integrated chitosan–hyaluronate hydrogels have shown both reduced porosity and strong antimicrobial activity, providing a protective yet functional microenvironment for biointerfaces. Complementing this, electrospun chitosan nanofibers loaded with delaminated $Ti_3C_2T_x$ flakes have exhibited significant antibacterial efficacy by achieving up to 95% reduction in *E. coli* and 62% in *S. aureus*[143]. These nanofibrous mats offer a dual advantage of barrier protection and passive antimicrobial action, reinforcing the potential of MXene–polymer encapsulation systems for extended use in wearable biosensing and wound healing applications. In another work, a hydrogel composite system incorporating $Ti_3C_2T_x$ MXene into a chitosan–hyaluronate matrix demonstrated the potential of polymeric encapsulation to enhance stability and functionality of MXene-based materials [144].

The hydrogel maintained structural integrity while supporting ionic permeability and offering antibacterial protection, even with low MXene loading (1–5 wt.%). Additionally, the reduced porosity of the matrix, stabilized with vitamin C, contributed to a more uniform microstructure, positioning such encapsulated designs as promising candidates for extended on-body use, such as in biosensing or wound monitoring applications [144].

The introduction of heteroatoms or secondary terminations during synthesis may also provide protective effects or improved compatibility with sweat components [26, 145]. For example, co-doping Nb_2C MXene with nitrogen and sulfur via a one-step thiourea-assisted treatment has been shown to significantly enhance its electrochemical properties [146]. This heteroatom incorporation not only expands interlayer spacing and increases surface area but also enriches the material with additional active sites and improved conductivity.

As demonstrated in acidic environments such as simulated gastric juice, the doped MXene displayed superior sensitivity, selectivity, and long-term stability during dopamine (DA) detection [146]. Compared to multilayered and delaminated Nb_2C, the co-doped structure exhibits markedly superior redox activity, highlighting the effectiveness of heteroatom engineering in preserving MXene performance under physiologically challenging conditions [146]. Such strategies offer promising avenues for extending the functional lifespan of MXene-based biosensors exposed to chloride-rich biofluids like sweat.

3.4. Surface Functionalization Strategies

Recent efforts toward integrating these advanced materials into textile-based platforms and epidermal electronics have reinforced the importance of addressing these stability concerns holistically [147]. By leveraging multiple stabilization strategies such as layered heterostructures, redox-inert coatings, and dynamic self-healing polymers MXene-based biosensors are increasingly able to meet the stringent demands of wearable healthcare, operating reliably in real-world environments while maintaining sensitivity to trace-level biomarkers in sweat [117]. Recent advancements have focused on various strategies to functionalize MXenes, tailoring their surface chemistry to meet the demands of biosensing applications [25, 110, 117].One prominent approach involves the covalent attachment of biomolecules to MXene surfaces. Lee *et al.* (2021) demonstrated a surface functionalization strategy where polyethylene glycol carboxylic acid (PEG_6-COOH) was covalently grafted onto $Ti_3C_2T_x$ MXene via esterification [148]. This modification significantly improved dispersibility in nonpolar organic solvents while preserving the structural integrity and electrical conductivity of the flakes. The engineered PEG-functionalized MXenes formed well-ordered microstructures and conductive thin films (~16,200 $S \cdot cm^{-1}$), and the approach also enabled tunable surface valency through the incorporation of ω-functionalized PEG ligands (e.g., $-NH_2$, $-N_3$). These findings highlight the potential of controlled covalent modification for enhancing MXene processability and expanding their functional versatility in bioelectronic applications [148]. In a related study, MXene flakes were covalently functionalized with first-generation poly(amidoamine) (PAMAM) dendrimers to form a stable hybrid structure (MXene@PAMAM) that effectively mitigated restacking and anodic oxidation [149]. This modification preserved MXene's conductivity while introducing a three-dimensional (3D) architecture with high surface area and abundant functional groups. The amino-rich PAMAM layer served both as a structural stabilizer and as an anchoring matrix for gold nanoparticles (AuNPs), enabling the construction of a highly sensitive immunosensor for cardiac troponin-T detection. The resulting biosensor achieved a wide detection range with excellent sensitivity and long-term signal retention, underscoring the potential of covalent biomolecular grafting strategies to enhance the electrochemical performance and stability of MXene-based devices [149]. Fig. 4 illustrates the enhanced electrochemical performance of the AuNPs/MXene@PAMAM hybrid sensor. As shown by cyclic voltammetry (Fig. 4a–c), the composite electrode exhibits superior redox stability and significantly improved signal retention across repeated cycles. The impedance analysis (Fig. 4d) and peak current measurements (Fig. 4e, f) further confirm that the hierarchical architecture reduces charge transfer resistance and enhances electron transfer kinetics, contributing to a >5-fold increase in current response compared to bare electrodes [149].

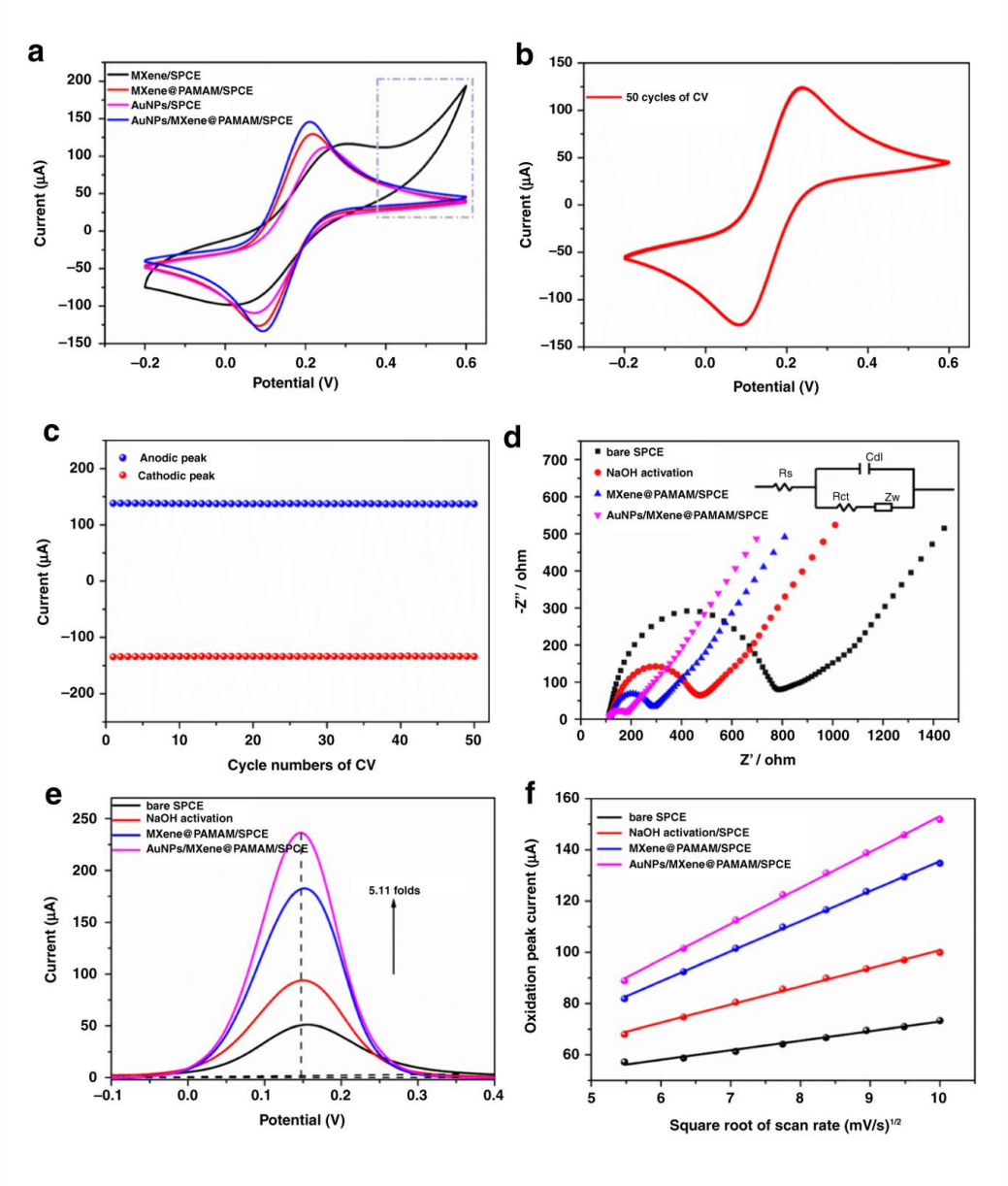

Figure 4. Electrochemical characterization of AuNPs/MXene@PAMAM-modified SPCE for enhanced biosensing performance. Reproduced from [149] under the Creative Commons Attribution (CC-BY) 4.0 license

Non-covalent functionalization methods have also been explored to preserve the intrinsic properties of MXenes. These include π–π stacking interactions, hydrogen bonding, and electrostatic interactions with polymers or biomolecules, facilitating the immobilization of enzymes or aptamers without compromising MXene conductivity. Such strategies have been employed to develop sensors with enhanced sensitivity and selectivity for various analytes. Thurakkal *et al.* (2022) demonstrated a non-covalent functionalization approach where $Ti_3C_2T_x$ MXene was stabilized using cationic porphyrins through electrostatic interactions. The Fig. 5. illustrates the synthesis of delaminated $Ti_3C_2T_x$ MXene via LiF/HCl etching followed by electrostatic interaction with positively charged porphyrins, forming stable MXene–porphyrin hybrids through non-covalent assembly [150]. This strategy effectively suppressed oxidation in aqueous environments while preserving the structural integrity and electronic characteristics of MXene. The resulting hybrids exhibited strong energy/electron transfer behavior and pH-responsive porphyrin release, showcasing the potential of non-covalent modification in enhancing both stability and functional versatility of MXenes for biosensing and biomedical applications [150].

Composite formation is another strategy wherein MXenes are combined with other nanomaterials to synergistically improve sensor performance. For example, integrating MXenes with gold nanoparticles or graphene has been shown to amplify redox signals and enhance electron transfer rates, thereby increasing the sensitivity of electrochemical biosensors. For instance, Fan *et al.* (2024) developed a highly sensitive DNA biosensor by integrating amino-functionalized $Ti_3C_2T_x$ MXene with AuNPs, forming a $Ti_3C_2NH_2$ MXene@Au composite.

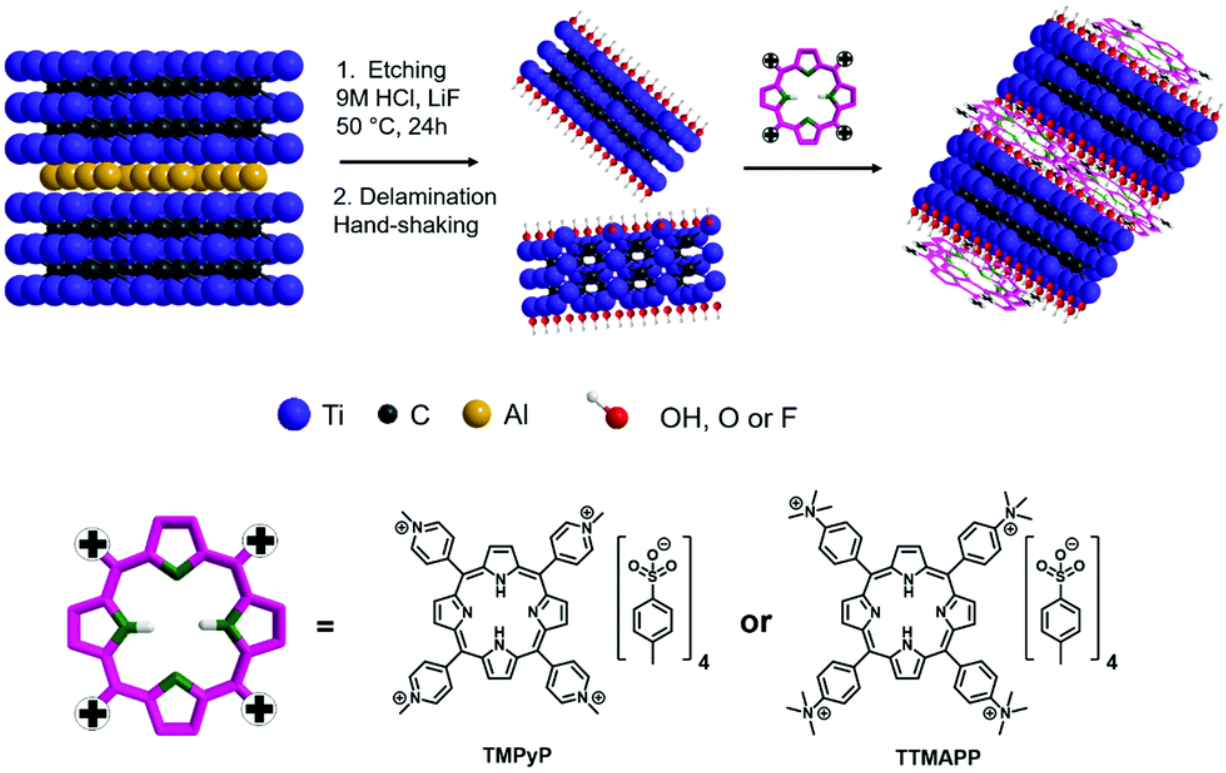

Figure 5. Schematic representation of non-covalent functionalization of $Ti_3C_2T_x$ MXene. Reprinted from [150] under a Creative Commons Attribution-NonCommercial 3.0 Unported License

By tuning the amino group content during exfoliation, they precisely controlled the AuNP density via Au–N interactions, thereby optimizing probe DNA immobilization[151] performance.

The resulting nanocomposite sensor exhibited exceptional sensitivity and selectivity for HBV-DNA, achieving detection down to 1.05×10^{-14} M across a wide dynamic range, even in artificial serum [151]. This work highlights how compositing MXenes with AuNPs can synergistically enhance redox activity and electron transfer efficiency in electrochemical biosensors In other work, Mao *et al.* (2024) proposed a hybrid photonic crystal fiber biosensor integrating gold, graphene, and $Ti_3C_2T_x$ MXene as a multilayered surface plasmon resonance structure for cancer cell detection. This composite configuration, modeled using finite element analysis, leveraged the synergistic optical properties of the three materials to achieve ultra-high sensitivity reaching up to 9286 nm/RIU for MCF-7 breast cancer cells [152]. The strategic manipulation of cladding geometry and material layering significantly enhanced SPP coupling, enabling label-free, cost-effective cancer diagnostics with remarkable specificity [152]. This study exemplifies how MXene-based hybrid composites can be tailored for advanced photonic biosensing platforms. A recent study by Saraswathi *et al.* (2024) introduced enzyme-free, disposable glucose sensors based on 2D $Ti_3C_2T_x$ MXene-modified screen-printed gold electrodes, optimized for non-invasive sweat analysis. By tailoring surface terminations through direct and in-situ etching strategies, the researchers achieved controlled surface chemistry, which significantly influenced the electrocatalytic.

Among the variants, LiF/HCl-etched MXene exhibited the highest sensitivity (569.70 μA mM^{-1} cm^{-2}) and a remarkably low detection limit of 5 nM. The sensor enabled accurate glucose detection in natural sweat samples without requiring dopants or enzymatic layers, highlighting the potential of pristine MXene-modified electrodes as practical, cost-effective tools for wearable glucose monitoring platforms [153]. Chen *et al.* (2024) developed a 3D electrochemical glucose sensor using a porous aerogel composed of $Ti_3C_2T_x$ MXene and reduced graphene oxide, aimed at continuous and noninvasive sweat glucose monitoring. The 3D architecture significantly enhanced electron transfer efficiency by minimizing the distance between the redox center of the immobilized enzyme and the electrode surface, while also ensuring stable enzyme retention [154]. A key innovation was the integration of a real-time adaptive calibration system that simultaneously accounts for pH fluctuations in sweat, enabling dynamic and accurate glucose sensing during physical activity. This work underscores the potential of multifunctional MXene-based composites for next-generation personalized health monitoring platforms [154]. Dai *et al.* (2017) reported the development of multifunctional tantalum carbide (Ta_4C_3) MXene-based nanosheets engineered for imaging-guided photothermal cancer therapy. By leveraging the reductive nature of the MXene surface, manganese oxide (MnOx) nanoparticles were grown *in-situ,* creating MnOx/Ta_4C_3 composites with

synergistic functionalities. The Ta component provided strong X-ray attenuation for enhanced CT imaging, while MnOx contributed pH-responsive contrast in T1-weighted MRI. In addition, the composite exhibited efficient photothermal conversion for photoacoustic imaging and effective tumor ablation through localized hyperthermia. This study exemplifies how rational composition tuning and surface functionalization of MXenes can expand their role in noninvasive, multimodal cancer theragnostic [155]. Furthermore, surface passivation techniques have been employed to mitigate the oxidation of MXenes in aqueous environments. Coating MXene surfaces with biocompatible polymers such as chitosan or polyethylene glycol not only enhances their stability but also provides functional groups for further bioconjugation, extending the operational lifespan of wearable sensors. Yin *et al.* (2025) developed a high-performance non-invasive electrochemical glucose sensor by integrating MXene with nickel–cobalt layered double hydroxide (NiCo-LDH) and subsequently coating the composite with chitosan. The MXene component provided excellent conductivity and a large active surface area, while NiCo-LDH enhanced catalytic activity for glucose oxidation. Critically, the chitosan layer served as a biocompatible passivation coating, improving structural integrity and sensor stability in complex media such as saliva. The incorporation of NiCo-LDH and chitosan onto MXene-modified electrodes significantly improves redox activity and reduces R_{ct}. The scan rate-dependent measurements confirm the sensor's excellent linearity and fast electron transfer kinetics, demonstrating its high sensitivity and stability for glucose detection. The resulting sensor exhibited excellent sensitivity (154.05 μA mM^{-1} cm^{-2}), a wide linear range, and a low detection limit, underscoring the effectiveness of polymer coatings like chitosan in extending sensor lifespan and ensuring biocompatibility in wearable monitoring systems [156]. In a similar manner, Pan *et al.* (2024) developed a wearable electrochemical biosensor by integrating $Ti_3C_2T_x$ MXene with a biocompatible poly(3,4-ethylenedioxythiophene)polystyrenesulfonate (PEDOT:PSS) based conductive hydrogel for continuous, noninvasive glucose monitoring in sweat. MXene and glucose oxidase (GOx) were mixed into a PEDOT:PSS hydrogel matrix, forming a flexible electrochemical patch capable of noninvasive glucose detection in sweat during physical activity [157]. Ethylene glycol was introduced during synthesis to enhance polymer chain mobility, resulting in improved film formation, flexibility, and electrical conductivity. This structural optimization also addressed material agglomeration and delamination, enhancing sensor stability. The device exhibited a low detection limit of 1.9 μM and a sensitivity of 21.7 $\mu A \cdot mM^{-1} \cdot cm^{-2}$. When applied on human skin using screen-printed carbon electrodes, the hydrogel patch demonstrated strong agreement with conventional glucose meters, confirming its potential for real-time wearable diabetes management [157].

Emerging strategies also include the development of porous MXene structures to increase the surface area available for biomolecule immobilization, thereby improving the sensitivity and response time of biosensors. These porous architectures facilitate efficient mass transport and rapid analyte diffusion, which are critical for real-time monitoring applications [158, 159]. These surface functionalization strategies are pivotal in harnessing the full potential of MXenes for wearable biosensing applications, enabling the development of devices that are not only sensitive and selective but also robust and adaptable to the complex environment of human sweat [160, 161].

3.5. Integration of MXenes into Wearable Biosensing Platforms

The transition from laboratory-based electrochemical measurements to real-time, on-body monitoring requires sensor materials that are not only functionally superior at the molecular level but also compatible with scalable fabrication techniques and flexible device architectures [162]. Among the most widely adopted integration methods is the fabrication of thin, flexible MXene films via vacuum-assisted filtration or drop-casting, followed by transfer onto stretchable elastomeric substrates such as PDMS or Ecoflex [163].

These platforms enable conformal contact with skin and preserve signal fidelity under motion-induced deformation. For example, in a recent study, Zahed *et al.* (2023) demonstrated a fully integrated, flexible patch system combining microfluidic glucose sensing and dry electrophysiological monitoring using scalable, skin-conformal fabrication strategies. Their device employed laser-patterned MXene–PVDF-derived carbon nanofiber electrodes and reduced graphene oxide-based glucose sensors, achieving reliable signal acquisition even under physical movement.

This platform maintained the sensitivity during bending and enabled real-time adjustment based on dynamic sweat pH and temperature, underscoring the role of MXene-derived materials in multimodal, miniaturized biosensing platforms tailored for continuous on-body monitoring [164]. Beyond simple film-based configurations, MXenes have also been incorporated into stretchable hydrogels, which provide a dual advantage of mechanical softness and ionic permeability, both desirable for interfacing with human skin and sweat glands.

In a recent report, Wang *et al.* (2020) introduced a rapid self-assembly method to fabricate $Ti_3C_2T_x$ MXene-based poly(acrylic acid) (PAA) hydrogels with exceptional

conductivity and stretchability (~1400%), specifically designed to overcome nanosheet restacking. By inducing in-situ TiO_2 nanoparticle growth on MXene surfaces, the strategy not only prevented aggregation but also enabled ultrafast polymerization without external heating. The resulting hydrogels exhibited tunable mechanical and ionic properties, making them highly suitable for wearable bioelectronics and skin-interfacing applications where both softness and signal permeability are essential [165]. Gong *et al. (2023)* developed a novel MXene nanochannel hydrogel by embedding $Ti_3C_2T_x$ within the aligned microstructure of electrospun fiber textiles, forming a neuron-like, interconnected conductive network (Fig. 6A) [166].

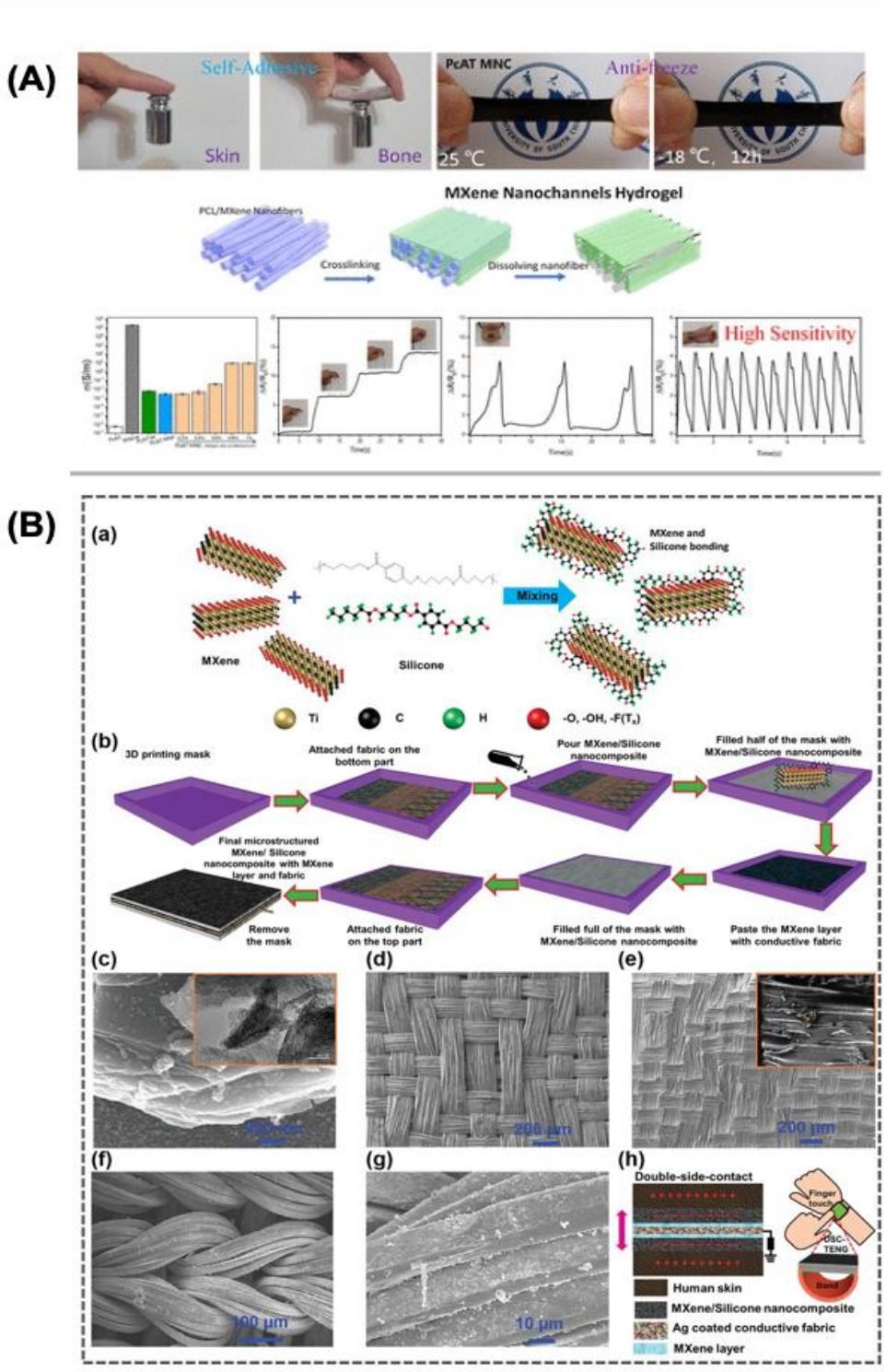

Figure 6. Representative MXene–hybrid architectures for flexible wearable sensing. **(A)** MXene nanofiber–reinforced hydrogel exhibiting strong self-adhesion to skin and bone, antifreezing capability, and high mechanical sensitivity enabled by aligned nanofiber channels. Reprinted with permission from [166] Copyright © 2023, American Chemical Society (**B)** Microstructured MXene–silicone nanocomposite fabricated via 3D-masked casting and integrated with conductive fabrics for double-sided skin contact and robust physiological signal monitoring
Reprinted with permission from [167] © 2021 Wiley-VCH GmbH

10.57647/jnsc.2026.1601.05

Unlike conventional MXene-filled hydrogels, this architecture provided greater mobility and alignment of the nanosheets, significantly enhancing conductivity, mechanical resilience, and sensitivity. As can be seen from Fig. 6A, the resulting hydrogel exhibited self-adhesion, antifreezing capability, and excellent performance in detecting subtle physiological signals such as pulse, highlighting its potential for next-generation flexible and wearable biosensing applications [166].

In pursuit of fully integrated, wearable systems, screen printing and inkjet printing of MXene-based inks onto flexible substrates have gained momentum. These techniques allow scalable, low-cost patterning of sensor electrodes and interconnects. These techniques offer scalable and cost-effective patterning for sensor electrodes and interconnects, advancing the manufacturability of next-generation wearables. Yi *et al.* (2021) demonstrated a self-powered, fully integrated wearable platform using 3D-printed MXene-based inks coupled with stretchable SEBS substrates. The system included a triboelectric nanogenerator (TENG), high-sensitivity pressure sensors, and near-field communication modules, enabling continuous and wireless monitoring of physiological signals such as radial artery pulse—without the need for external power. In this multifunctional platform, MXene ink is 3D-printed into sensing components and energy harvesters, enabling self-charging from biomechanical energy and seamless data transmission to mobile devices. This approach exemplifies the role of printed MXene technology in realizing autonomous, skin-interfacing biosensor systems [168].

Textile-based MXene integration is an emerging area of interest, as it enables biosensors to be embedded directly into garments for large-area, non-invasive sensing. Dip-coating or spraying of MXene suspensions onto conductive textile fibers, followed by functionalization with selective biorecognition layers, has yielded promising results for on-cloth sensing of sweat analytes. In a recent demonstration, Wang *et al.* (2021) developed a superhydrophobic, wearable textile sensor by assembling 2D $Ti_3C_2T_x$ MXene nanosheets and zero-dimensional (0D) silicon nanoparticles (SiNPs) onto cotton fibers, forming a hierarchically structured MX@SiNPs cotton composite [169]. This hybrid textile platform exhibited exceptional multi-mode sensing capabilities with high sensitivity (up to 12.23 kPa^{-1}) and long-term durability, even under wet or corrosive environments. The low surface energy of the SiNP coating preserved MXene's conductivity while improving wash resistance, showcasing the feasibility of integrating MXenes into fabric-based substrates for scalable, flexible, and waterproof biosensing applications[169]. Interfacing MXene sensors with readout electronics and data communication modules is essential for developing complete wearable systems[168, 170]. Integration with flexible printed circuit boards, Bluetooth low-energy modules, and smartphone apps has enabled real-time visualization and data logging in multiple studies. Furthermore, some research efforts have explored energy-autonomous systems, where MXene sensors are paired with triboelectric or thermoelectric energy harvesters to support continuous monitoring without external batteries, a key step toward sustainable, untethered bioelectronic devices.

In a study by Salauddin *et al* (2022), a fabric-assisted micropatterning strategy was developed to engineer hierarchical surface microstructures on MXene/silicone nanocomposites (Fig. 6B) [167]. This approach enabled controlled alignment and confinement of MXene flakes within the silicone matrix, significantly enhancing interfacial charge generation and trapping without requiring high-temperature processing or complex lithography.

The resulting double-side-contact TENG demonstrated nearly a 10-fold increase in output voltage and more than a 20-fold enhancement in current density compared with unstructured silicone counterparts. Beyond energy harvesting, the system reliably powered wearable electronics and enabled real-time motion sensing and wireless interfacing, illustrating a scalable pathway toward battery-free MXene-based platforms for continuous physiological and biomechanical monitoring [167].The compatibility of MXenes with both solution-based processing and dry-transfer techniques offers design freedom across multiple device form factors. Whether integrated into soft patches, textile bands, or even tattoo-like epidermal electronics, MXenes provide a robust platform for the translation of high-performance materials into clinically and commercially viable biosensing solutions.

The ongoing refinement of printing methods, device encapsulation, and biorecognition layer integration continues to expand the capabilities of MXene-based systems for real-time health monitoring.

4. Advanced-Material Engineering Strategies Toward Personalization

4.1. MXene–Polymer Composites for Adaptive Interface Engineering

The integration of MXenes into wearable biosensors offers compelling opportunities for high-fidelity biochemical monitoring. However, the effective interfacing of these 2D materials with soft, dynamically changing biological surfaces such as human skin presents significant engineering challenges.

To bridge this mechanical and biochemical mismatch, MXene–polymer composites have emerged as a powerful

platform for building adaptive sensing interfaces that are not only structurally compliant and stretchable, but also capable of tuning their interfacial properties in response to user-specific sweat compositions. The interfacial structure of MXene–polymer composites directly dictates the analyte transport and charge-transfer behavior in sweat sensing. Uniformly dispersed MXene nanosheets establish continuous electron-conduction networks, while polymer-swelling kinetics regulate ion diffusion from sweat into these networks. Highly crosslinked polymers provide mechanical robustness but restrict ion transport, whereas loosely crosslinked or hydrophilic matrices enhance sensitivity at the cost of slower recovery times. These tunable couplings between microstructure, hydration behavior, and electron/ion mobility form a rational framework for future MXene composite design.

In wearable sweat biosensors, sensor interfaces must endure not only cyclic mechanical deformation from bodily movement but also variations in hydration, temperature, salt concentration, and surface chemistry arising from inter-individual and intra-individual sweat variability. The polymer matrix in MXene–polymer composites acts as a dynamic medium that can be engineered to respond intelligently to these changes, modulating analyte diffusion, ion exchange rates, and even surface charge distribution [171, 172]. This creates a feedback-competent interface where sensor performance can be dynamically matched to the user's biochemical environment.

A key functional parameter is swelling behavior the ability of the composite to absorb water and expand, thereby altering internal porosity, ionic diffusivity, and interfacial contact area. Hydrophilic polymers such as polyvinyl alcohol (PVA), PEG, and polyacrylamide have been widely employed to form hydrogels with embedded $Ti_3C_2T_x$, Mo_2CT_x, or Nb_2CT_x flakes. In these systems, the polymer not only stabilizes the MXene against oxidation but also serves as a tunable ionic conductor. For instance, a recent study by Liu *et al.* (2021) addressed the common challenge of MXene aggregation in hydrogels by introducing a chitosan-induced self-assembly method to fabricate a dispersion-enhanced MXene hydrogel. In this system, polyacrylamide serves as the swelling matrix, while chitosan forms a positively charged scaffold that interacts electrostatically with MXene nanosheets, preventing their restacking [173]. This strategy not only preserves the hydrophilicity and swelling capability of the hydrogel but also creates a highly interconnected 3D conductive network, improving both ionic transport and electron mobility. The resulting composite exhibits exceptional mechanical flexibility (up to 1900% strain), conductivity, self-adhesion, and antibacterial functionality, demonstrating the critical role of hydrophilic polymers in stabilizing MXenes and tailoring hydrogel properties for wearable biosensing and soft electronic applications [173]. Peng *et al.* (2023) developed a multifunctional ionotronic hydrogel composed of polyvinyl alcohol, polyacrylamide, $CaCl_2$, and MXene esigned for bionic skin sensors. By integrating both electron- and ion-conductive pathways through the combined effects of MXene and $CaCl_2$, the hydrogel overcomes the limitations of conventional electronic or ionic skins. Notably, the $CaCl_2$ component imparts a moisture self-regenerative capability, allowing the hydrogel to retain water and functional stability for over 70 days under ambient conditions. The composite also demonstrates remarkable features such as anti-freezing performance down to −50 °C, high strain sensitivity, and strong self-adhesion. These properties collectively position PPCM hydrogels as robust, long-lasting platforms for practical applications in wearable electronics, prosthetics, and human–machine interfaces [174]. In other work, Sun *et al.* (2024) introduced a MXene-based polyampholyte hydrogel engineered to suppress excessive swelling in aqueous environments while maintaining high stretchability (up to 1391%), reliable conductivity, and self-healing capability. The anti-swelling design enabled stable underwater sensing performance across a wide strain range (2–400%), making it suitable for real-time aquatic applications. Additionally, the hydrogel exhibited rapid photoresponsiveness and was successfully integrated into an underwater warning system, demonstrating its potential for environmental monitoring, marine technology, and smart urban infrastructure [175].

The interfacial ion transport properties of MXene–polymer systems are also highly tunable through polymer chain architecture, crosslinking density, and ionic functional group incorporation. Nafion, a sulfonated tetrafluoroethylene-based fluoropolymer, has been co-cast with $Ti_3C_2T_x$ to yield composites that exhibit directional ion conductivity and enhanced selectivity for cationic analytes, critical in multiplexed sweat electrolyte sensing. Shahzad *et al.* (2019) demonstrated that coating $Ti_3C_2T_x$ MXene-modified electrodes with Nafion significantly enhanced the electrochemical detection of DA, achieving high sensitivity (~3 nM), excellent selectivity, and a broad detection range (0.015–10 μM). The negatively charged MXene surface and the ion-selective nature of Nafion worked synergistically to favor cationic DA transport, enabling discrimination from interfering species. Compared to reduced graphene oxide-based sensors, the MXene–Nafion composite exhibited superior performance in real-sample testing, highlighting how ionic functional polymers like Nafion can modulate interfacial ion transport and improve selectivity in MXene-based biosensing platforms [176]. Further demonstrating the role of polymer-assisted ion transport in MXene-based sensing systems, Cao *et al. (2022)* fabricated a DA electrochemical sensor by co-assembling ZnO nanoparticles with

monolayer $Ti_3C_2T_x$ and coating the composite with Nafion. The resulting ZnO/$Ti_3C_2T_x$/Nafion-modified Au electrode exhibited a broad linear detection range (0.1–1200 µM), a low detection limit (0.076 µM), and high sensitivity (96 nA/µM), with excellent reproducibility and recovery (97.8%–102.2%) in biological samples [177].

Guo *et al.* (2023) developed a zwitterionic MXene-based conductive hydrogel with rapid synthesis, antifreeze capability, and long-term environmental stability. The hydrogel was prepared within one minute through an autocatalytic reaction system involving tannic acid-modified cellulose nanofibers and $ZnCl_2$, into which $Ti_3C_2T_x$ nanosheets were incorporated to enhance conductivity (~30 mS cm^{-1}) and mechanical flexibility (stretchability ~980%). The resulting material demonstrated durable adhesion even after prolonged air exposure, remained functional across an ultra-wide temperature range (−60 °C to 40 °C), and was effective for high-resolution physiological signal monitoring, including handwriting and voice recognition. Its versatility and robustness make it a strong candidate for wearable healthcare devices and intelligent sensing systems in challenging environments [178]. These hybrid systems exploit the synergy between the electronic transport of MXenes and the ionic transport of hydrated polymer chains, resulting in stable signal transduction under physiological strain.

Beyond linear composites, recent advances in self-healing and thermoresponsive polymer matrices have enabled the development of MXene–polymer systems that adapt their morphology and conductivity over time. For example, Zhang *et al.* (2020) reported a self-healing, stretchable MXene/silicone composite engineered through biomolecule-assisted modification. By functionalizing MXenes and amino-terminated PDMS via esterification and Schiff base reactions, the resulting material achieved uniform MXene dispersion, high electrical conductivity, and robust mechanical performance. The reversible hydrogen and imine bonding networks imparted excellent self-healing efficiency, restoring up to 98.4% of tensile strength and 97.6% of conductivity after damage. The composite, containing 10 wt% modified MXene, exhibited reliable strain-sensing capabilities and was able to detect subtle physiological movements such as speech and swallowing, even after repeated cut-heal cycles. This work highlights a scalable approach for developing multifunctional, wearable electronics combining mechanical resilience and sensing precision [179].

Importantly, MXene–polymer composites serve as not just structural or transport media but as information-processing layers. Their tunable permselectivity, redox buffering capacity, and dynamic swelling can be exploited to perform on-material preprocessing of biochemical signals such as filtering pH shifts, smoothing ionic noise, or biasing diffusion of larger interferents prior to downstream signal capture and digitization[134, 172]. This built-in biochemical filtering can be particularly valuable when analyzing sweat from users with altered physiology (e.g., hyperhidrosis, cystic fibrosis, or dehydration), where standard sensor calibrations may fail.

In the context of personalized bioelectronics, the use of adaptable MXene–polymer composites thus offers a materials-first approach to user matching. Rather than relying exclusively on software-based calibration, these materials can be pre-engineered or in situ tuned to match specific user sweat profiles. This paradigm shift, from calibrating signal output to calibrating the material input, represents a fundamental innovation in biosensor personalization strategy, and lays the groundwork for biosensors that are tailored not only to a measurement but to a person.

4.2. Structuring and Patterning for Signal Fidelity

In personalized sweat biosensing platforms, the design of the sensor interface must go beyond basic conductivity or sensitivity and focus on optimizing signal fidelity under dynamic, real-world conditions[18]. As wearable sensors are continuously exposed to mechanical motion, heterogeneous sweat diffusion, and biochemical variability, achieving stable and reproducible signal transduction becomes increasingly challenging[78, 180]. Micro- and nanostructuring of MXene-based sensing materials offers a powerful engineering route to address this problem by enhancing analyte accessibility, increasing signal-to-noise ratio, and improving interfacial coupling with both the skin and the analyte-rich fluid.

At the nanoscale, structuring techniques such as template-assisted synthesis, laser-induced patterning, and freeze-casting have been utilized to create MXene films and composites with controlled porosity, hierarchical surface roughness, and anisotropic channel architectures [99, 101, 159].

These features facilitate mass transport of ions and small molecules, minimize local analyte depletion zones, and promote uniform contact between the sensor and sweat film. For instance, novel enzymatic glucose sensors were fabricated using synthesized molybdenum carbide (Mo_3C_2) MXene and dPIn-modified screen-printed electrodes, demonstrating their first reported application in glucose sensing; although MWCNT-dPIn composites exhibited superior electrochemical performance, Mo_3C_2-based sensors still provided stable, selective, and reproducible detection across physiologically relevant glucose ranges, supporting the utility of structured MXene composites in biosensing platforms [181]. In other work, MXene-wrapped cationic polystyrene spheres have been pyrolyzed to synthesize highly graphitic carbon quantum dots

(CQDs), where the $Ti_3C_2T_x$ shell not only catalyzed dehydrogenation via C–Ti–O active sites but also acted as a confinement barrier to regulate the diffusion and carbonization of decomposition products, demonstrating a templated approach to control nanoscale architecture and enhance material uniformity [182].

Beyond increasing electrochemically active area, microstructuring can improve mechanical interlocking between the sensor surface and the skin, reducing motion-induced noise. Patterning MXene layers into interdigitated microelectrodes (IDEs) or micropillar arrays not only amplifies the capacitance signal but also enhances adhesion under strain [183]. For wearable platforms, this translates into improved robustness of measurements during movement, sweat accumulation, or hydration changes. For instance, Turcan *et al.* (2024) demonstrated the successful dielectrophoretic assembly of pristine MXene flakes across interdigitated microelectrodes, forming uniaxial conductive bridges whose alignment and density could be precisely tuned via frequency and voltage parameters, paving the way for reproducible, directionally oriented MXene architectures in miniaturized chemi-resistive sensors [184]. In another work, Cai *et al.* (2018) designed a MXene/CNT-based percolation network with a woven microstructure that synergistically combined 2D $Ti_3C_2T_x$ nanosheets and 1D carbon nanotubes to achieve ultrathin, highly stretchable strain sensors with excellent adhesion, stability, and a detection limit as low as 0.1% strain. This demonstrates how microstructural engineering can enhance both sensitivity and mechanical robustness for continuous physiological monitoring during movement. [138]. Similarly, Lu *et al.* (2020) developed highly stretchable and pressure-sensitive MXene-based hydrogel sensors by embedding uniformly dispersed $Ti_3C_2T_x$ nanosheets into a double-network PVA/PVP hydrogel, forming a 3D conductive architecture that enhanced mechanical interlocking, resilience (up to 2400% strain), and signal fidelity under dynamic deformation. This is ideal for real-time monitoring of complex human motions such as facial expressions, phonation, and handwriting. [185]. Zhang *et al*. (2021) developed a fully self-powered smart sensor system by integrating MXene/black phosphorus (BP) lamellar structures into both flexible pressure sensors and laser-written micro-supercapacitors, enabling high sensitivity (77.61 kPa^{-1}), rapid response (10.9 ms), and real-time heart signal monitoring without external power [186].

Signal fidelity is also closely linked to spatial resolution, particularly in multiplexed or patch-based devices designed to monitor multiple analytes in parallel. Microfluidic-guided patterning, such as using wax printing or laser-engraved microchannels, can spatially isolate MXene sensing regions for selective analyte detection while avoiding cross-talk between adjacent regions. In such designs, patterned MXene zones can be functionalized individually, enabling simultaneous sensing of lactate, glucose, and electrolytes from the same sweat sample. These modular architectures are critical for translating MXene-based materials into wearable biochemical arrays, where local signal integrity and minimal interference are essential. For instance, Nah *et al.* (2021) developed a wearable microfluidic electrochemical immunosensor by integrating $Ti_3C_2T_x$ MXene into a LBG 3D electrode network on a PDMS substrate, enabling localized and selective detection of cortisol in sweat**.** The microfluidic channel guided sweat into a defined chamber, allowing spatial isolation of the sensing zone and minimizing cross-talk. This configuration not only improved signal fidelity and detection sensitivity (LOD: 88 pM) but also demonstrated the potential of MXene-integrated microfluidic patch systems for multiplexed, point-of-care biomarker analysis [187]. In other work, Liu *et al. (2022)* demonstrated a high-throughput microfluidic synthesis platform for producing $Ti_3C_2T_x$ MXene functionalized with uniformly dispersed Pt–Pd nanoparticles, achieving precise control over nanoparticle size (2.4–9.3 nm), composition, and distribution under tunable flow rates. The resulting $Ti_3C_2T_x$/Pt–Pd composites exhibited superior electrocatalytic activity for hydrogen peroxide sensing, with a broad detection range (1–12,000 µM), low detection limit (0.3 µM), and high sensitivity (300 µA mM^{-1} cm^{-2}), outperforming batch-synthesized counterparts and highlighting the promise of microfluidic strategies for scalable, high-performance MXene-based sensor fabrication [188]. Similarly, Wen *et al.* (2022) developed a FRET-based fluorescent biosensor for the ultrasensitive detection of amyloid β oligomers (AβO), a key biomarker of Alzheimer's disease, by integrating carboxyfluorescein-labeled aptamers with 3D Fe_3O_4/MXene nanospheres as novel quenchers on a PDMS microfluidic chip. The platform achieved a wide linear detection range (0.10–200 nM) with a remarkably low detection limit (~0.05 nM) using minimal sample volume (~4.5 µL), demonstrating the promise of MXene-based nanostructures in early-stage neurodegenerative disease diagnostics and miniaturized smart healthcare systems [189].

At the interface with electronics, structuring also improves impedance matching and charge transfer efficiency. Techniques such as microcrack engineering and fracture-controlled patterning, wherein cracks are introduced intentionally in composite films to segment conductive paths, have been used to maintain electrical performance under bending and torsion while reducing noise from capacitive drift [190, 191]. These crack-insensitive patterns are especially relevant for devices operating over long durations on regions prone to flexion (e.g., wrists, elbows), where mechanical noise could

otherwise compromise baseline drift [191, 192]. On the other hand, the choice of substrate and its compatibility with patterned MXene layers is another crucial design factor. Recent approaches have utilized stretchable, breathable materials such as electrospun polyurethane meshes or porous PDMS membranes, onto which patterned MXene electrodes are deposited via screen-printing or layer-by-layer assembly [136, 185]. These systems improve sweat permeation, reduce hydration lag, and preserve intimate contact with the skin, three conditions that significantly influence the electrochemical signal fidelity in wearable formats. Moreover, emerging structuring strategies also incorporate bio-inspired geometries, such as honeycomb microchannels or lotus-leaf-like textures, which can facilitate self-cleaning, anti-fouling behavior, and rapid sweat wicking [193]. Such features contribute not only to mechanical and chemical stability but also to consistent analyte delivery and minimized contamination from skin lipids, dead cells, or exogenous molecules (e.g., cosmetics). Bio-inspired structuring may also assist in extending the operation window for sensors worn continuously over multiple days, aligning with the goal of long-term, personalized health monitoring[193–195]. For example, Chen *et al.* (2025) developed a leaf-inspired MXene-composited hydrogel using tannic acid encapsulation and cellulose nanofiber intercalation, forming a stable 3D nano-motif that preserved MXene integrity for over 10 days under oxidative conditions. The resulting PCM-TENG demonstrated robust mechanical resilience, high stretchability (>800%), and sustained performance as a self-powered biosensor, highlighting how bio-inspired structuring strategies can extend operational longevity in wearable health monitoring applications [195].

As personalized biosensing applications demand high-resolution, drift-free signal acquisition over extended durations, micro- and nanoscale structuring of MXene-based materials will play a central role in achieving stable and reliable device performance [18]. Structuring not only amplifies sensing performance but serves as a foundational design layer that complements the chemistry and electronics in realizing adaptive, user-specific biosensing systems.

4.3. Tuning Surface Charge and Ion Exchange Behavior

In the design of personalized wearable biosensors, one of the most underappreciated yet critically important engineering variables is the surface charge of the sensing material [111, 115].

This becomes particularly relevant when the biosensor operates in a medium as chemically dynamic as human sweat, where ionic composition, pH, and the presence of competing species vary both across individuals and temporally within the same user.

Because sweat composition varies widely among individuals, tuning MXene surface charge emerges as a potent strategy for selective analyte recognition. Modulating the zeta potential of MXenes by tuning the density and distribution of surface terminations is a direct approach to influence this behavior [25, 111]. MXenes with negative zeta potentials preferentially attract cationic metabolites (NH_4^+, Ca^{2+}), while positively modified surfaces favor anionic species such as lactate or chloride. Termination engineering, pH-induced charge modulation, and functional coatings can therefore be strategically leveraged to match target analytes and reduce cross-sensitivity. This direct mapping between surface chemistry and selectivity establishes clear guidelines for personalized and multi-analyte sweat sensor design.

In a recently published work, Venkatesan *et al.* (2024) demonstrated that incorporating TiO_2-functionalized MXene into a polystyrene nanofiber membrane introduced effective charge-trapping behavior in a triboelectric nanogenerator, significantly enhancing surface charge retention and electric field distribution. This result emphasizes how tailoring MXene surface chemistry, specifically by modifying its termination groups and zeta potential, can optimize interfacial charge dynamics in ionically complex environments, thereby improving stability and performance in bio-interfacing applications such as wound healing and sweat-powered wearable sensors [196]. On the other hand, Hajian *et al.* (2018) employed first-principles density functional theory (DFT) simulations to demonstrate that tuning the ratio of surface terminations on $Ti_3C_2T_x$ MXene (particularly reducing fluorine content in favor of oxygen and hydroxyl groups) enhances ammonia adsorption by increasing charge transfer and adsorption energy. This study underscores how surface termination engineering directly influences zeta potential and interfacial electrostatics, offering a strategic route to improve selectivity and sensitivity of MXene-based chemical sensors in complex biological environments[197]. In another DFT-based study, it was revealed that the adsorption behavior of Ti_2C MXenes toward various flue gas molecules is highly dependent on surface terminations, with oxygenated groups (e.g., =O, –OH) enabling strong chemisorption of polar species like NH_3 and NO, while halogenated (Br, Cl) and amine (–NH) terminations primarily promote physisorption with weaker, reversible interactions. The findings highlight that surface termination not only governs adsorption strength and selectivity but also impacts structural stability under reactive conditions—providing a theoretical framework for tailoring MXene interfaces in selective gas sensing and separation technologies[198]. In the concept of wearable sensors, Li *et al.* (2022) enhanced the VOC selectivity and

humidity tolerance of $Ti_3C_2T_x$ MXene by introducing hydrocarbon surface terminations, which significantly suppressed water vapor interference (by 71%) while increasing ethanol sensitivity fivefold at room temperature [199]. Fig. 7 illustrates the design and operation of the hydrocarbon-terminated $Ti_3C_2T_x$-M_2 MXene sensor integrated into a flexible wearable platform for real-time breath ethanol monitoring. Fig. 7a shows the device architecture, highlighting the flexible substrate, patterned MXene sensing layer, and wireless module for on-body deployment. Fig. 7b presents the fabrication procedure, including MXene surface termination, electrode patterning, and encapsulation into a breathable wearable patch. Fig. 7c depicts the wearable prototype positioned near the exhalation pathway for continuous on-body breath analysis. As shown in Fig. 7d, the hydrocarbon-terminated $Ti_3C_2T_x$-M_2 sensor delivers rapid and sensitive electrochemical responses to ethanol, closely correlating with commercial BrAC detector outputs. Fig. 7e–f further demonstrate the enhanced selectivity, reduced baseline drift, and improved operational stability of $Ti_3C_2T_x$-M_2 compared to pristine $Ti_3C_2T_x$, confirming the benefits of surface termination engineering for volatile organic compound (VOC) sensing. Collectively, the results highlight that surface-modified MXene electrodes significantly improve chemical specificity and long-term stability, enabling practical integration into wearable breath-analysis systems for intelligen -health monitoring. An equally powerful approach lies in surface charge inversion or patterning, where MXenes are chemically or physically modified to present regions of opposing or tunable polarity. This has been achieved by grafting amine-functionalized silanes (e.g., 3-aminopropyl) triethoxysilane (APTES)) or zwitterionic polymers (e.g., poly(sulfobetaine methacrylate)) onto MXene surfaces, resulting in surfaces capable of capturing both anionic and cationic analytes in a pH-dependent fashion [88, 178].

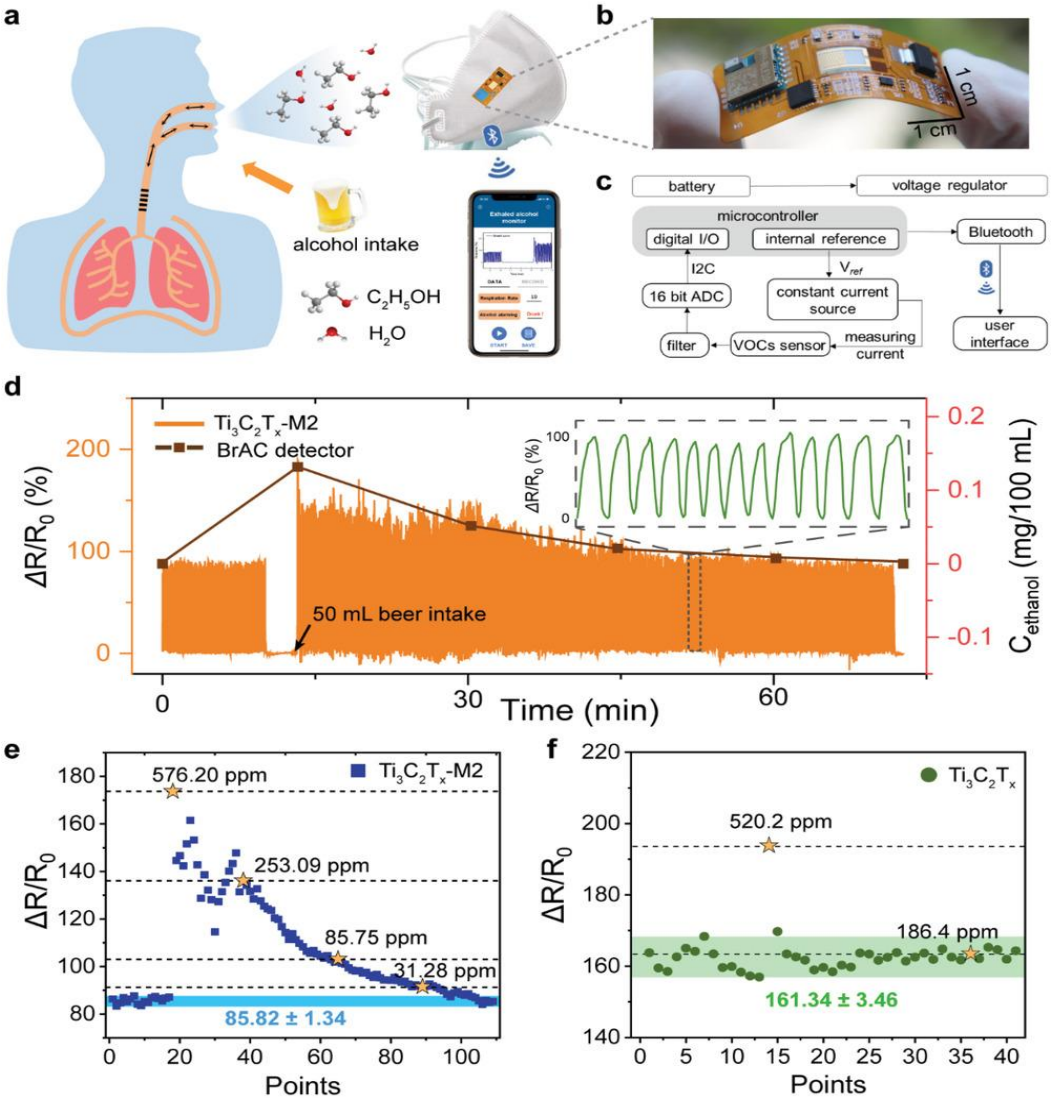

Figure 7. Wearable $Ti_3C_2T_x$-M_2 MXene sensor platform for real-time, wireless monitoring of exhaled ethanol (a) Schematic illustration of breath alcohol monitoring using a mask-integrated MXene sensor. (b) Optical image of the flexible sensor device. (c) System architecture detailing signal processing and wireless transmission. (d) Real-time resistance change ($\Delta R/R_0$) in response to ethanol following beer intake, showing strong correlation with a commercial BrAC detector. (e–f) Comparative ethanol sensing performance of $Ti_3C_2T_x$-M_2 versus unmodified $Ti_3C_2T_x$, highlighting the enhanced sensitivity and signal clarity of the modified sensor. Reprinted with permission from [199] © 2021 Wiley-VCH GmbH

10.57647/jnsc.2026.1601.05

Such dual-affinity systems offer flexibility for simultaneous monitoring of multiple sweat constituents with opposite charges—e.g., lactate (negatively charged at physiological pH) and ammonium (positively charged)—without mutual signal interference. Moreover, as sweat pH can vary between 4.5 and 7.5 depending on body region, hydration state, and individual physiology, the pH responsiveness of MXene interfaces is another critical dimension of design. In practical terms, this means that sweat sensors lacking pH normalization or charge control may misinterpret analyte concentrations due to confounding electrochemical signals arising from proton flux or ionic masking [29, 78, 200].

Integrating pH-stable MXene–polymer composites or applying real-time signal correction algorithms based on electrostatic modeling, provides a pathway to compensate for these confounding factors and move closer to accurate, personalized sensing. Surface charge engineering of MXenes thus constitutes a material-level calibration mechanism one that can be embedded directly into the sensor structure. As personalization becomes a cornerstone of biosensor design, MXenes offer a unique opportunity to match their interfacial behavior to an individual's sweat signature, whether it reflects their diet, hydration habits, disease state, or even genetic makeup.

5. Case Studies and Experimental Advances of Sweat-Responsive MXene-Based Sensors

While this review focuses on MXene-based wearable sweat sensors, a limited number of non-MXene examples are intentionally incorporated in this section to serve as benchmark comparisons. These reference systems, such as carbon nanostructures, metal oxides, and polymer-based sensing platforms, provide essential contextual baselines for evaluating MXene performance in terms of conductivity, electrocatalytic activity, mechanical compliance, and interface stability. Their inclusion is strictly comparative and enables a clearer distinction of the advantages and remaining challenges of MXene-based architectures relative to widely adopted material classes in wearable biosensing. This framing ensures that the discussion remains MXene-centered while delivering a scientifically meaningful assessment of design trade-offs relevant to real-world sensor deployment. In recent years, a growing body of experimental work has validated the feasibility of MXenes as core sensing materials for sweat diagnostics, yet challenges remain in ensuring their robustness under physiologically variable conditions and translating laboratory prototypes into real-world use. The diversity of sweat biomarkers necessitates MXene-based sensing architectures that are not only compositionally tuned but performance-matched to the analytical demands of each target analyte. In recent experimental demonstrations, sensitivity, LOD, response time, and stability are strongly dictated by the interplay between MXene flake chemistry, termination profile, hybrid assembly, and polymer or hydrogel interfaces. For example, sensors designed for electrolytes prioritize rapid ion transport and broad linearity, whereas glucose and lactate platforms emphasize catalytic enhancement and interference rejection through composite engineering. Cortisol and other low-abundance biomarkers require termination-controlled MXenes or biofunctional surfaces to achieve nM-level detection fidelity. By analyzing these case studies through the lens of performance–structure coupling, Section 5 highlights how experimental MXene designs strategically align material properties with application-specific performance requirements.

Electrochemical sensing platforms leveraging $Ti_3C_2T_x$ have been the most extensively explored. In a representative example, *Zhang et al. (2025)* reported a wearable biosensing system based on a Ga@MXene/chitosan (CS) hydrogel composite that combines high conductivity with excellent mechanical stretchability. By forming a three-dimensional conductive network, the Ga-integrated MXene enhanced signal transduction, while the CS hydrogel provided sweat absorption, adhesion, and softness for skin-conformal application. The biosensor demonstrated a low detection limit of 0.77 μM, high sensitivity (1.122 $\mu A \cdot \mu M^{-1} \cdot cm^{-2}$), and a wide linear detection range (10–1000 μM), making it well-suited for continuous sweat analysis and personalized health monitoring [201]. Myndrul *et al.* (2022) reported a skin-attachable and stretchable electrochemical glucose sensor integrating ZnO tetrapods with $Ti_3C_2T_x$ MXene nanoflakes, enabling non-invasive, real-time monitoring of glucose in sweat with high sensitivity (29 $\mu A\ mM^{-1}\ cm^{-2}$), a low detection limit (~17 μM), and mechanical stretchability up to 30%. The sensor demonstrated strong correlation with conventional blood glucose readings, highlighting its clinical promise for continuous, painless glucose tracking during physical activity or postprandial states [202]. Beyond the ZnO/MXene-based example, strain-dependent behavior is broadly observed across flexible and stretchable biosensor architectures. Tensile deformation can modulate the electrochemical response by altering conductive percolation pathways in MXene–polymer composites, where stretching disrupts or reorients flake networks and increases resistance [203–205]. In hydrogel-based enzymatic sensors, strain influences mass-transport dynamics and the local hydration environment, leading to changes in response time or baseline drift [206, 207]. Stretchable microfluidic platforms may also experience deformation-induced changes in channel geometry that affect sweat sampling efficiency and analyte concentration stability [208–210]. Therefore, it can be stated that strain sensitivity is strongly dependent on the

sensor's material composition and structural design, underscoring the need for strain-aware engineering in MXene-enabled wearable systems. In another work, Zahed *et al.* (2022) introduced a butterfly-inspired hybrid epidermal biosensing (bi-HEB) patch that integrates nanoporous carbon/MXene (NPC@MXene) transducers for the real-time, multiplexed detection of sweat glucose, pH, temperature, and electrophysiological (ECG) signals (Fig. 8). The sensor demonstrated high glucose sensitivity (100.85 μA mM^{-1} cm^{-2}) within physiological ranges and incorporated a compensation strategy for dynamic sweat pH and temperature fluctuations, while also providing reliable ECG data comparable to standard Ag/AgCl electrodes. This multifunctional wearable platform highlights the value of integrating electrochemical and electrophysiological monitoring in a unified patch for enhanced physiological assessment during physical activity [211]. While $Ti_3C_2T_x$ dominates most demonstrations, alternative MXene chemistries such as Mo_2CT_x and Nb_2CT_x are gaining traction due to their distinct electronic properties and different surface terminations. Chavan *et al.* (2025) developed a minimally invasive electrochemical biosensor for real-time progesterone monitoring based on an aptamer displacement mechanism, integrating AuNPs-decorated APTES-functionalized Nb_2C MXene nanosheets on a screen-printed carbon electrode. The sensor achieved high sensitivity (0.159 μA pM^{-1}) and low detection limits (14–17 pM) in both PBS and sweat samples, enabling accurate in situ hormone tracking with high selectivity and stability for point-of-care female health diagnostics [212].Laochai *et al.* (2022) demonstrated a thread-based electrochemical immunosensor for non-invasive cortisol detection in sweat, utilizing a conductive thread electrode modified with MXene and AuNPs to enhance surface area and facilitate anti-cortisol immobilization. The sensor employed EDC/NHS chemistry for aptamer conjugation and achieved high sensitivity (LOD: 0.54 ng/mL) across a broad linear range (5–180 ng/mL). Designed for wearable use, this robust platform maintained performance for over 6 weeks and proved effective for cortisol detection in artificial sweat, offering promising integration potential into wristband-based real-time biosensing systems [213].Multi-analyte systems based on patterned MXene films have also been explored to reflect the biochemical complexity of sweat [94, 96]. In a recent demonstration, Zhang *et al.* (2025) introduced a flexible, multifunctional sweat sensor platform by integrating reduced graphene oxide electrodes with a hybrid nanocomposite consisting of nitrogen/sulfur co-doped holey graphene and TiO_2-decorated MXene**.** This architecture enhances conductivity, increases electrocatalytic activity, and maximizes ion/electron transport via porous and doped structures. The device enables simultaneous detection of K^+, AA, UA, and DA in sweat with high sensitivity and selectivity. Validated during physical activity, the system successfully monitored biomarker fluctuations in real time, offering a robust approach for continuous, non-invasive health assessment [96]. Emerging approaches have begun to explore non-enzymatic detection routes using MXenes to overcome stability issues associated with biomolecular degradation. For instance, Subramania *et al.* (2023) reported the fabrication of a non-enzymatic electrochemical glucose sensor by in-situ decorating $NiCo_2O_4$ nanoparticles (~82 nm) onto Ti_2NbC_2 MXene nanosheets, forming a hybrid material with enhanced electrocatalytic properties. The synergistic integration of $NiCo_2O_4$'s high surface area and Ti_2NbC_2's superior electrical conductivity enabled the sensor to achieve a high sensitivity of 425.6 μA mM^{-1} cm^{-2}, along with a low detection limit and rapid response time. This work highlights the potential of Ti_2NbC_2-based nanohybrids in developing efficient, low-cost, and scalable non-enzymatic wearable biosensors [214]. Similarly, Feng *et al.* (2024) developed a $Ti_3C_2T_x$ MXene/Cu_xO composite glucose sensor via acid etching followed by electrochemical deposition. The composite exhibited a synergistic catalytic effect where the MXene matrix enhanced Cu_xO nanoparticle dispersion and electron transfer efficiency, resulting in an ultrasensitive non-enzymatic glucose sensing platform. Operating at 0.55 V (vs. Ag/AgCl), the sensor showed dual linear detection ranges (1 μM–4.655 mM and 5.155 mM–16.155 mM), an excellent sensitivity (up to 361 μA mM^{-1} cm^{-2}), and a low detection limit of 0.065 μM. It demonstrated high selectivity against common interferents and accurate glucose quantification in sweat, confirming its promise for real-time wearable biosensing [215]. In another work, Ravitchandiran *et al.* (2024) reported the design of a non-enzymatic glucose biosensor by integrating a ZnFe Prussian Blue analogue [ZnFe(PBA)] with $Ti_3C_2T_x$ MXene via in-situ sonication, forming a nanohybrid with enhanced electrocatalytic activity. The cubic nanostructure of ZnFe(PBA) coupled with the conductive MXene nanosheets provided a large electroactive surface and superior electron transfer capability. This screen-printed electrode exhibited an impressive sensitivity of 973.42 μA mM^{-1} cm^{-2}, a low detection limit of 3.036 μM, and a wide linear range of 0.01–1 mM, demonstrating its strong potential for non-enzymatic glucose sensing in wearable diagnostic systems [216]. On the other hand, Damirchi *et al.* (2024) developed a paper-based electrochemical glucose sensor leveraging a novel MXene/NiSm-LDH porous nanocomposite electrode that operates under bipolar electrochemistry without the need for enzymes. The sensor design enables efficient electron transfer and high electrocatalytic activity, allowing enzyme-free glucose oxidation and real-time detection in sweat.

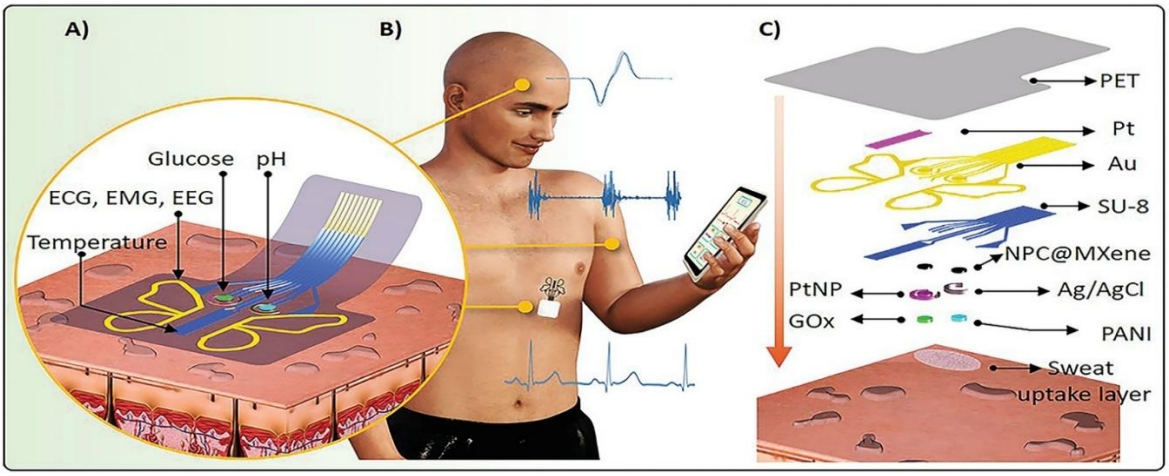

Figure 8. Multimodal on-skin epidermal MXene patch for detecting glucose, lactate, electrolytes, and temperature. Reprinted with permission from [211]

Table 1. Comparative performance of MXene-based wearable sweat biosensors

Table 1A. Electrolytes and pH

Analyte	Material	Sensing Mechanism	Platform	Performance Metrics	Advantages	Limitations	Ref
pH	$Ti_3C_2T_x$ MXene	Potentiometric	Wearable patch	Sensivity of −43.51 ± 0.53 mV/pH at pH 1–11	- Wide pH range - Good stability	MXene oxidation alters slope over time	[80]
Na^+	PEDOT:PSS + polypyrrole (PPy) / $Ti_3C_2T_x$ MXene	Potentiometric	Wearable electrochemical sensor	428 µF and signal drift of 0.02 mV/h	Highly stable cycling; dual-analyte detection	Polymer/MXene interface sensitive to humidity	[127]

Table 1B. Hormones

Analyte	Material	Sensing Mechanism	Platform	Linear Range	LOD	Advantages	Limitations	Ref
Progesterone	AuNPs on APTES decorated Nb_2C MXene	Aptamer-based	Screen-printed aptasensor	50–160 pM	17 pM	-High aptamer specificity - Good stability in real-time clinical samples	Aptamer conformation depends on ionic strength	[212]
	$Ti_3C_2T_x$ MXene on laser-burned graphene	Immunosensor	Microfluidic wearable patch	0.01–100 nM	3.88 pM	-Improved electron transfer, -Low-cost, -Fast and easy sample collection	Antibody degradation over time	[187]
Cortisol	L-cys/AuNPs/$Ti_3C_2T_x$ MXene	Label-free immunosensor	Flexible chip (conductive thread electrode)	5–180 $ng{\cdot}mL^{-1}$	0.54 $ng{\cdot}mL^{-1}$	- High reproducibility - Long-term stability (≥6 weeks)	Biofouling vulnerability	[213]
	MXene + CNTs	Immunosensor	Polyethyleneterephthalate (PET)-based wearable	0.1 fg/mL–1 µg/mL	0.03 fg/mL	- CNT and MXene synergy boosts sensitivity -Non-invasive real-time monitoring	PET limits high-strain flexibility	[48]

Table 1C. Small-molecules (metabolites, antioxidants, catecholamines, alkaloid, etc.)

Analyte	Material System	Sensing Mechanism	Platform	Sensitivity	Linear Range	LOD	Advantages	Limitations	Ref
Glucose	*in-situ* LiF and HCl etched $Ti_3C_2T_x$ MXene	Non-enzymatic	Screen printed electrode	569.7 $\mu A \cdot mM^{-1} \cdot cm^{-2}$	5–350 µM	5 µM	- Strong catalytic activity - Compatibl	Interlayer collapse risk on drying	[153]
	$Ti_3C_2T_x$ MXene–PEDOT:PS S- GOx hydrogel	Enzymatic	Flexible hydrogel biosensor	21.7 $\mu A \cdot mM^{-1} \cdot cm^{-2}$	1- 94 µM	1.9 µM	Soft, conformal; high conductivit y	Hydrogel slows recovery at low sweat	[157]
	ZnO tetrapods decorated $Ti_3C_2T_x$ MXene	Enzymatic	Skin-attachable sensor	29 $\mu A \cdot mM^{-1} \cdot cm^{-2}$	0.05–0.7 mM	17 µM	-High stretchabilit y *-In-vivo* correlation	Enzyme instability under acidic sweat	[202]
	$NiCo_2O_4$ / Ti_2NbC_2 double MXene	Non-enzymatic	Flexible patch	425.6 $\mu A \cdot mM^{-1} \cdot cm^{-2}$	—	0.298 mM	- Promising electrical conductiv ity	Transition metal oxide oxidation	[214]
	Gallium grafted MXene/C hitosan	Non-enzymatic	Wearable sensor	1.122 $\mu A \cdot \mu M^{-1} \cdot cm^{-2}$	10–1,000 µM	0.77 µM	Self-heating module increases charge	Transition metal oxide oxidation	[201]
	$Ti_3C_2T_x$ MXene decorated with enzyme mimetic	Enzymatic	Wearable sensor	7.6 µA/µM	100 µM and 10 mM	0.49 µM	- 3D porous structure boosts	Fabric fibers affect analyte diffusion	[218]
Ascorbic Acid	Ti_3C_2 MXene-MoS_2	Enzymatic	3-electrode sensor	54.6 $nA \cdot \mu M^{-1}$	10-5000 µM	4.2 µM	- High catalytic amplificatio n -Swift	Redox potential pH-dependent	[219]
Nicotine	Palladium Hydroxide Supported Carbon Doped $Ti_3C_2T_x$ MXene	Non-enzymatic /Amperometric	Wearable transducer	0.286 $\mu A \cdot \mu M^{-1} \cdot cm^{-2}$	0.25–37.5 µM	27 nM	-The 3D heterostruct ure-based working electrode	-Pd susceptible to chloride interference - High cost	[220]
Uric Acid	1,3,6,8-pyrene tetrasulfoni c acid sodium salt functionaliz	Non-nenzymatic	Microfluidi c wearable flexible	0.215 $\mu A \cdot \mu M^{-1} \cdot c m^{-2}$	5 µM–100 µM	0.48 µM	-High selectivity towards Na^+, Mg^{2+}, Ca^{2+}, hydrogen	- High conductivit y and large active surface	[221]
Multiplex analysis of AA, DA, and UA	NiO–$Ti_3C_2T_x$ MXene modified laser-induced graphene (LIG)	Non-enzymatic	Flexible sensor	0.14, 2.02 and 5.94 µA μM^{-1} for AA, DA and UA, respectively	- 10 µM–2 mM for AA, - 0.1–200 µM for DA, - 0.5–100 µM for UA	16, 1.97 and 0.78 µM for AA, DA and UA,	-Simultaneous real-time analysis	-Possible degradation under variable	[222]

With a linear detection range of 10–200 µM and a limit of detection of 3.6 µM, the system demonstrated reliable sensitivity and strong practical applicability when validated with real sweat samples [217]. A comparative analysis of recent MXene-based sweat biosensors is summarized in Table 1, highlighting how variations in material architecture, fabrication strategies, and sensing mechanisms govern device performance across different

analyte classes. As shown, sensing platforms using pristine or functionalized $Ti_3C_2T_x$ excel in electrolyte and pH detection owing to their stable ion-responsive surface terminations, whereas aptamer-based and immunosensing modalities enable high specificity for low-abundance hormones such as progesterone and cortisol. Non-enzymatic glucose sensors benefit from MXene–metal or MXene–carbon hybrids that enhance catalytic activity and charge-transport kinetics, while enzymatic hydrogel-based systems provide superior conformability at the expense of recovery time and biochemical stability. Importantly, the table also illustrates key limitations intrinsic to each design such as enzyme degradation, MXene oxidation, polymer interface drift, or microfluidic flow variability emphasizing the need for tailored material–mechanism alignment for each biochemical target.

This comparative framework underscores the diversity of MXene-enabled sensing pathways and identifies the structure–property relationships that should guide the rational design of next-generation wearable bioelectronic platforms. Despite these promising developments, challenges remain in fully understanding the influence of real sweat matrices on sensor performance. Many experimental studies still rely on artificial sweat standards, which often lack the complexity of native sweat, particularly in terms of protein content, variable pH, and skin-derived contaminants. This gap is particularly significant for personalized biosensors, where interindividual sweat composition can differ markedly in ion content, pH, and metabolite concentration. While the functional performance of MXene-based materials has been thoroughly demonstrated in controlled laboratory environments, their practical implementation within skin-conformal, self-contained wearable platforms presents a unique set of engineering and physiological challenges. Successful integration involves not only establishing stable electrical and electrochemical connections but also ensuring biomechanical compatibility, biochemical resilience, power autonomy, and real-time data interfacing.

The translation from a testbed sensor to a fully operable wearable requires harmonization across material science, device architecture, and user ergonomics. As a result, MXene-based biosensor research is now increasingly shifting toward on-body testing with diverse user groups, real-time monitoring during physical activity, and longitudinal studies under variable environmental and physiological conditions.

The development of sweat-responsive MXene-based sensors thus represents a critical junction where material chemistry, device engineering, and physiological variability converge. The growing experimental literature provides clear validation of their technical viability, yet also highlights the need for standardized protocols, personalized calibration frameworks, and multi-parameter validation to fully leverage these materials in individualized, real-world health monitoring applications.

6. Toward Data-Driven Personalization and Intelligent Modeling

Data-driven methodologies represent a critical layer of intelligence in modern wearable biosensors. In MXene-based platforms, ML and digital twin modeling serve complementary functions. ML enables real-time signal correction and adaptive calibration, while digital twins provide physics-guided simulations of sweat chemistry, device behavior, and long-term performance. The following subsections detail these approaches and their integration into next-generation MXene-enabled wearable systems.

6.1. Machine Learning–Enabled Calibration and Signal Adaptation

The operational fidelity of wearable MXene-based biosensors increasingly depends on advanced signal-processing strategies capable of compensating for environmental, physiological, and device-specific variability. During real-world wear, factors such as fluctuations in sweat composition, pH, electrolyte concentration, skin temperature, mechanical deformation, and hydration state introduce dynamic sources of noise and drift that static, laboratory-based calibration cannot reliably address [4, 5]. As a result, real-time recalibration has become essential for maintaining long-term reliability. As a result, real-time recalibration has become essential for maintaining long-term reliability. Static calibration protocols, while effective under controlled conditions, often fail during continuous operation due to drift, analyte cross-sensitivity, and temporal signal instability [79]. ML has emerged as a powerful enabling tool for maintaining accuracy *in-situ*, offering adaptive recalibration without manual baseline resets or repeated reference measurements [223, 224]. ML algorithms learn nonlinear mappings between raw sensor outputs and ground-truth analyte concentrations using labeled training datasets [96, 200]. Once trained, these models can infer reliable analyte levels even in the presence of noise, variable sweat chemistry, or sensor drift. Algorithms such as support vector regression, artificial neural networks, and random forest regressors [225, 226] have demonstrated strong predictive capability for time-series electrochemical data, enabling extraction of richer information from amperometric, voltammetric, or impedance-based measurements and capturing complex dependencies between MXene surface chemistry, physiological

parameters, and temporal signal evolution. While the intrinsic electrochemical response of MXene-based sensors is dictated by material properties and interfacial redox behavior, real-time ML and digital twin approaches provide important complementary advantages under dynamic on-body conditions. ML algorithms can continuously adapt calibration by learning relationships between raw signals and true analyte levels, enabling correction for pH fluctuations, electrolyte variations, sweat-rate changes, temperature shifts, and mechanical deformation. By extracting multidimensional waveform features, ML reduces cross-sensitivity and improves interpretability beyond traditional peak-based analysis. Digital twin frameworks further enhance robustness by providing physics-informed simulations of how sweat chemistry, hydration, temperature, and electrode degradation influence sensor behavior over time, enabling predictive drift correction and virtual optimization. Together, these computational tools support more stable, accurate, and personalized operation of MXene-based wearable biosensors during continuous real-world use.

In a representative example, Chen *et al.* (2025) developed a noninvasive wearable diagnostic platform for cardiovascular disease by combining surface-enhanced Raman spectroscopy (SERS) with ML. Utilizing AgNW/MXene hydroxyl composite membranes as flexible SERS substrates, the system enables ultrasensitive detection of cholesterol in sweat down to 10^{-8} M, while maintaining performance over 50 stretch-release cycles. Importantly, a random forest classifier was employed to distinguish between healthy individuals and cardiovascular patients, achieving an accuracy of 83.5%, thereby demonstrating the power of ML in enhancing diagnostic precision. This approach showcases a durable, highly sensitive, and ML-integrated sensing strategy that holds promise for real-time, noninvasive monitoring in personalized cardiovascular health management [227]. Das *et al.* (2024) present a comprehensive review emphasizing how ML integration enhances the performance of 2D materials-based sensors, such as those utilizing graphene and transition metal dichalcogenides. While 2D materials offer unique electrical and surface properties, their sensing capabilities are often constrained by environmental variability and material-specific limitations.

ML approaches are shown to address these challenges by enabling pattern recognition, real-time signal correction, and adaptive calibration, which significantly improve sensitivity, selectivity, and overall reliability. The study systematically reviews ML techniques applied across healthcare, industrial, and environmental monitoring use cases, showcasing how they reduce false positives and elevate accuracy. This work positions ML-assisted 2D sensing systems as a transformative path forward for smart, high-performance detection technologies[225].

In a study regarding smart sweat sensors, Zhou *et al.* (2024) developed a low-cost, battery-free colorimetric wearable sensor for non-invasive detection of pH and glucose levels in sweat**,** utilizing cotton-based textiles and smartphone-assisted image acquisition. The sensor system employs newly synthesized pH indicators and enzymatic glucose sensing layers, which exhibit visible color changes corresponding to physiological ranges. To interpret the results with high accuracy, three different ML algorithms were applied to image data, achieving up to 90% accuracy in classifying pH and glucose levels. This study underscores the value of ML in automating signal interpretation, improving reliability, and eliminating user bias in wearable diagnostics—offering a promising solution for chronic disease management, especially in resource-limited settings [228].

Similarly, Zhou *et al.* (2024b) developed a machine learning-integrated non-enzymatic wearable sweat sensor capable of selectively detecting tyrosine, tryptophan, and pH levels during physical activity, even under resource-constrained conditions typical of portable systems. The device features a compact two-electrode design embedded within a microsystem that handles real-time signal processing and wireless data transmission. By extracting four explainable ML-derived features, the system accurately predicts biomarker concentrations with strong statistical reliability. Tested during cycling trials, the platform demonstrated consistent biomarker detection across varied pH conditions and nutritional states, highlighting its potential for cost-effective, accurate, and portable physiological monitoring in real-world biomedical applications [229]. ML does not resolve the underlying electrochemical overlap between tyrosine and tryptophan. Instead, it enables *computational discrimination* by extracting latent waveform features such as curvature, derivative behavior, and temporal evolution that remain distinguishable even when the redox peaks overlap in the 1D voltammetric trace. This approach allows reliable quantification under varying pH conditions where traditional peak-based analysis fails. By extracting key electrochemical features and applying classification algorithms such as k-nearest neighbors (KNN), the system accurately quantified sweat biomarkers. The resulted design enabled wireless, real-time monitoring of exercise-related physiological changes [229]**.**

In addition to signal correction and noise suppression, ML algorithms are increasingly being employed for drift compensation. Long-term exposure of MXene electrodes to sweat constituents such as chloride ions and proteins can lead to surface oxidation, enzymatic degradation, or electrochemical fatigue, resulting in baseline shifts that conventional analytical models cannot account for. By

integrating time-dependent features and incorporating historical sensor performance data, recurrent neural network models and long short-term memory architectures have been developed to capture such temporal effects, enabling continuous recalibration during device operation. These models are particularly effective in wearable platforms used over extended periods or in applications requiring uninterrupted monitoring, such as glucose tracking in diabetic patients or electrolyte management during endurance sports.

Wang *et al.* (2024) developed a multifunctional MXene-based bioadhesive hydrogel epidermal sensor designed for seamless integration with the human skin. This hydrogel sensor offers not only excellent mechanical and electrical adhesion for high-quality electrophysiological signal acquisition (e.g., Electromyography (EMG)) but also provides robust UV protection, photothermal therapeutic effects, antibacterial properties, and efficient hemostasis. Notably, the integration with machine learning enabled the accurate recognition of sign language gestures based on EMG signals, highlighting its potential for intelligent diagnostics and human–machine interfaces. This work exemplifies the advancement of bioadhesive, multifunctional epidermic sensors for next-generation wearable healthcare technologies [230]. In another work, Guo *et al.* (2024) reported a high-performance MXene-functionalized piezoresistive sensor based on a surface-modified PDMS (FPDMS) sponge, fabricated through plasma treatment to enhance hydrogen bonding and material integration. The resulting MXene-FPDMS sponge achieved excellent sensitivity (14.2 kPa^{-1}), mechanical softness (modulus of 9.7 kPa), and structural integrity in a compact 450 µm-thick configuration, making it highly responsive to subtle pressure variations. When paired with deep learning algorithms, the sensor demonstrated remarkable capability in classifying 26 spoken letters and polite expressions with ~94% accuracy, showcasing the promise of MXene-based soft electronics in intelligent voice-interactive healthcare platforms and wearable systems [231].

A promising trend in wearable sensor development is the integration of soft, tissue-like materials with machine learning for advanced, intelligent interfacing. In this context, Wang *et al.* (2024) introduced a flexible conductive hydrogel engineered through hydrogen bonding between trisodium citrate dihydrate and MXene nanosheets. The resulting material demonstrates mechanical compliance with human skin (Young's modulus: 23.5–92 kPa), high sensitivity under both tensile and compressive modes, and long-term durability over 1000 deformation cycles. Notably, its ability to detect fine human motions such as joint movement or gait changes was extended into the digital realm through successful machine-learning-assisted handwriting recognition, achieving an accuracy of 97.44%. This convergence of hydrogel mechanics and AI-powered analysis signals a significant advancement for next-generation human-machine interfaces in healthcare and smart living environments.

The integration of adaptive machine learning with wearable electronics marks a major advancement in real-time, intelligent human–machine interfacing. In this regard, Duan *et al.* (2024) developed a smart MXene-based data glove incorporating 10-channel textile bending sensors and a near-sensor adaptive ML model for high-accuracy gesture recognition. The sensors, fabricated using a thermal transfer printing and MXene-infiltrated textile method, provide stable mechanical contact and high sensitivity. The embedded adaptive ML model achieved 99.5% accuracy for 14 gestures and maintained 98.1% accuracy even when expanded to 20 gestures, recovering 27.6% in performance through local updates without offloading computations. The system's successful deployment in robotic sorting tasks underscores its potential for next-generation applications in healthcare, the Metaverse, and intelligent robotics [232].

In evaluating algorithmic performance, comparative studies have highlighted distinctions in robustness, generalizability, and computational efficiency. Recent advancements in wearable biosensing have increasingly integrated machine learning to overcome limitations in selectivity, sensitivity, and real-time signal interpretation. By combining MXene-based electrochemical and optical sensors with various ML algorithms, including random forest, KNN, neural networks, and adaptive learning models researchers have demonstrated accurate, on-body detection of biomarkers such as glucose, cortisol, tyrosine, tryptophan, and dopamine, even in the presence of overlapping signals and environmental fluctuations. ML enhances the robustness of biosensors by enabling real-time correction for dynamic factors such as sweat pH, temperature, or motion artifacts, while also allowing multiplexed and explainable classification tasks, such as gesture recognition or disease risk profiling. These studies collectively show that integrating ML with next-generation MXene-based flexible sensors holds great promise for advancing personalized, non-invasive, and autonomous health monitoring platforms.

6.2. Digital Twin Technology for Biosensor Customization and In Silico Optimization

The integration of digital twin technology into the design and development pipeline of wearable biosensors represents a significant advancement in personalized diagnostics and precision health engineering [233, 234]. A digital twin, in this context, is not merely a real-time

digital replica of a user's physiological state, but a predictive and computationally tractable model that allows for the simulation, optimization, and iterative refinement of biosensor systems prior to physical deployment [233, 235]. When applied to the field of material-focused sensor development, digital twins provide a feedback-enabled framework through which virtual testing environments parameterized by user-specific sweat chemistry, temperature, and skin hydration can guide the rational design of sensing materials and architectures [234, 235]. In, digital twin–driven personalization framework for MXene-based wearable biosensors, real-time physiological data acquired from MXene-integrated sweat sensors, combined with user-specific metadata (e.g., hydration, activity level), are processed through a digital twin model. The system simulates physiological dynamics, predicts health trajectories, and provides adaptive feedback to optimize sensor calibration and enable personalized, non-invasive health monitoring.

One of the most promising applications of this approach lies in the use of simulated sweat environments for screening sensor performance across a physiologically relevant range of conditions. Instead of relying on a limited set of empirical test cases, computational sweat libraries generated from population-level biochemistry data can be used to evaluate sensor responses in silico [236]. These synthetic datasets, informed by wearable datasets or clinical reference values, can emulate edge cases such as hypo/hypernatremia, abnormal pH ranges, or stress-induced hormonal surges. Such models are critical for designing sensors that are not only sensitive within standard ranges but remain robust across interindividual and intraindividual variability. Recent works have shown that digital twin-based simulation platforms can model real-time ion dynamics at the skin–sensor interface and predict response degradation due to signal interference or biomolecular fouling, reducing the need for extensive empirical iteration in the early design stages [235, 237].

Beyond environmental simulation, digital twins are increasingly being used to guide in silico optimization of biosensor architecture, particularly in systems where multi-layered materials, enzymatic interfaces, or microfluidic modules are involved [234, 238]. Computational fluid dynamics (CFD) models coupled with finite element analysis (FEA) can simulate sweat diffusion, ion transport, and heat dissipation across flexible sensor platforms, enabling the refinement of microchannel dimensions, electrode geometries, and permeable membrane configurations [239, 240]. Material-level modeling further extends the utility of digital twins. Atomistic and mesoscopic simulations such as DFT (Mukasa et al., 2023; C. Wang et al., 2025a) and coarse-grained molecular dynamics (MD) (Deshpande et al., 2022; C. Wang et al., 2025b) have been employed to predict analyte–surface interactions, surface charge behavior, and ion transport mechanisms for emerging sensor materials, including MXenes. These predictive models can be integrated into multi-scale digital twin frameworks that span from nanoscopic surface chemistry to macroscopic signal behavior. Through iterative coupling between simulation and experimental feedback, material candidates can be rapidly screened, functionalization strategies can be virtually tested, and degradation profiles under simulated use can be mapped with time-dependent boundary conditions reflective of real-world usage patterns. The broader implication of embedding biosensor development into digital twin ecosystems is a shift toward material-by-design methodologies, where sensor components are no longer empirically derived but computationally generated, screened, and refined in silico before fabrication. This approach not only reduces material waste and accelerates development cycles but also increases the likelihood that the final sensor will exhibit reproducibility and resilience when deployed in personalized health monitoring scenarios. It also enables a move toward co-optimization, where sensing materials, device geometry, and data processing algorithms are designed together within a unified simulation framework.

As biosensors become increasingly integrated into decentralized care, athletic monitoring, and chronic disease management, the predictive power of digital twins will play a growing role in enabling devices that are not only reactive but anticipatory. The next generation of biosensors will likely be "born digital," with their structure, surface chemistry, and performance constraints defined not just in the lab, but within computational environments that model the physiological realities of the users they are intended to serve.

7. Challenges, Limitations, and Future Outlook

While MXene-based wearable biosensors hold significant promise for personalized health monitoring, several scientific, engineering, and translational challenges must be addressed before these systems can achieve reliable real-world deployment. These limitations extend across material stability, device integration, computational adaptation, and regulatory validation each of which shapes the long-term performance and clinical readiness of MXene-enabled platforms.From a materials standpoint, although certain MXene compositions have demonstrated strong operational stability under optimized laboratory conditions and short-term wear, their long-term performance in real-world sweat environments remains a critical challenge. MXenes, particularly $Ti_3C_2T_x$, exhibit

susceptibility to oxidative degradation in aqueous or humid environments, leading to changes in surface terminations, conductivity, and electrochemical activity. This issue becomes more pronounced during extended exposure to chloride-rich and protein-containing sweat. Achieving durable MXene electrodes requires advances in minimally oxidative synthesis, controlled surface termination engineering, antioxidant or zwitterionic coatings, and encapsulation strategies that maintain ion accessibility while preventing surface decay. Moreover, the broader MXene family beyond $Ti_3C_2T_x$ remains underexplored in biosensing applications, and comparative studies are needed to establish composition–performance relationships under physiologically variable conditions. Recent efforts have explored oxidation-resistant MXene architectures by integrating MXene sheets with chemically robust carbon frameworks. For example, several studies have demonstrated that *in-situ* functionalization of MXene on porous LIG creates a stabilizing interfacial microenvironment that suppresses oxidation and preserves conductivity [243–246]. Such MXene–LIG hybrids have enabled stable glucose sensing over extended periods, owing to improved oxygen barrier properties, enhanced electron transport, and reduced surface defect reactivity. These findings highlight the value of structural confinement and conductive carbon scaffolds in prolonging MXene electrochemical stability and represent a promising direction for future wearable biosensor design.

Another key challenge is the intrinsic specificity and selectivity of MXene-based sensors toward target analytes**.** Although MXenes possess rich surface chemistry and tunable terminations, their broad redox activity and high surface reactivity can lead to interference from structurally similar species in sweat, such as uric acid, ascorbic acid, dopamine, lactate, or electroactive amino acids. Improving chemical specificity will require more deliberate molecular engineering strategies, such as introducing selective recognition layers (aptamers, MIPs, zwitterionic polymers), leveraging MXene–metal or MXene–oxide heterostructures to modulate adsorption energetics, or tailoring surface terminations to enhance affinity toward the target analyte. Additionally, incorporating catalytic nanoparticles or enzymatic interfaces can reinforce selectivity by introducing biochemical orthogonality. Coupling these material-level strategies with ML-based signal deconvolution is expected to substantially elevate specificity in complex sweat matrices, particularly for multiplexed wearable platforms.

On the device level, challenges in ensuring stable skin–sensor contact, minimizing motion artifacts, and optimizing multi-analyte selectivity persist. Wearable platforms must not only detect target biomarkers with high fidelity but also maintain performance across different skin types, anatomical locations, and environmental settings. Biofouling from proteins, oils, and skin cells can lead to signal degradation, particularly in non-enzymatic or passive sensing formats. Furthermore, the integration of MXene electrodes with microfluidics, stretchable electronics, and wireless communication modules must be scalable, low-cost, and compatible with standard manufacturing processes.

In terms of computational adaptation, while machine learning and digital twin strategies significantly enhance personalization, their effectiveness depends heavily on the availability of large, diverse, and high-quality datasets. Most wearable sensor studies to date are limited in sample size and demographic diversity, raising concerns about generalizability and bias in model predictions. Real-time signal normalization, drift compensation, and cross-sensor harmonization are computationally intensive tasks, and their implementation on low-power, wearable hardware platforms remains constrained by trade-offs in latency and energy consumption. Furthermore, the interpretability of ML models remains a challenge in clinical settings, where transparency and accountability in decision-making are essential.

Regulatory and translational hurdles are also significant. Biocompatibility of MXene materials, especially for long-term skin contact or transdermal applications, must be thoroughly evaluated under ISO and FDA guidelines. Translating MXene-based sensors into healthcare environments also necessitates compliance with cybersecurity and patient data privacy standards, especially when integrated with telemedicine platforms or electronic health record systems. Secure encryption, authenticated wireless transmission, and robust data governance frameworks are therefore essential for clinical viability.

Despite these limitations, the outlook for MXene-enabled personalized biosensors remains highly promising. Several emerging directions offer clear pathways to overcome the above challenges. Advances in surface termination engineering [25, 111], heterostructures and –MXene hybrids [161]may yield improved biomolecular selectivity and enhanced chemical resilience. Scalable, oxidation-resistant synthesis routes such as fluorine-free etching, molten-salt routes, and gel-state delamination are expected to improve batch uniformity and environmental stability. Integrating MXenes into multimodal platforms that combine electrochemical sensing with strain, or optical readouts, supported by microfluidic sweat management and stretchable encapsulation, may enable more comprehensive physiological monitoring. Moreover, recent progress in high-performance MXene architectures, multimodal sensors capable of decoupling

simultaneous mechanical and biochemical stimuli, and fully stretchable standalone platforms further underscores the rapid technological evolution of the field and provides additional promising avenues for next-generation MXene-enabled wearable systems. These research opportunities establish a future trajectory toward MXene-based wearable biosensors that are more stable, intelligent, and individualized. This positions the field to deliver next-generation tools for precision diagnostics, preventive healthcare, and continuous real-world monitoring.

8. Conclusion

This review has presented a comprehensive exploration of MXene-based wearable biosensors, highlighting their potential to serve as key enablers of personalized and adaptive health monitoring through sweat analysis. The unique physiochemical features of MXenes, including high surface area, redox activity, and tunable surface terminations, have positioned them at the forefront of flexible bioelectronic platforms. Yet, as real-world deployment demands move beyond conventional performance metrics, material science alone is no longer sufficient. The next frontier lies in integrating these materials into intelligent, context-aware systems capable of adapting to dynamic physiological states and individual biochemical signatures.

Through this lens, we examined how engineering strategies, from surface functionalization and composite design to micro/nanostructuring and ion-exchange control,I can tailor MXene interfaces for personalized sweat sensing. We further demonstrated how recent advances in adaptive signal processing, machine learning–driven calibration, and digital twin modeling allow biosensors to evolve from static detectors into predictive, self-correcting systems. These computational frameworks not only enhance real-time accuracy under variable conditions but also enable simulation-driven sensor design, material optimization, and health trajectory forecasting.

Digital twin technology represents a paradigm shift in biosensor development, bridging virtual environments with real-time data streams to allow for in silico customization, physiological modeling, and closed-loop decision-making. When coupled with a deep understanding of sweat variability and human-specific biomarker expression, this framework facilitates the development of biosensors that are not only wearable and sensitive, but also meaningfully responsive to the uniqueness of each user.

Despite significant progress, the path toward clinical and commercial adoption still demands solutions to challenges related to long-term material stability, data interpretability, signal reproducibility, and regulatory compliance. Nevertheless, the convergence of MXene chemistry, advanced fabrication, machine learning, and digital physiology points toward a future in which biosensors are seamlessly embedded into personalized digital health ecosystems. These systems will not merely record data, but actively guide interventions, adapt to the user, and contribute to a more anticipatory, precise, and accessible model of healthcare.

Author Contribution

Onur Karaman: Writing – review & editing, Writing – original draft, Visualization, Conceptualization.
Ceren Karaman: Writing – review & editing, Writing – original draft, Visualization, Conceptualization.
Jun Jiang: Writing – Writing – original draft
Zhao Taotao: Writing – review & editing, Writing – original draft.

Competing Interests

There is no financial, personal, or professional relationships that could influence this manuscript to declare between the authors.

Declaration of generative AI and AI-assisted technologies in the writing process

During the preparation of this work the authors used ChatGPT to improve the readability and language of the manuscript. After using this tool/service, the authors reviewed and edited the content as needed and take full responsibility for the content of the publication.

Research Funding

This paper was supported by Medical and Health Talent Research Initiation Fund Class G (Grant Number KYQD2024-020), The Quzhou Affiliated Hospital of Wenzhou Medical University.

Data availability

References

[1] S. Gong, Y. Lu, J. Yin, A. Levin, and W. Cheng. “Materials-driven soft wearable bioelectronics for connected healthcare.”. *Chem Rev*, **124**: 455-553, (2024).

[2] M. Kim, D.J. Joe, I. Doh, and Y.H. Cho. “Piezoelectric nanocomposite-based multifunctional wearable bioelectronics for mental stress analysis utilizing physiological signals.”. *Adv Mater Technol*, **9**: 2301610, (2024).

[3] J. Xu, Y. Fang, and J. Chen. “Wearable biosensors for non-invasive sweat diagnostics.”. *Biosensors*, **11**:245, (2021).

[4] M. Chen, D. Cui, H. Haick, and N. Tang. “Artificial intelligence-based medical sensors for healthcare system.”. *Adv Sensor Res,* **3**: 2300009, (2024).

[5] H. Haick and N. Tang. “Artificial intelligence in medical sensors for clinical decisions.”. *ACS Nano,* **15**: 3557-3567, (2021).

[6] S. Shajari, K. Kuruvinashetti, A. Komeili, and U. Sundararaj. “The emergence of ai-based wearable sensors for digital health technology: a review.”. *Sensors*, **23**: 9498, (2023).

[7] Z. Zhang, Z. Li, K. Wei, Z. Cao, Z. Zhu, and R. Chen. “Sweat as a source of non-invasive biomarkers for clinical diagnosis: an overview.”. *Talanta,* **273**: 125865, (2024).

[8] R.D. Munje, S. Muthukumar, B. Jagannath, and S. Prasad. "A new paradigm in sweat based wearable diagnostics biosensors using room temperature ionic liquids (RTILs).". *Sci Rep*, **7**:1950, (2017).

[9] S.M. Khor, J. Choi, P. Won, and S.H. Ko."Challenges and strategies in developing an enzymatic wearable sweat glucose biosensor as a practical point-of-care monitoring tool for type ii diabetes.". *Nanomater*, **12**:221, (2022).

[10] C. Wu."Non-invasive wearable sweat and tear-based biosensors for continuous health monitoring.". *Highlights Sci Eng Technol,* **55:** 9959*, (*2023).

[11] R.F.R. Ursem, A. Steijlen, M. Parrilla, J. Bastemeijer, A. Bossche, and K. De Wael. "Worth your sweat: wearable microfluidic flow rate sensors for meaningful sweat analytics.". *Lab Chip*, **25**: 1296–1315, (2025).

[12] J.N. Hussain, N. Mantri, and M.M. Cohen. "Working up a good sweat - the challenges of standardising sweat collection for metabolomics analysis.". *Clin Biochem Rev*, **38**: 13, (2017).

[13] L.B. Baker. "Physiology of sweat gland function: the roles of sweating and sweat composition in human health.". *Temperature*, **6:** 211-259, (2019).

[14] J. Min, J. Tu, C. Xu, H. Lukas, S. Shin, Y. Yang, S.A. Solomon, D. Mukasa, and W. Gao. "Skin-interfaced wearable sweat sensors for precision medicine.". *Chem Rev,* **123:** 5049-5138. (2023).

[15] H. Ehtesabi and S.O. Kalji. "Carbon nanomaterials for sweat-based sensors: a review.". *Microchim Acta,* **191**:77, (2024).

[16] H. Li and D. Wang."Progress and applications of nanotechnology-based wearable sensors in human motion and posture detection.". *J Nanostruct Chem*, **15**: 152504, (2025).

[17] V. Kedambaimoole, K. Harsh, K. Rajanna, P. Sen, M.M. Nayak, and S. Kumar. "MXene wearables: properties, fabrication strategies, sensing mechanism and applications.". *Mater Adv*, **3:**3784-3808, (2022).

[18] W. Ji, J. Zhu, W. Wu, N. Wang, J. Wang, J. Wu, Q. Wu, X. Wang, C. Yu, G. Wei, L. Li, and F. Huo. "Wearable sweat biosensors refresh personalized health/medical diagnostics.". *Research*, **2021**: 9757126, (2021).

[19] D. Mohanapriya, J. Satija, S. Senthilkumar, V. Kumar Ponnusamy, and K. Thenmozhi. "Design and engineering of 2D MXenes for point-of-care electrochemical detection of bioactive analytes and environmental pollutants.". *Coord Chem Rev,* **507**:215746, (2024).

[20] M.R. Ali, M.S. Bacchu, M.R. Al-Mamun, M.I. Hossain, A. Khaleque, A. Khatun, D.D. Ridoy, M.A.S. Aly, and M.Z.H. Khan. "Recent advanced in MXene research toward biosensor development.". *Crit. Rev. Anal. Chem.***, 54:**1381-1398, (2024).

[21] L. Jia, Zh. Lei, N. Zare, T. Wu, M. Ghalkhani, L. Wan, and Y. Xu."Ti3C2 MXene-enhanced electro- chemical biosensors for prostate-specific antigen (psa) detection in prostate cancer.". *J Nanostruct Chem*, **1**: 152502, (2025).

[22] M. Safarkhani, B. Farasati Far, E.C. Lima, S. Jafarzadeh, P. Makvandi, R.S. Varma, Y.S. Huh, M. Ebrahimi Warkiani, and N. Rabiee. "Integration of mxene and microfluidics: a perspective.", *ACS Biomater sci Eng,* **10:**657-676, (2024).

[23] A. Khosla, Sonu, H.T.A. Awan, K. Singh, Gaurav, R. Walvekar, Z. Zhao, A. Kaushik, M. Khalid, and V. Chaudhary. "Emergence of MXene and MXene–polymer hybrid membranes as future-environmental remediation strategies.". *Adv Sci*, **9:**2203527, (2022).

[24] T. Zhang, L. Chang, and X. Xiao. "Surface and interface regulation of mxenes: methods and properties.". *Adv Sci,* **9:** 2203527, (2023).

[25] V. Natu and M.W. Barsoum. "MXene surface terminations: a perspective.". *J. Phys. Chem. C,* **127:** 20197-20206, (2023).

[26] N. Li, J. Peng, W.J. Ong, T. Ma, Arramel, P. Zhang, J. Jiang, X. Yuan, and C. (John) Zhang. "MXenes: an emerging platform for wearable electronics and looking beyond.". *Matter*, **4:** 377-407, (2021).

[27] S. Moradi, A. Firoozbakhtian, M. Hosseini, O. Karaman, S. Kalikeri, G.G. Raja, and H. Karimi-Maleh. "Advancements in wearable technology for monitoring lactate levels using lactate oxidase enzyme and free enzyme as analytical approaches: a review.". *Int J Biol Macromol*, **254**: 127577, (2024).

[28] R. Ibragimova, M.J. Puska, and H.P. Komsa. "PH-dependent distribution of functional groups on titanium-based mMXenes.". *ACS Nano*, **13**: 9171-9181, (2019).

[29] S. Patle and D. Rotake. "Recent advances, technological challenges and requirements to predict the future treads in wearable sweat sensors: a critical review.". *Microchemical Journal*, **200**: 110457, (2024).

[30] A. Cazalé, W. Sant, F. Ginot, J.C. Launay, G. Savourey, F. Revol-Cavalier, J.M. Lagarde, D. Heinry, J. Launay, and P. Temple-Boyer. "Physiological stress monitoring using sodium ion potentiometric microsensors for sweat analysis.". *Sens Actuators B Chem*, **225**:1-9, (2016).

[31] L.B. Baker and A.S. Wolfe. "Physiological mechanisms determining eccrine sweat composition.". *Eur J Appl Physiol,* **120:** 719-752, (2020).

[32] L. Klous, C.J. de Ruiter, S. Scherrer, N. Gerrett, and H.A.M. Daanen. "The (in)dependency of blood and sweat sodium, chloride, potassium, ammonia, lactate and glucose concentrations during submaximal exercise.". *Eur J Appl Physiol*, **121**: 803-816, (2021).

[33] H. Zafar, A. Channa, V. Jeoti, and G.M. Stojanović. "Comprehensive review on wearable sweat-glucose sensors for continuous glucose monitoring.". *Sensors*, **22:**638, (2022).

[34] P.J. Derbyshire, H. Barr, F. Davis, and S.P.J. Higson."Lactate in human sweat: a critical review of research to the present day.". *J Physiol Sci,* **62**:429-440**, (**2012).

[35] E.C. Nakajima and B. Van Houten."Metabolic symbiosis in cancer: refocusing the warburg lens." . *Mol Carcinog*, **52**: 329-337, (2013).

[36] A. Futane, M. Senthil, S. Jayashree, A. Srinivasan, R. Kalpana, and V. Narayanamurthy. "Sweat analysis for urea sensing: trends and challenges.". *Analytical Methods*, **15**:4405-4426, (2023).

[37] S. Sudha, R. Kalpana, and P. Soundararajan. "Quantification of sweat urea in diabetes using electro-optical technique.". *Physiol Meas*, **42**: 095002, (2021).

[38] Y. Zhang, H. Guo, S.B. Kim, Y. Wu, D. Ostojich, S.H. Park, X. Wang, Z. Weng, R. Li, A.J. Bandodkar, Y. Sekine, J. Choi, S. Xu, S. Quaggin, R. Ghaffari, and J.A. Rogers. "Passive sweat collection and colorimetric analysis of biomarkers relevant to kidney disorders using a soft microfluidic system." . *Lab Chip*, **19**: 1545-1555, (2019).

[39] C.T. Huang, M.L. Chen, L.L. Huang, and I.F. Mao."Uric acid and urea in human sweat." . *Chinese J Physiol*, **45**:109-115, (2002).

[40] T. Laochai, C. Moonla, J. Moon, K. Sakdaphetsiri, L. Yin, L.F. Mendes, A. Abbas, O. Djassemi, S. Seker, K. Mahato, O. Chailapakul, J. Wang, and N. Rodthongkum. "Touch–based potentiometric sensors for simultaneous detection of urea and ammonium from fingertip sweat.". *Sens Actuators B Chem*, **413**: 135898, (2024).

[41] Y. Araki and S. Ando. "Urea, amino acid and ammonia in human sweat.". *Japanese Journal of Physiology*, **3**:211-218, (1952).

[42] S. Itoh and T. Nakayama."Ammonia in human sweat and its origin.". *Japanese J Physiol*, **3**:133-137, (1952).

[43] D. Czarnowski, J. Górski, J. Jóźwiuk, and A. Boroń-Kaczmarska. "Plasma ammonia is the principal source of ammonia in sweat.". *Eur J Appl Physiol Occup Physiol*, **65**:135-137, (1992).

[44] M.A. King, S.D. Brown, K.A. Barnes, P.J.D. De Chavez, and L.B. Baker. "Regional and time course differences in sweat cortisol, glucose, and select cytokine concentrations during exercise.". *Eur J Appl Physiol*, **123**: 1727-1738, (2023).

[45] C.J. Weber, O.M. Clay, R.E. Lycan, G.K. Anderson, and O. Simoska. "Advances in electrochemical biosensor design for the detection of the stress biomarker cortisol.". *Anal Bioanal Chem,* **416**: 87-106, (2024).

[46] M. Sekar, M. Pandiaraj, S. Bhansali, N. Ponpandian, and C. Viswanathan."Carbon fiber based electrochemical sensor for sweat cortisol measurement.". *Sci Rep*, **9**:403, (2019).

[47] P. Pearlmutter, G. DeRose, C. Samson, N. Linehan, Y. Cen, L. Begdache, D. Won, and A. KOH. "Sweat and saliva cortisol response to stress and nutrition factors." . *Sci Rep*, **10**:19050, (2020).

[48] L. Tian, M. Jiang, M. Su, X. Cao, Q. Jiang, Q. Liu, and C. Yu. "Sweat cortisol determination utilizing MXene and multi-walled carbon nanotube nanocomposite functionalized immunosensor.". *Microchemical Journal*, **185**: 108172, (2023).

[49] M. Ding, S. Zhang, J. Wang, Y. Ding, and C. Ding. "Ultrasensitive ratiometric electrochemiluminescence sensor with an efficient antifouling and antibacterial interface of PSBMA@SiO2-MXene for oxytetracycline trace detection in the marine environment.". *Anal Chem*, **95**: 16327-16334, (2023).

[50] J.C.C. Sheng, B.D. La Franier, and M. Thompson. "Assembling surface linker chemistry with minimization of non-specific adsorption on biosensor materials.". *Materials*, **14**:472, (2021).

[51] A. Karrat and A. Amine. "Innovative approaches to suppress non-specific adsorption in molecularly imprinted polymers for sensing applications.". *Biosens Bioelectron*, **250**: 116053, (2024).

[52] N.R. Jalal, T. Madrakian, M. Ahmadi, A. Afkhami, S. Khalili, M. Bahrami, and M. Roshanaei. "Wireless wearable potentiometric sensor for simultaneous determination of ph, sodium and potassium in human sweat.". *Sci Rep*, **14**: 11526, (2024).

[53] K. Zhao, B. Kang, and B. Zhou."Wearable electrochemical sensors for monitoring of inorganic ions and ph in sweat.". *Int J Electrochem Sci*, **17**: 220452, (2022).

[54] V. Couturaud."Biophysical characteristics of the skin in relation to race, sex, age, and site." Handbook of Cosmetic Science and Technology, Third Edition,pp. 5-24, (2009).

[55] X. Sun, X. Gao, Z. Li, X. Zhang, X. Zhai, Q. Zhang, L. Li, N. Gao, G. He, and H. Li. "Nanowires framework supported porous lotus-carbon anode boosts lithium-ion and sodium-ion batteries.". *Small Methods*, **8**: 2300746, (2024).

[56] A.C. Gonçalves, F.A.L. Marson, R.M.H. Mendonça, C.S. Bertuzzo, I.A. Paschoal, J.D. Ribeiro, A.F. Ribeiro, and C.E. Levy. "Chloride and sodium ion concentrations in saliva and sweat as a method to diagnose cystic fibrosis.". *J Pediatr (Rio J)*, **95**: 443-450, (2019).

[57] J.J. Wine."How the sweat gland reveals levels of cftr activity.", *J Cystic Fibros*, 2022, **21**:396-406 (2022).

[58] P. Braconnier, B. Milani, N. Loncle, J.M. Lourenco, W. Brito, J. Delacoste, M. Maillard, M. Stuber, M. Burnier, and M. Pruijm. "Short-term changes in dietary sodium intake influence sweat sodium concentration and muscle sodium content in healthy individuals.". *J Hypertens*, **38**: 159-166, (2020).

[59] D.S. Bari, H.Y. Yacoob Aldosky, and Ø.G. Martinsen. "Simultaneous measurement of electrodermal activity components correlated with age-related differences.". *J Biol Phys*, **46**: 177-188, (2020).

[60] N.A. Coull, A.M. West, S.G. Hodder, P. Wheeler, and G. Havenith. "Body mapping of regional sweat distribution in young and older males.". *Eur J Appl Physiol*, **121**: 109-125, (2021).

[61] M. Villiger, R. Stoop, T. Vetsch, E. Hohenauer, M. Pini, P. Clarys, F. Pereira, and R. Clijsen. "Evaluation and review of body fluids saliva, sweat and tear compared to biochemical hydration assessment markers within blood and urine.". *Eur J Clin Nutr*, **72**: 69-76, (2018).

[62] J. Surapongchai, V. Saengsirisuwan, I. Rollo, R.K. Randell, K. Nithitsuttibuta, P. Sainiyom, C.H.W. Leow, and J.K.W. Lee. "Hydration status, fluid intake, sweat rate, and sweat sodium concentration in recreational tropical native runners.". *Nutrients*, **13**: 1374, (2021).

[63] S.N. Cheuvront and R.W. Kenefick."Dehydration: physiology, assessment, and performance effects.". *Compr Physiol*, **4**: 257-285, (2014).

[64] S. Pham, D. Yeap, G. Escalera, R. Basu, X. Wu, N.J. Kenyon, I. Hertz-Picciotto, M.J. Ko, and C.E. Davis. "Wearable sensor system to monitor physical activity and the physiological effects of heat exposure.". *Sensors*, **20**: 855, (2020).

[65] J. Siquier- Coll, I. Bartolomé, M. Pérez-Quintero, F.J. Grijota, D. Muñoz, and M. Maynar-Mariño. "Effect of heat exposure and physical exercise until exhaustion in normothermic and hyperthermic conditions on serum, sweat and urinary concentrations of magnesium and phosphorus.". *J Therm Biol*, **84**: 176-184, (2019).

[66] L. Klous, C. de Ruiter, P. Alkemade, H. Daanen, and N. Gerrett. "Sweat rate and sweat composition following active or passive heat re-acclimation: a pilot study.". *Temperature*, **8**: 90-104, (2021).

[67] N.K.M. Churcher, S. Upasham, P. Rice, C.F. Greyling, and S. Prasad. “Sweat based-multiplexed detection of npy-cortisol for disease diagnostics and stress management.”. *Electroanalysis*, **34**: 375-386, (2022).

[68] S. Upasham, A. Bhide, K.C. Lin, and S. Prasad. “Point-of-use sweat biosensor to track the endocrine-inflammation relationship for chronic disease monitoring.”. *Future Sci OA*, **7**: FSO628, (2021).

[69] C. Cheng, X. Li, G. Xu, Y. Lu, S.S. Low, G. Liu, L. Zhu, C. Li, and Q. Liu. “Battery-free, wireless, and flexible electrochemical patch for in situ analysis of sweat cortisol via near field communication.”. *Biosens Bioelectron*, **172**: 112782, (2021).

[70] A.D. Grant, T.J. Upton, J.R. Terry, B.L. Smarr, and E. Zavala. “Analysis of wearable time series data in endocrine and metabolic research.”. *Curr Opin Endocr Metabol Res,* **25:** 100380, (2022).

[71] X. Yuan, C. Li, X. Yin, Y. Yang, B. Ji, Y. Niu, and L. Ren.“Epidermal wearable biosensors for monitoring biomarkers of chronic disease in sweat.”. *Biosensors*, **13:**313, (2023).

[72] N. Tiwari, S. Chatterjee, K. Kaswan, J.H. Chung, K.P. Fan, and Z.H. Lin. “Recent advancements in sampling, power management strategies and development in applications for non-invasive wearable electrochemical sensors.”. *J Electroanal Chem*, **907**:116064, (2022).

[73] J. Foster, J.W. Smallcombe, S. Hodder, O. Jay, A.D. Flouris, and G. Havenith. “Quantifying the impact of heat on human physical work capacity; part ii: the observed interaction of air velocity with temperature, humidity, sweat rate, and clothing is not captured by most heat stress indices.”. *Int J Biometeorol*, **66**: 507-520, (2022).

[74] B. Zhong, K. Jiang, L. Wang, and G. Shen. “Wearable sweat loss measuring devices: from the role of sweat loss to advanced mechanisms and designs.”, A*dv Sci*, **9:**2103257, (2022).

[75] U. Amara, I. Hussain, M. Ahmad, K. Mahmood, and K. Zhang. “2D mxene-based biosensing: a review.”. *Small*, 19: 2205249, (2023).

[76] Y. Yang, S. Yang, X. Xia, S. Hui, B. Wang, B. Zou, Y. Zhang, J. Sun, and J.H. Xin. “MXenes for wearable physical sensors toward smart healthcare.”. *ACS Nano*, **18**: 24705–24740, (2024).

[77] C.G. Ann Maria, A. Varghese, and M. Nidhin. “Recent advances in nanomaterials based molecularly imprinted electrochemical sensors.”. *Critical Rev Anal Chem,* 53:88-97, (2023).

[78] S. Patle and D. Rotake.“Recent advances, technological challenges and requirements to predict the future treads in wearable sweat sensors: a critical review.”. *Microchemical Journal*, **200**: 110457, (2024).

[79] A. Childs, B. Mayol, J.A. Lasalde-Ramírez, Y. Song, J.R. Sempionatto, and W. Gao. “Diving into sweat: advances, challenges, and future directions in wearable sweat sensing.” . *ACS Nano*, **18**: 24605–24616, (2024).

[80] R. Liang, L. Zhong, Y. Zhang, Y. Tang, M. Lai, T. Han, W. Wang, Y. Bao, Y. Ma, S. Gan, and L. Niu. “Directly using ti3c2tx mxene for a solid-contact potentiometric pH sensor toward wearable sweat ph monitoring.”. *Membranes*, **13**: 376, (2023).

[81] D. Jiang, X. Liu, W. Zhan, M. Fu, J. Liu, J. He, Y. Li, Y. Li, X. Chen, and C. Yu. “Skin-interfaced wearable sensor for long-term reliable monitoring of uric acid and pH in sweat.”. *Nano Lett*, **25**: 1427–1435, (2025).

[82] Q. Ning, S. Feng, Y. Cheng, T. Li, D. Cui, and K. Wang. “Point-of-care biochemical assays using electrochemical technologies: approaches, applications, and opportunities.”. *Microchim Acta*, **189**:310, (2022).

[83] D.H. Ho, Y.Y. Choi, S.B. Jo, J.M. Myoung, and J.H. Cho. “Sensing with Mxenes: progress and prospects.”. *Adv Mater*, **33:** 2005846, (2021).

[84] N. Davis, J. Heikenfeld, C. Milla, and A. Javey. “The challenges and promise of sweat sensing.”. *Nat Biotechnol*, **42**: 860-871, (2024).

[85] P. Zhao, E.D. Patamia, and T.L. Andrew. “Strategies to combat the fouling and surface texture issues associated with fabric-based colorimetric sensors.”. *Sens Actuators B Chem*, **377**: 133099, (2023).

[86] X. Qiao, Y. Cai, Z. Kong, Z. Xu, and X. Luo. “A wearable electrochemical sensor based on anti-fouling and self-healing polypeptide complex hydrogels for sweat monitoring.” . *ACS Sens*, **8**: 2834-2842, (2023).

[87] Z. Xu, Y. Liu, M. Lv, X. Qiao, G.C. Fan, and X. Luo. “An anti-fouling wearable molecular imprinting sensor based on semi-interpenetrating network hydrogel for the detection of tryptophan in sweat.”. *Anal Chim Acta*, **1283**: 341948, (2023).

[88] S. Liu, J. Tang, F. Ji, W. Lin, and S. Chen. “Recent advances in zwitterionic hydrogels: preparation, property, and biomedical application.”, *Gels*, **8:**46. (2022).

[89] Z. Song, R. Han, K. Yu, R. Li, and X. Luo. “Antifouling strategies for electrochemical sensing in complex biological media.” *Microchimica Acta*, **191**:138, (2024).

[90] X. Yin, E. Peri, E. Pelssers, J. Den Toonder, and M. Mischi.“Estimation of blood glucose levels by sweat sensing based on biophysical modeling of glucose transport.” 2023 IEEE International Symposium on Medical Measurements and Applications, MeMeA 2023 - Conference Proceedings (2023).

[91] W. Gao, G.A. Brooks, and D.C. Klonoff.“Wearable physiological systems and technologies for metabolic monitoring.”. *J Appl Physiol,* **124:** 548-556, *(*2018).

[92] M. Hemdan, M.A. Ali, A.S. Doghish, S.S.A. Mageed, I.M. Elazab, M.M. Khalil, M. Mabrouk, D.B. Das, and A.S. Amin. “Innovations in biosensor technologies for healthcare diagnostics and therapeutic drug monitoring: applications, recent progress, and future research challenges.”. *Sensors*, **24**: 5143, (2024).

[93] U. Chadha, P. Bhardwaj, R. Agarwal, P. Rawat, R. Agarwal, I. Gupta, M. Panjwani, S. Singh, C. Ahuja, S.K. Selvaraj, M. Banavoth, P. Sonar, B. Badoni, and A. Chakravorty. “Recent progress and growth in biosensors technology: a critical review.”. *J Ind Eng Chem,* **109**:21-51*, (*2022).

[94] Y. Huang, C. Luo, F. Xia, Y. Song, L. Jiang, and F. Li. “Multi-analyte sensing strategies towards wearable and intelligent devices.”. *Chem Sci*, **13:** 12309-12325, (2022).

[95] F. Beygnezhad, K. Dashtian, R. Zare-Dorabei, and Z. Zangouei.“Biological ce/fe-metal organic framework multifunctional nanozyme-based colorimetric sensor array for multi-analyte detection in human sweat.”. *Sens Actuators B Chem*, **423**: 136769, (2025).

[96] Y. Zhang, Y. Sun, J. Han, M. Zhang, F. Li, and D. Yang."High-sensitivity flexible electrochemical sensor for real-time multi-analyte sweat analysis.". *Talanta*, **287**: 127644, (2025).

[97] Q. ul A. Zahra, S. Ullah, F. Shahzad, B. Qiu, X. Fang, A. Ammar, Z. Luo, and S. Abbas Zaidi. "MXene-based aptasensors: advances, challenges, and prospects.". *Prog Mater Sci*, 129:100967, (2022).

[98] M.A.K. Purbayanto, V. Presser, K. Skarżyński, M. Słoma, M. Naguib, and A.M. Jastrzębska. "MXenes: multifunctional materials for the smart cities of tomorrow.". *Adv Funct Mater*, **35**: 2409953, (2025).

[99] M. Naguib, M.W. Barsoum, and Y. Gogotsi. "Ten years of progress in the synthesis and development of Mxenes.". *Advanced Materials*, **33**: 2103393, (2021).

[100] J.C. Lei, X. Zhang, and Z. Zhou. "Recent advances in Mxene: preparation, properties, and applications.". *Frontiers of Physics*, **10**:276-286, (2015).

[101] S.M.M. Raj, A.K. Sundramoorthy, R. Atchudan, D. Ganapathy, and A. Khosla."Review—recent trends on the synthesis and different characterization tools for Mxenes and their emerging applications.". *J Electrochem Soc*, **169**: 077501, (2022).

[102] Y. Xu, L. Wan, N. Zare, S.-W. Wang, and Zh. Lei. "Cr2C Mxene modification of an electrochemical platform allows for highly selective and sensitive detection of PSMA, a prostate cancer biomarker.". *J Nanostruct Chem*, **15**: 152517, (2025).

[103] Z. Zhang and H. Karimi-Maleh."Label-free electrochemical aptasensor based on gold nanoparticles/titanium carbide Mxene for lead detection with its reduction peak as index signal.". *Adv Compos Hybrid Mater*, **6**: 68, (2023).

[104] N. Zare, H. Karimi-Maleh, Z. Zhang, L. Fu, J. Rouhi, N. Zhong, Y. Wen, and M. Ghalkhani. "Enhancing cancer biomarker identification: precise monitoring of muc1 using V2C/Au nanocomposite-amplified electrochemical biosensor.". *Carbon Letters*, **35**: 1691–1700, (2025).

[105] N. Zare, H. Karimi-Maleh, Z. Zhang, Y. Wen, N. Zhong, and L. Fu. "Enhanced detection of HER2 using a TiVC Xenes/gold nanocomposite amplified analytical biosensor for precise cancer biomarker monitoring.". *Adv Compos Hybrid Mater*, **7**: 165, (2024).

[106] C.B. Subba, D.P. Rai, M.E. Tursunov, A.T. Dekhkonov, and Z. Pachuau. "Comprehensive review of max phase and Mxene materials: synthesis, properties, and applications.". *Carbon Letters*, **35:** 2485-2570, (2025).

[107] N.H. Solangi, S.A. Mazari, N.M. Mubarak, R.R. Karri, N. Rajamohan, and D.V.N. Vo."Recent trends in Mxene-based material for biomedical applications." . *Environ Res*, **222**: 115337, (2023).

[108] C. Sen Liu, J. Li, and H. Pang. "Metal-organic framework-based materials as an emerging platform for advanced electrochemical sensing.". *Coor Chem Rev*, 410:213222, (2020).

[109] B.C. Wyatt, A. Rosenkranz, and B. Anasori. "2D Mxenes: tunable mechanical and tribological properties.". *Adv Mater*, **33**: 2007973, (2021).

[110] G. Li, S. Lian, J. Wang, G. Xie, N. Zhang, and X. Xie. "Surface chemistry engineering and the applications of Mxenes.". *Journal of Materiomics*, **9**: 1160-1184, (2023).

[111] X. Wang, G.M.C. Ong, M. Naguib, and J. Wu. "Theoretical insights into Mxene termination and surface charge regulation.". *J Phys Chem C*, **125**: 21771-21779, (2021).

[112] L. Liu, E. Raymundo-Piñero, S. Sunny, P.L. Taberna, and P. Simon. "Role of surface terminations for charge storage of Ti3C2Tx Mxene electrodes in aqueous acidic electrolyte.". *Angewandte Chemie*, **63**: e202319238, (2024).

[113] F. Shahzad, S.A. Zaidi, and R.A. Naqvi. "2D transition metal carbides (Mxene) for electrochemical sensing: a review.". *Critical Reviews in Analytical Chemistry*, **52:**848-864, (2022).

[114] M. Pantrangi, E. Ashalley, M.K. Hadi, H. Xiao, Y. Zhang, W. Ahmed, N. Singh, A. Alam, U. Younis, F. Ran, P. Liang, and Z. Wang. "Flexible micro-supercapacitors: materials and architectures for smart integrated wearable and implantable devices.". *Energy Storage Mater*, **73**: 103791, (2024).

[115] J.L. Hart, K. Hantanasirisakul, A.C. Lang, B. Anasori, D. Pinto, Y. Pivak, J.T. van Omme, S.J. May, Y. Gogotsi, and M.L. Taheri. "Control of Mxenes' electronic properties through termination and intercalation.". *Nat Commun*, **10**:522, (2019).

[116] A.A.A. Abdelazeez, A. Ben Gouider Trabelsi, F.H. Alkallas, S. AlFaify, M. Shkir, T.A. Alrebdi, K.S. Almugren, F. V. Kusmatsev, and M. Rabia. "Tuning the structural, electronic, and optical properties of monolayer graphene through heteroatom doping: a first-principles study with future light sensing applications.". *Photonics*, **10**:838, (2023).

[117] A. Wojciechowska, M. Chandel, and A.M. Jastrzębska. "Surface functionalization and interfacial design of Mxenes.". *MXene Nanocomposites: Design, Fabrication, and Shielding Applications, CRC Press,* 37-66. (2023).

[118] X. Han, K. Cao, Y. Yao, J. Zhao, C. Chai, and P. Dai. "A novel electrochemical sensor for glucose detection based on a Ti3X2Tx/ZIF-67 nanocomposite.". *RSC Adv*, **12**: 20138-20146, (2022).

[119] M. Lounasvuori, T. Zhang, Y. Gogotsi, and T. Petit. "Tuning the microenvironment of water confined in Ti3C2Tx Mxene by cation intercalation." . *Journal of Physical Chemistry C*, **128**: 2803-2813, (2024).

[120] M. Hu, L. Chen, Y. Jing, Y. Zhu, J. Dai, A. Meng, C. Sun, J. Jia, and Z. Li. "Intensifying electrochemical activity of Ti3C2Tx Mxene via customized interlayer structure and surface chemistry.". *Molecules*, **28**: 5776, (2023).

[121] S. Kumar."Fluorine-free mxenes: recent advances, synthesis strategies, and mechanisms.". *Small*, *20*:2308225, (2024).

[122] Y. Long, Y. Tao, T. Shang, H. Yang, Z. Sun, W. Chen, and Q.H. Yang. "Roles of metal ions in Mxene synthesis, processing and applications: a perspective.". *Adv Sci*, **9:** 2200296, (2022).

[123] M. Okubo, A. Sugahara, S. Kajiyama, and A. Yamada. "MXene as a charge storage host." . *Acc Chem Res*, **51**: 591-599, (2018).

[124] R.K. Sen, P. Prabhakar, N. Bisht, M. Patel, S. Mishra, A.K. Yadav, D. V. Venu, G.K. Gupta, P.R. Solanki, S. Ramakrishnan, D.P. Mondal, A.K. Srivastava, N. Dwivedi, and C. Dhand. "2D materials-based aptamer biosensors: present status and way forward.". *Curr Med Chem*, **29**: 5815-5849, (2021).

[125] R. Khan and S. Andreescu. "Mxenes-based bioanalytical sensors: design, characterization, and applications.". *Sensors*, **20:**5434, (2020).

[126] J. Wen, Q. Fu, W. Wu, H. Gao, X. Zhang, and B. Wang. "Understanding the different diffusion mechanisms of hydrated protons and potassium ions in titanium carbide Mxene.". *ACS Appl Mater Interfaces*, **11**: 7087-7095, (2019).

[127] S. Kalasin and P. Sangnuang."Multiplex wearable electrochemical sensors fabricated from sodiated polymers and Mxene nanosheet to measure sodium and creatinine levels in sweat.". *ACS Appl Nano Mater*, **6**: 18209–18221, (2023).

[128] A. Prasad, J. Hasse, T. Steimle, D. Nepal, G.J. Frank, and V. Varshney."Mechanical behavior of Mxene-polymer layered nanocomposite using computational finite element analysis.". *Compos B Eng*, **284**: 111689, (2024).

[129] S. Wan, X. Li, Y. Chen, N. Liu, S. Wang, Y. Du, Z. Xu, X. Deng, S. Dou, L. Jiang, and Q. Cheng. "Ultrastrong Mxene films via the synergy of intercalating small flakes and interfacial bridging.". *Nat Commun*, **13**: 7340, (2022).

[130] C. Liang, Y. Meng, Y. Zhang, H. Zhang, W. Wang, M. Lu, and G. Wang. "Insights into the impact of interlayer spacing on Mxene-based electrodes for supercapacitors: a review.". *J Energy Storage*, **65:**107341, (2023).

[131] K. Arole, S.E. Pas, R.M. Thakur, L.A. Amiouny, M.H. Kabir, M. Dujovic, M. Radovic, J.L. Lutkenhaus, M.J. Green, and H. Liang."Effects of intercalation on ml-$Ti_3C_2T_z$ mxene properties and friction performance.". *ACS Appl Mater Interfaces*, **16**: 64156–64165, (2024).

[132] A. Altan and M. Namvari."Multifunctional, flexible, and mechanically robust polyimide-Mxene nanocomposites: a review." . *2d Mater*, **10**: 042001, (2023).

[133] C. Ma, M.G. Ma, C. Si, X.X. Ji, and P. Wan."Flexible mxene-based composites for wearable devices.". *Advanced Functional Materials*, **31:**2009524, (2021).

[134] H. Cao, N.N. Neal, S. Pas, M. Radovic, J.L. Lutkenhaus, M.J. Green, and E.B. Pentzer."Architecting mxenes in polymer composites." . *Prog Polym Sci*, **153**: 101830, (2024).

[135] J.H. Pu, X. Zhao, X.J. Zha, L. Bai, K. Ke, R.Y. Bao, Z.Y. Liu, M.B. Yang, and W. Yang."Multilayer structured Ag NW/WPu-Mxene fiber strain sensors with ultrahigh sensitivity and a wide operating range for wearable monitoring and healthcare." . *J Mater Chem A Mater*, **7**: 15913-15923, (2019).

[136] S. Seyedin, S. Uzun, A. Levitt, B. Anasori, G. Dion, Y. Gogotsi, and J.M. Razal. "MXene composite and coaxial fibers with high stretchability and conductivity for wearable strain sensing textiles.". *Adv Funct Mater*, **30**: 1910504, (2020).

[137] H. Li and Z. Du. "Preparation of a highly sensitive and stretchable strain sensor of Mxene/silver nanocomposite-based yarn and wearable applications.". *ACS Appl Mater Interfaces*, **11**: 45930-45938, (2019).

[138] Y. Cai, J. Shen, G. Ge, Y. Zhang, W. Jin, W. Huang, J. Shao, J. Yang, and X. Dong."Stretchable ti3c2tx mxene/carbon nanotube composite based strain sensor with ultrahigh sensitivity and tunable sensing range.". *ACS Nano*, **12**: 56-62, (2018).

[139] Y. Yang, Z. Cao, P. He, L. Shi, G. Ding, R. Wang, and J. Sun. "Ti3C2Tx Mxene-graphene composite films for wearable strain sensors featured with high sensitivity and large range of linear response.". *Nano Energy*, **66**: 104134, (2019).

[140] L. Chen, F. Chen, G. Liu, H. Lin, Y. Bao, D. Han, W. Wang, Y. Ma, B. Zhang, and L. Niu. "Superhydrophobic functionalized Ti3C2Tx Mxene-based skin-attachable and wearable electrochemical pH sensor for real-time sweat detection.". *Anal Chem*, **94**: 7319-7328, (2022).

[141] H. Riazi, S.K. Nemani, M.C. Grady, B. Anasori, and M. Soroush. "Ti_3C_2 Mxene–polymer nanocomposites and their applications.". *J Mater Chem A Mater*, **9**: 8051–8098, (2021).

[142] F. Damiri, Md.H. Rahman, M. Zehravi, A.A. Awaji, M.Z. Nasrullah, H.A. Gad, M.Z. Bani-Fwaz, R.S. Varma, M.O. Germoush, H.S. Al-malky, A.A. Sayed, S. Rojekar, M.M. Abdel-Daim, and M. Berrada."MXene (Ti3C2Tx)-embedded nanocomposite hydrogels for biomedical applications: a review." . *Materials*, **15**: 1666, (2022).

[143] E.A. Mayerberger, R.M. Street, R.M. McDaniel, M.W. Barsoum, and C.L. Schauer. "Antibacterial properties of electrospun Ti3C2Tz (Mxene)/chitosan nanofibers.". *RSC Adv*, **8**: 35386-35394, (2018).

[144] A. Rozmysłowska-Wojciechowska, E. Karwowska, M. Gloc, J. Woźniak, M. Petrus, B. Przybyszewski, T. Wojciechowski, and A.M. Jastrzębska. "Controlling the porosity and biocidal properties of the chitosan-hyaluronate matrix hydrogel nanocomposites by the addition of 2D Ti3C2Tx Mxene." . *Materials*, **13**: 4587, (2020).

[145] S. De and B.P. Bastakoti."Doped and functionalized non-Ti-Mxenes for flexible and wearable electronic devices." . *J Mater Chem A Mater*, **13**: 855–888, (2025).

[146] M. Lian, Y. Shi, W. Zhang, J. Zhao, and D. Chen. "Nitrogen and sulfur co-doped Nb2C-Mxene nanosheets for the ultrasensitive electrochemical detection dopamine under acidic conditions in gastric juice.". *Journal of Electroanalytical Chemistry*, **904**: 115849, (2022).

[147] C.-B. Ma, X. Shang, M. Sun, X. Bo, J. Bai, Y. Du, and M. Zhou. "Emerging multifunctional wearable sensors: integrating multimodal sweat analysis and advanced material technologies for next-generation health monitoring." . *ACS Sens*, **10:** 2388-2408, (2025).

[148] J.T. Lee, B.C. Wyatt, G.A. Davis, A.N. Masterson, A.L. Pagan, A. Shah, B. Anasori, and R. Sardar." Covalent surface modification of Ti3C2Tx Mxene with chemically active polymeric ligands producing highly conductive and ordered microstructure films.". *ACS Nano*, **15**: 19600-19612, (2021).

[149] X. Liu, Y. Qiu, D. Jiang, F. Li, Y. Gan, Y. Zhu, Y. Pan, H. Wan, and P. Wang."Covalently grafting first-generation PAMAM dendrimers onto Mxenes with self-adsorbed Au NPs for use as a functional nanoplatform for highly sensitive electrochemical biosensing of ctnt.". *Microsyst Nanoeng*, **8**: 35, (2022).

[150] S. Thurakkal and X. Zhang."Noncovalent functionalization of ti3c2tx using cationic porphyrins with enhanced stability against oxidation.". *Mater Chem Front*, **6**: 561-569, (2022).

[151] P. Fan, E. Ma, C. Liu, Y. Zhao, X. Wen, L. Wang, L. Li, and Q. Qu."A new electrochemical DNA biosensor based on the density control strategy of Ti3C2NH2 Mxene@Qu nanocomposites for the detection of hepatitis b virus-dna.". *Ionics*, **30**: 541-552, (2024).

[152] Y. Mao, F. Ren, D. Zhou, and Y. Li."Highly sensitive pcf-spr ri sensor for cancer detection using gold/graphene/Ti3C2Tx-Mxene hybrid layer.". *Plasmonics*, **20**: 2279–2290, (2024).

[153] K.A. Saraswathi, M. Sai Bhargava Reddy, N. Jayarambabu, K. Venkateswara Rao, S. Aich, and T. Venkatappa Rao. "Non-invasive disposable 2D Ti3C2T based enzyme free electrochemical sweat glucose biosensor.". *Microchemical Journal*, **205**: 111302, (2024).

[154] Y. Chen, H. Xiao, Q. Fan, W. Tu, S. Zhang, X. Li, and T. Hu."Fully integrated biosensing system for dynamic monitoring of sweat glucose and real-time ph adjustment based on 3D graphene Mxene aerogel.". *ACS Appl Mater Interfaces*,**16:** 55155-55165, (2024).

[155] C. Dai, Y. Chen, X. Jing, L. Xiang, D. Yang, H. Lin, Z. Liu, X. Han, and R. Wu."Two-dimensional tantalum carbide (Mxenes) composite nanosheets for multiple imaging-guided photothermal tumor ablation.". *ACS Nano*, **11**: 12696-12712, (2017).

[156] J. Yin, H. Zhang, Y. Wang, Y. Hasebe, Y. Dong, and Z. Zhang."Highly sensitive non-invasive glucose sensing based on chitosan-coated Mxene/NiCO-ldh composites." . *Journal of Electroanalytical Chemistry*, **984**: 119064, (2025).

[157] Y. Pan, M. He, J. Wu, H. Qi, and Y. Cheng."One-step synthesis of Mxene-functionalized PEDOT:PSS conductive polymer hydrogels for wearable and noninvasive monitoring of sweat glucose.". *Sens Actuators B Chem*, **401**: 135055, (2024).

[158] Q. Yan, Y. Cheng, R. Wang, and J. Sun."Recent advances in 3D porous Mxenes: structures, properties and applications.". *J Phys D Appl Phys*, **55**: 093001, (2022).

[159] F. Bu, M.M. Zagho, Y. Ibrahim, B. Ma, A. Elzatahry, and D. Zhao."Porous Mxenes: synthesis, structures, and applications.". *Nano Today*, *30*, 100803, (2020).

[160] W. Hao, S. Ren, X. Wu, X. Shen, and S. Cui."Recent advance in the construction of 3d porous structure Ti3C2Tx Mxene and their multi-functional applications.". *Journal of Alloys and Compounds*, **968:** 172219, (2023).

[161] J. Jiang, F. Li, J. Zou, S. Liu, J. Wang, Y. Zou, K. Xiang, H. Zhang, G. Zhu, Y. Zhang, X. Fu, and J.P. Hsu."Three-dimensional Mxenes heterostructures and their applications.". *Science China Materials*, **65**: 2895-2910, (2022).

[162] H.C. Ates, P.Q. Nguyen, L. Gonzalez-Macia, E. Morales-Narváez, F. Güder, J.J. Collins, and C. Dincer."End-to-end design of wearable sensors.". *Nature Reviews Materials*, **7**:887-907, (2022).

[163] K. Manibalan and J.-T. Chen."Recent progress on mxene–polymer composites for soft electronics applications in sensing and biosensing: a review." . *J Mater Chem A Mater*, **12**: 27130–27156, (2024).

[164] M.A. Zahed, D.K. Kim, S.H. Jeong, M. Selim Reza, M. Sharifuzzaman, G.B. Pradhan, H. Song, M. Asaduzzaman, and J.Y. Park."Microfluidic-integrated multimodal wearable hybrid patch for wireless and continuous physiological monitoring." . *ACS Sens*, **8**: 2960-2974, (2023).

[165] Q. Wang, X. Pan, C. Lin, H. Gao, S. Cao, Y. Ni, and X. Ma."Modified ti3c2tx (mxene) nanosheet-catalyzed self-assembled, anti-aggregated, ultra-stretchable, conductive hydrogels for wearable bioelectronics.". *Chemical Engineering Journal*, **401**: 126129, (2020).

[166] T. Gong, Z. ngyang Li, H. Liang, Y. Li, X. Tang, F. Chen, Q. Hu, and H.Q. Wang."High-sensitivity wearable sensor based on a mxene nanochannel self-adhesive hydrogel.". *ACS Appl Mater Interfaces*, **15**: 19349-19361, (2023).

[167] M. Salauddin, S.M.S. Rana, M.T. Rahman, M. Sharifuzzaman, P. Maharjan, T. Bhatta, H. Cho, S.H. Lee, C. Park, K. Shrestha, S. Sharma, and J.Y. Park."Fabric-assisted Mxene/silicone nanocomposite-based triboelectric nanogenerators for self-powered sensors and wearable electronics.". *Adv Funct Mater*, **32**: 2107143, (2022).

[168] Q. Yi, X. Pei, P. Das, H. Qin, S.W. Lee, and R. Esfandyarpour. "A self-powered triboelectric mxene-based 3d-printed wearable physiological biosignal sensing system for on-demand, wireless, and real-time health monitoring.". *Nano Energy*, **101**: 107511, (2022).

[169] S. Wang, X. Du, Y. Luo, S. Lin, M. Zhou, Z. Du, X. Cheng, and H. Wang."Hierarchical design of waterproof, highly sensitive, and wearable sensing electronics based on Mxene-reinforced durable cotton fabrics.". *Chemical Engineering Journal*, **408**: 127363, (2021).

[170] L. Kong, W. Li, T. Zhang, H. Ma, Y. Cao, K. Wang, Y. Zhou, A. Shamim, L. Zheng, X. Wang, and W. Huang."Wireless technologies in flexible and wearable sensing: from materials design, system integration to applications." . *Advanced Materials*, **36**: 2400333, 2024.

[171] S. He, X. Sun, H. Zhang, C. Yuan, Y. Wei, and J. Li."Preparation strategies and applications of Mxene-polymer composites: a review.". *Macromolecular Rapid Communications*, **42:**2100324, (2021).

[172] J. Jimmy and B. Kandasubramanian."Mxene functionalized polymer composites: synthesis and applications.". *European Polymer Journal*, 122:109367, (2020).

[173] Y. Liu, D. Xu, Y. Ding, X. Lv, T. Huang, B. Yuan, L. Jiang, X. Sun, Y. Yao, and J. Tang."A conductive polyacrylamide hydrogel enabled by dispersion-enhanced mxene@chitosan assembly for highly stretchable and sensitive wearable skin." . *J Mater Chem B*, **9**: 8862-8870, (2021).

[174] W. Peng, X. Pan, X. Liu, Y. Gao, T. Lu, J. Li, M. Xu, and L. Pan."A moisture self-regenerative, ultra-low temperature anti-freezing and self-adhesive Polyvinyl alcohol/Polyacrylamide/CaCl2/Mxene ionotronics hydrogel for bionic skin strain sensor.". *J Colloid Interface Sci*, **634**: 782-792, (2023).

[175] Y. Sun, Y. Du, Y. Zhang, J. Yang, J. Liu, R. Tian, J. Wang, Q. Li, X. He, and J. Fu."Anti-swelling and photoresponsive Mxene-based polyampholyte hydrogel sensors for underwater positioning and urban waterlogging pre-warning." . *J Mater Chem A Mater*, **12**: 22166–22179, (2024).

[176] F. Shahzad, A. Iqbal, S.A. Zaidi, S.W. Hwang, and C.M. Koo."Nafion-stabilized two-dimensional transition metal carbide (Ti3C2Tx Mxene) as a high-performance electrochemical sensor for neurotransmitter.". *Journal of Industrial and Engineering Chemistry*, **79**: 338-344, (2019).

[177] M. Cao, S. Liu, S. Liu, Z. Tong, X. Wang, and X. Xu."Preparation of ZnO/Ti3C2Tx/Nafion/Au electrode.". *Microchemical Journal*, **175**: 107068 , (2022).

[178] W.Y. Guo, T. Mai, L.Z. Huang, W. Zhang, M.Y. Qi, C. Yao, and M.G. Ma."Multifunctional Mxene conductive zwitterionic hydrogel for flexible wearable sensors and arrays." . *ACS Appl Mater Interfaces*, **15**: 24933-24947, (2023).

[179] K. Zhang, J. Sun, J. Song, C. Gao, Z. Wang, C. Song, Y. Wu, and Y. Liu."Self-healing Ti_3C_2 Mxene/PDMS supramolecular

elastomers based on small biomolecules modification for wearable sensors.". *ACS Appl Mater Interfaces*, **12**: 45306–45314, (2020).

[180] C.C. dos Santos, G.N. Lucena, G.C. Pinto, M.J. Júnior, and R.F.C. Marques."Advances and current challenges in non-invasive wearable sensors and wearable biosensors—a mini-review.". *Med Devices Sens*, **4**: e10130, (2021).

[181] K. Phasuksom, N. Ariyasajjamongkol, and A. Sirivat."Screen-printed electrode designed with mxene/doped-polyindole and mwcnt/doped-polyindole for chronoamperometric enzymatic glucose sensor.". *Heliyon*, **10**: e24346, (2024).

[182] H.R. Chen, W.M. Meng, R.Y. Wang, F.L. Chen, T. Li, D.D. Wang, F. Wang, S.E. Zhu, C.X. Wei, H.D. Lu, and W. Yang."Engineering highly graphitic carbon quantum dots by catalytic dehydrogenation and carbonization of ti3c2tx-mxene wrapped polystyrene spheres." . *Carbon N Y*, **190**: 319-328, (2022).

[183] P. Das, P.K. Marvi, S. Ganguly, X. Tang, B. Wang, S. Srinivasan, A.R. Rajabzadeh, and A. Rosenkranz."MXene-based elastomer mimetic stretchable sensors: design, properties, and applications.". *Nano-Micro Letters*, **16**:135, (2024).

[184] I. Turcan, T.A. Filip, T. Vlad-Bubulac, D. Rusu, and M.A. Olariu."Dielectrophoretic direct assembling of mxene flakes at the level of screen-printed interdigitated microelectrodes and their evaluation in gas sensing applications." . *2d Mater*, **11**: 045014, (2024).

[185] Y. Lu, X. Qu, W. Zhao, Y. Ren, W. Si, W. Wang, Q. Wang, W. Huang, and X. Dong."Highly stretchable, elastic, and sensitive mxene-based hydrogel for flexible strain and pressure sensors." . *Research*, **2020**: 2038560, (2020).

[186] Y. Zhang, L. Wang, L. Zhao, K. Wang, Y. Zheng, Z. Yuan, D. Wang, X. Fu, G. Shen, and W. Han."Flexible self-powered integrated sensing system with 3d periodic ordered black phosphorus@mxene thin-films.". *Advanced Materials*, **33**: 2007890, (2021).

[187] J.S. Nah, S.C. Barman, M.A. Zahed, M. Sharifuzzaman, H. Yoon, C. Park, S. Yoon, S. Zhang, and J.Y. Park."A wearable microfluidics-integrated impedimetric immunosensor based on ti3c2tx mxene incorporated laser-burned graphene for noninvasive sweat cortisol detection." . *Sens Actuators B Chem*, **329**: 129206, (2021)

[188] B. Liu, B. Ran, C. Chen, L. Shi, J. Jin, and Y. Zhu."High-throughput microfluidic production of bimetallic nanoparticles on mxene nanosheets and application in hydrogen peroxide detection." . *ACS Appl Mater Interfaces*, **14**: 56298-56309, (2022).

[189] X.H. Wen, X.F. Zhao, X.H. Wang, Y. Wang, J.C. Guo, H.G. Zhou, C.T. Zuo, and H.L. Lu."Fe3O4/mxene nanosphere-based microfluidic chip for the accurate diagnosis of alzheimer's disease." . *ACS Appl Nano Mater*, **5**: 15925-15933, (2022).

[190] D.H. Lee, J.C. Yang, J.Y. Sim, H. Kang, H.R. Kim, and S. Park."Bending sensor based on controlled microcracking regions for application toward wearable electronics and robotics." . *ACS Appl Mater Interfaces*, **14**: 31312-31320, (2022).

[191] Y. Yu, S. Peng, P. Blanloeuil, S. Wu, and C.H. Wang."Wearable temperature sensors with enhanced sensitivity by engineering microcrack morphology in pedot:pss–pdms sensors." . *ACS Appl Mater Interfaces*, **12**: 36578–36588, (2020).

[192] Y. Zhou, H. Lian, Z. Li, L. Yin, Q. Ji, K. Li, F. Qi, and Y.A. Huang."Crack engineering boosts the performance of flexible sensors.". *View*, **3:** 20220025, (2022).

[193] H. Dai, J. Chang, J. Yang, H. Wang, J. Zhou, and G. Sun."Bio-inspired interfacial engineering of mxene fibers toward synergistic improvement in mechanical strength and electrochemical performance." . *Adv Funct Mater*, **34**: 2312654, (2024).

[194] Y. Wang, C. Xu, Z. Mao, X. Peng, W. Cui, H. Deng, and H. Chen."Bio-inspired bi-directional design: mxene@mof as a light-driven integrated platform for mrsa management and monitoring." . *Compos B Eng*, **292**: 112086, (2025).

[195] Y. Chen, Y. Hao, L. Feng, J. Meng, Z. Yang, H. Wu, P. Li, Z. Zhu, B. Zhao, and Q. Wei."A flexible multifunctional triboelectric nanogenerator based on bio-inspired nanocellulose/tannic acid@mxene-composited hydrogel for human healthcare." . *Int J Biol Macromol*, **306**: 141261, (2025).

[196] M. Venkatesan, J. Chandrasekar, Y. Hsu, T. Sun, P. Li, X. King, M. Chung, R. Chung, W. Lee, Y. Zhou, J. Lin, and C. Kuo. "Rationally improved surface charge density of triboelectric nanogenerator with TiO_2-Mxene/polystyrene nanofiber charge trapping layer for biomechanical sensing and wound healing application.". *Advanced Science*, **11:**2404019, (2024).

[197] S. Hajian, P. Khakbaz, M. Moshayedi, D. Maddipatla, B.B. Narakathu, V.S. Turkani, B.J. Bazuin, M. Pourfath, and M.Z. Atashbar."Impact of different ratios of fluorine, oxygen, and hydroxyl surface terminations on ti3c2t x mxene as ammonia sensor: a first-principles study." Proceedings of IEEE Sensors (2018).

[198] J.D. Gouveia and J.R.B. Gomes."Effect of the surface termination on the adsorption of flue gas by the titanium carbide mxene." . *Mater Today Chem*, **29**: 101441, (2023).

[199] X. Li, Z. An, Y. Lu, J. Shan, H. Xing, G. Liu, Z. Shi, Y. He, Q. Chen, R.P.S. Han, D. Wang, J. Jiang, F. Zhang, and Q. Liu."Room temperature vocs sensing with termination-modified Ti3C2Tx Mxene for wearable exhaled breath monitoring." . *Adv Mater Technol*, **7**: 2100872, (2022).

[200] R. Ghaffari, D.S. Yang, J. Kim, A. Mansour, J.A. Wright, J.B. Model, D.E. Wright, J.A. Rogers, and T.R. Ray."State of sweat: emerging wearable systems for real-time, noninvasive sweat sensing and analytics.". *ACS sensors*, **6**: 2787-2801, (2021).

[201] W. Zhang, S. Jiang, H. Yu, S. Feng, and K. Zhang."Ga@MXene-based flexible wearable biosensor for glucose monitoring in sweat." . *iScience*, **28**: 111737, (2025).

[202] V. Myndrul, E. Coy, N. Babayevska, V. Zahorodna, V. Balitskyi, I. Baginskiy, O. Gogotsi, M. Bechelany, M.T. Giardi, and I. Iatsunskyi. "MXene nanoflakes decorating zno tetrapods for enhanced performance of skin-attachable stretchable enzymatic electrochemical glucose sensor.". *Biosens Bioelectron*, **207**: 114141, 2022.

[203] Z. Zheng, Y. Zhao, Z. Ye, J. Hu, and H. Wang."Electrically conductive porous mxene-polymer composites with ultralow percolation threshold via pickering high internal phase emulsion templating strategy." . *J Colloid Interface Sci*, **618**: 290-299, (2022).

[204] H. Cao, Y. Wang, A. Sarmah, K.W. Liu, Z. Tan, K.D. Arole, J.L. Lutkenhaus, M. Radovic, M.J. Green, and E.B. Pentzer."Electrically conductive porous ti3c2t x mxene-polymer

composites from high internal phase emulsions (hipes).” . *2d Mater*, **9**: 044004, (2022).

[205] M. Liu, Y. Zhuo, A. Sarycheva, Y. Gogotsi, M.A. Bissett, R.J. Young, and I.A. Kinloch.“Deformation of and interfacial stress transfer in Ti3C2 mxene-polymer composites.” . *ACS Appl Mater Interfaces*, **14**: 10681-10690, (2022).

[206] K. Völlmecke, R. Afroz, S. Bierbach, L.J. Brenker, S. Frücht, A. Glass, R. Giebelhaus, A. Hoppe, K. Kanemaru, M. Lazarek, L. Rabbe, L. Song, A. Velasco Suarez, S. Wu, M. Serpe, and D. Kuckling.“Hydrogel-based biosensors.”. *Gels*, **8:** 768, (2022).

[207] J. Tavakoli and Y. Tang.“Hydrogel based sensors for biomedical applications: an updated review.”. *Polymers*, **9:** 364, (2017).

[208] X. Fu, Y. Qiu, H. Zhang, Y. Tian, A. Liu, and H. Wu.“Microfluidic sweat patch based on capillary force and evaporation pump for real-time continuous sweat analysis.” . *Biomicrofluidics*, **18**: 034106, (2024).

[209] C.H. Wu, H.J.H. Ma, P. Baessler, R.K. Balanay, and T.R. Ray.“Skin-interfaced microfluidic systems with spatially engineered 3d fluidics for sweat capture and analysis.” . *Sci Adv*, **9**: eadg4272, (2023).

[210] X. He, T. Xu, Z. Gu, W. Gao, L.P. Xu, T. Pan, and X. Zhang.“Flexible and superwettable bands as a platform toward sweat sampling and sensing.” . *Anal Chem*, **91**: 4296-4300, (2019).

[211] M.A. Zahed, M. Sharifuzzaman, H. Yoon, M. Asaduzzaman, D.K. Kim, S. Jeong, G.B. Pradhan, Y. Do Shin, S.H. Yoon, S. Sharma, S. Zhang, and J.Y. Park.“A nanoporous carbon-mxene heterostructured nanocomposite-based epidermal patch for real-time biopotentials and sweat glucose monitoring.” . *Adv Funct Mater*, **32**: 2208344, (2022).

[212] S.G. Chavan, P.R. Rathod, A. Koyappayil, G. Karuppaiah, A. Go, E. Jin, J. Park, and M.-H. Lee.“Self-assembled aunps on niobium carbide (Nb2C) mxene-based apta-sensor for progesterone recognition in female sweat and serum sample.” . *Sens Actuators B Chem*, **437**: 137722, (2025).

[213] T. Laochai, J. Yukird, N. Promphet, J. Qin, O. Chailapakul, and N. Rodthongkum.“Non-invasive electrochemical immunosensor for sweat cortisol based on l-cys/aunps/ mxene modified thread electrode.” . *Biosens Bioelectron*, **203**: 114039, (2022).

[214] A.K. Subramania, S. Sugumaran, P. Sethuramalingam, R. Ramesh, P. Dhandapani, and S. Angaiah.“NiCo2O4/ti2nbc2 (double mxene) nanohybrid-based non-enzymatic electrochemical biosensor for the detection of glucose in sweat.” . *Bioprocess Biosyst Eng*, **46**: 1755-1763, (2023).

[215] L. Feng, J. Chen, M. Yang, J. Wang, S. Yin, D. Zhang, W. Qin, and J. Song.“CuxO decorated ti3c2tx mxene composites for non-enzymatic glucose sensing with large linear ranges.” . *Microchimica Acta*, **191**: 451, (2024).

[216] A. Ravitchandiran, S. AlGarni, M.S. AlSalhi, R. Rajaram, T. Malik, and S. Angaiah.“ZnFe(pba)@ti3c2tx nanohybrid-based highly sensitive non-enzymatic electrochemical sensor for the detection of glucose in human sweat.” . *Sci Rep*, **14**: 23835, (2024).

[217] Z. Damirchi, A. Firoozbakhtian, M. Hosseini, and M.R. Ganjali.“Ti3C2/ni/sm-based electrochemical glucose sensor for sweat analysis using bipolar electrochemistry.” . *Microchimica Acta*, **191**: 137, (2024).

[218] R. Khan and S. Andreescu.“Catalytic mxceo2 for enzyme based electrochemical biosensors: fabrication, characterization and application towards a wearable sweat biosensor.” . *Biosens Bioelectron*, **248**: 115975, (2024).

[219] Y. Zhang, Z. Wang, X. Liu, Y. Liu, Y. Cheng, D. Cui, F. Chen, and W. Cao.“A mxene/mos2 heterostructure based biosensor for accurate sweat ascorbic acid detection.” . *FlatChem*, **39**: 100503, (2023).

[220] V. Magesh, A.K. Sundramoorthy, D. Ganapathy, R. Atchudan, S. Arya, R.A. Alshgari, and A.M. Aljuwayid.“Palladium hydroxide (pearlman’s catalyst) doped mxene (ti3c2tx) composite modified electrode for selective detection of nicotine in human sweat.” . *Biosensors,* **13**:54, (2023).

[221] F. Chen, J. Wang, L. Chen, H. Lin, D. Han, Y. Bao, W. Wang, and L. Niu.“A wearable electrochemical biosensor utilizing functionalized ti3c2tx mxene for the real-time monitoring of uric acid metabolite.” . *Anal Chem*, **96**: 3914-3924, (2024).

[222] S. Choudhury, S. Zafar, D. Deepak, A. Panghal, B. Lochab, and S.S. Roy.“A surface modified laser-induced graphene based flexible biosensor for multiplexed sweat analysis.” . *J Mater Chem B*, **13**: 274–287, (2025).

[223] Z. Chen, Y. Liu, W. Yu, S. Liu, and Y. Huang.“Machine learning-driven wearable sweat sensors with agnw/mxene for non-invasive sers-based cardiovascular disease detection.” . *ACS Appl Nano Mater*, **8**: 5602–5610, (2025).

[224] Z. Zhou, X. He, J. Xiao, J. Pan, M. Li, T. Xu, and X. Zhang.“Machine learning-powered wearable interface for distinguishable and predictable sweat sensing.” . *Biosens Bioelectron*, **265**: 116712, (2024).

[225] S. Das, H. Mazumdar, K.R. Khondakar, and A. Kaushik.“Machine learning assisted enhancement in a two-dimensional material’s sensing performance.” . *ACS Appl Nano Mater*, **7**: 13893–13918, (2024).

[226] X. Xiao, J. Yin, J. Xu, T. Tat, and J. Chen.“Advances in machine learning for wearable sensors.” . *ACS Nano*, **18**: 22734–22751, (2024).

[227] Z. Chen, Y. Liu, W. Yu, S. Liu, and Y. Huang.“Machine learning-driven wearable sweat sensors with agnw/mxene for non-invasive sers-based cardiovascular disease detection.” . *ACS Appl Nano Mater*, **8**: 5602–5610, (2025).

[228] L. Zhou, S.S. Menon, X. Li, M. Zhang, and M.H. Malakooti.“Machine learning enables reliable colorimetric detection of ph and glucose in wearable sweat sensors.” . *Adv Mater Technol*, **10**: 2401121, (2025).

[229] Z. Zhou, X. He, J. Xiao, J. Pan, M. Li, T. Xu, and X. Zhang.“Machine learning-powered wearable interface for distinguishable and predictable sweat sensing.” . *Biosens Bioelectron*, **265**: 116712, (2024).

[230] W. Wang, H. Zhou, Z. Xu, Z. Li, L. Zhang, and P. Wan.“Flexible conformally bioadhesive mxene hydrogel electronics for machine learning-facilitated human-interactive sensing.” . *Advanced Materials*, **36**: 2401035, (2024).

[231] W. Guo, Z. Ma, Z. Chen, H. Hua, D. Wang, M. Elhousseini Hilal, Y. Fu, P. Lu, J. Lu, Y. Zhang, D. Ho, and B.L. Khoo.“Thin and soft ti3c2tx mxene sponge structure for highly sensitive pressure sensor assisted by deep learning.” . *Chemical Engineering Journal*, **485**: 149659, (2024).

[232] S. Duan, Y. Lin, Q. Shi, X. Wei, D. Zhu, J. Hong, S. Xiang, W. Yuan, G. Shen, and J. Wu."Highly sensitive and mechanically stable mxene textile sensors for adaptive smart data glove embedded with near-sensor edge intelligence." . *Advanced Fiber Materials*, **6**: 1541–1553, (2024).

[233] L. Uhlenberg, A. Derungs, and O. Amft."Co-simulation of human digital twins and wearable inertial sensors to analyse gait event estimation." . *Front Bioeng Biotechnol*, **11**: 1104000, (2023).

[234] Y.C. Zhao, Z. Wang, H. Zhao, N.A. Yap, R. Wang, W. Cheng, X. Xu, and L.A. Ju."Sensing the future of thrombosis management: integrating vessel-on-a-chip models, advanced biosensors, and ai-driven digital twins." . *ACS Sens*, **10**: 1507–1520, (2025).

[235] A. Vallée."Digital twin for healthcare systems.". *Digital Health*, **5:**1253050, (2023).

[236] P. Deshpande, B. Ravikumar, S. Tallur, D. Paul, and B. Rai."Development of an insilico model of eccrine sweat using molecular modelling techniques." . *Sci Rep*, **12**: 20263, (2022).

[237] C. Tang, W. Yi, E. Occhipinti, Y. Dai, S. Gao, and L.G. Occhipinti."A roadmap for the development of human body digital twins." . *Nature Reviews Electrical Engineering*, **1**: 199-207, (2024).

[238] S. Sen and K.D. Kilic."Digital twins in medicine, ai-driven personalized healthcare, and predictive analytics." In: *AI-Powered Digital Twins for Predictive Healthcare: Creating Virtual Replicas of Humans*. IGI Global Scientific Publishing, (2025). p. 359-396.

[239] S. Kumar, S. Kumar, M.A. Ali, P. Anand, V.V. Agrawal, R. John, S. Maji, and B.D. Malhotra."Microfluidic-integrated biosensors: prospects for point-of-care diagnostics.". *Biotech J*, **8:**1267-1279, (2013).

[240] F. Shahbazi, M. Jabbari, M.N. Esfahani, and A. Keshmiri."A computational simulation platform for designing real-time monitoring systems with application to covid-19." . *Biosens Bioelectron*, **171**: 112716, (2021).

[241] D. Mukasa, M. Wang, J. Min, Y. Yang, S.A. Solomon, H. Han, C. Ye, and W. Gao."A computationally assisted approach for designing wearable biosensors toward non-invasive personalized molecular analysis." . *Advanced Materials*, **35**: 2212161, (2023).

[242] C. Wang, Y. Zhang, X. Zeng, C. Jin, Y. Liu, M. Yang, D. Huo, and C. Hou."Boosted synergistic catalytic performance of pt single-atom catalyst nis2/pt on wearable hydrogel biosensor for sweat lactic acid analysis." . *Anal Chim Acta*, **1355**: 343971, (2025).

[243] S. Choudhury, S. Zafar, D. Deepak, A. Panghal, B. Lochab, and S.S. Roy."A surface modified laser-induced graphene based flexible biosensor for multiplexed sweat analysis." . *J Mater Chem B*, **13**: 274–287, (2025).

[244] X. Lei, H. Fan, Y. Zhao, M. Zhong, Z. Wu, L. Li, S. Li, X. Xing, J. Liu, Y. Sun, Y. Jiang, and G. Ren."MXene-enhanced laser-induced graphene flexible sensor with rapid response for monitoring pilots' body motion." . *Micromachines (Basel)*, **16**: 513, 2025.

[245] W. Sun, W. Li, C. Xue, W. Zhang, and Y. Jiang."MXene-silk composites integrated on laser-induced graphene platform for touch-free sensing." . *Chemical Engineering Journal*, **509**: 161317, (2025).

[246] A.M. Abdullah, M.A.S. Biswas, A. Dutta, J. Li, S. Das, X. Zhang, W. Zhang, F.T. Zohra, A. Moreno Calva, J.L. Gray, H. Jabelli, C. Wu, and H. Cheng."*In situ* functionalized mxene on porous laser-induced graphene for adsorption-dominated miniaturized multifunctional sensors." . *ACS Nano*, **19**: 33841–33856, (2025).